AKENTEN APPIAH-MENKA UNIVERSITY OF SKILLS TRAINING AND ENTREPRENEURIAL DEVELOPMENT

OPTIMAL CAPACITOR BANK PLACEMENT AND SIZING USING PARTICLE SWARM OPTIMIZATION (PSO): A CASE STUDY ON ECG 33 KV DISTRIBUTION NETWORK SYSTEM IN GHANA, ASHANTI REGION.

BY

PRINCE ASABERE

(8201200010)

A Thesis Submitted to the Department of Electrical and Electronic Technology Education,
Faculty of Technical Education, submitted to the School of Graduate Studies, in partial fulfilment of
the requirements for the award of the degree of Master of Philosophy Electrical Power System Engineering in the Akenten Appiah-Menka University of Skills Training and Entrepreneurial Development.

NOVEMBER 2023

DECLARATION

Student's Declaration

I, **Prince Asabere** declare that this thesis, with the exception of quotations and references contained in the published works which have all been identified and duly acknowledged, is entirely my original work, and it has not been submitted, either in part or whole, for another degree elsewhere.

SIGNATURE: .....

DATE: .....

Supervisor's Declaration

I hereby declare that the preparation and presentation of this work was supervised in accordance with guidelines for supervision of thesis as laid down by the Akenten Appiah-Menka University of Skills Training and Entrepreneurial Development.

NAME OF SUPERVISOR: FRANCOIS SEKYERE (MR)

SIGNATURE: .....

DATE: .....

ABSTRACT

Distribution systems always have high losses, maximum voltage drops, and bus voltage instability. This thesis examines the impact of integrating Distribution Static Synchronous Compensators (DSTATCOM) on the ECG distribution system in the Ashanti Region, Ghana. The study compares the system's performance before and after DSTATCOM integration. The Backward/Forward Sweep (BFS) was used to analyse the load flow, while the Particle Swarm Optimization (PSO) algorithm determined DSTATCOM's size and position. Three cases were analysed. The first case analysed a 50-bus system data without DSTATCOM, while the second and third cases employed PSO to determine the appropriate location and size of fixed and switched DSTATCOM to lessen active and reactive power loss, boost the voltage profile, and minimize energy cost. The results demonstrate that DSTATCOM integration increased the minimum bus voltage from 0.817 p.u. to 0.95 p.u. and maintaining the maximum bus voltage at 1 p.u. Additionally, DSTATCOM integration leads to substantial reductions in total active and reactive power losses. In Case 1, there is a reduction of 58.88% in active power loss and 57.48% in reactive power loss. Similarly, Case 2 shows a decrease of 58.72% in active power loss and an impressive 96.69% reduction in reactive power loss. Regarding the economic impact, Case 1 exhibits an annual energy cost of $1,004,433.60 and net savings of $1,436,606.40. In Case 2, these values are $1,007,867.76 for energy cost and $1,433,172.24 for net savings. Both Cases (Case 1 and Case 2) demonstrate a net savings percentage of 58.85% and 58.71% respectively, with a consistent seven-month payback period. The integration of DSTATCOMs into the ECG distribution system in the Ashanti Region has proven to be an effective strategy for improving voltage regulation, reducing power losses, and achieving significant economic savings.

ACKNOWLEDGEMENT

I would like to express my deepest gratitude to the Almighty GOD for providing me with knowledge, guidance, protection, strength, and blessings throughout the entire process of completing this thesis.

I am grateful to my supervisor, Mr Francois Sekyere for providing critical, analytical, and constructive feedback throughout the writing of this thesis. I am grateful to Dr Albert K. Awopone and Dr Patrick N. Ayambire for their directions, patience and guidelines throughout the thesis and also thank all the Electrical/Electronic Lab technicians of Akenten Appiah-Menka University of Skills Training and Entrepreneurial Development for their advice and motivation.

I would like to thank Ing. Appiah Alexander Winston and Ing. Ansah Antwi Boasiako, Electricity Company of Ghana (ECG) for their assistance of providing Ashanti Region network data and other resources during the project. I say a big thank you to all the ECG Control Room Engineers who helped me to have the data in each substation in Ashanti region.

Finally, I acknowledge all those who, in one way or another, supported me during my studies, especially my wife, Mavis Kyeremaa for her support.

DEDICATION

This thesis is dedicated to my wife, Mavis Kyeremaa and my Pastor, Aps. Emmanuel K. Adjei for their love, prayers, support, sacrifice, motivation, and patience during the period of my study.

TABLE OF CONTENTS

LIST OF TABLES

LIST OF FIGURES

GLOSSARY

AMA: Accra Metropolitan Assembly

AC: Alternating Current

AFSOA: Artificial Fish Swarm Optimization Algorithm

BCBV: Branch Current to the Bus Voltage

BIBC: Bus Injection to the Branch Current

CSA: Cuckoo Search Algorithm

CPD: Custom Power Devices

DLF: Decouple Load Flow

DC: Direct Current

DG: Distributed Generation

DLF: Distribution Load Flow

DSTATCOM: Distribution Static Compensator

EPC: Enclave Power Company

ECI: Equivalent Current Injection

FACTS: Flexible AC transmission system

GEDAP: Ghana Energy Development and Access Project

GridCO: Ghana Grid Company

GDP: Gross Domestic Product

IEEE: Institute of Electrical and Electronic Engineers

IEC: International Electrotechnical Commission

KVL: Kirchhoff’s Voltage Law

KCL: Kirchhoff's Current Law

KMA: Kumasi Metropolitan Assembly

KTI: Kumasi Technical Institute

LSA: Lightning Search Algorithm

LV: Low Voltage

NITS: National Interconnected Transmission System

NEDCo: Northern Electricity Distribution Company

PSO: Particle Swarm Optimization

PWD: Public Works Department

RDS: Radial Distribution System

R/X: Resistance to Reactance

SFLA: Shuffled Frog Leaping Algorithm

SSSC: Static Synchronous Series Compensator

SBU: Strategic Business Unit

TCSC: Thyristor Controlled Series Compensator

VALCO: Volta Aluminium Company

VRA: Volta River Authority

Vs: Voltage Magnitude

VSC: Voltage Source Converter

CHAPTER ONE

INTRODUCTION

1.1. Background of the study

Electricity is essential to modern living throughout public services, transportation, government, businesses, and homes due to globalization (Balakumar S., Akililu Getahun, Samuel Kefale, and Ramash Kumar K., 2021). Generation, transmission, and distribution make up an electric power system. The government of Ghana has mandated Volta River Authority (VRA) and Ghana Grid Company (GridCo) to undertake the operation of national power generation and national interconnected transmission system (NITS) respectively. The Electricity Company of Ghana (ECG) and Northern Electricity Distribution Company (NEDCo) are responsible for the distribution systems in southern and northern part of Ghana respectively while the Enclave Power Company (EPC) to supply power to Tema Free Zones Enclave and Dawa Industrial Zone, Ghana. The EPC was licensed to operate as private power distribution company on 2015 (Ebenezer Nyarko Kumi, 2017).

In Ghana, hydropower systems were the main means of generating electricity in 2000. By 2021, however, the power mix had changed to include 34.1% hydro, 65.3% thermal, and 0.55% renewable sources (Energy Commission Ghana, 2022). The national dependability on thermal power generation has negatively impacted the country's economy because of the cost of fuel for thermal plants and also because of global warming in Ghana (Felix Amankwah Diawuo, Ian J. Scott, Patricia C. Baptista, and Carlos A. Silva., 2020). The transmission system was created with the purpose of transferring large quantities of energy from distant power generation stations to load centres. The transmission system in Ghana is made up of a high-

voltage network, generally 161 – 330 kV a.c which was designed as National Interconnected Transmission System (Energy Commission, 2016).

The distribution system, categorized by primary/secondary and radial/ring characteristics, supplies electricity to consumers at various consumption stages (PNNL Seeks Visionary Leadership in Grid and Advanced Controls, 2013). The distribution system is crucial to the power system because it constitute a lot of power losses and voltage drops that affect load demand in power system (Iman Ziari, Gerard Ledwich, Arindam Ghosh, and Glenn Platt, 2013). When the distribution network is overloaded, the load current from the source increases, putting strain on the system and resulting in power loss and voltage fluctuations. A high resistance to reactance (R/X) ratio in a distribution system causes voltage drop, power factor lag, and system instability (Daiva Stanelyte & Virginijus Radziukynas, 2020).

Radial distribution systems use a single power source, experiencing low voltage and power losses at distant points (Ayodeji Olalekan Salau, Yalew Werkie Gebru & Dessalegn Bitew, 2020). Industrial sites with critical loads are prone to voltage collapse due to power losses and voltage drops. Demand fluctuations worsen these issues by lowering bus voltage and increasing reactive power demands. It has been reported that approximately thirteen percent (13%) of generated electricity is lost through the distribution system (Noramin Ismail & Wan Norainin Wan Abdullah, 2010; Ibrahim Dincer & Canan Acar, 2015). To enhance the voltage profile and minimize power losses, an effective reactive power mitigation tool with optimized size and position becomes essential.

In 2021, Ghana's distribution systems have caused annual losses of US$620.36 million (89.89%, 10.05%, and 0.06% for ECG, NEDCo and EPC respectively) (Energy Commission Ghana, 2022). Despite a surge from 2170 MW in 2011 to 5481 MW in 2021 which represent the annual average growth of 9.7%, the consumption demand also rose from 9187 GWh in

2011 to 18067 GWh in 2021. The distribution systems losses increased from 2347 GWh in 2011 to 4809 GWh in 2021 (Energy Commission Ghana, 2022). The corresponded distribution losses were 4,323 GWh (89.8%), 483 GWh (10.1%) and 3 (0.1%) GWh in 2021 for ECG, NEDCo and EPC, respectively (Energy Commission Ghana, 2022). Due to network layout, unauthorized access to electricity and inadequate energy capacity to solicit the load demand, the distribution system losses have become high and causing issues with electricity supply in Ghana.

Kumasi Metropolitan Assembly (KMA) leads Ghana's energy consumption with 836.5 GWh, followed by Accra (644.5 GWh), Sekondi Takoradi (661.9 GWh), Asokore Mampong (196.1 GWh), and Ga South (150.9 GWh). The Ashanti region has 26.1% of the national share of electricity demand, which is the highest among all the sixteen regions in the country (Energy Commission - Ghana, 2019).

The Ashanti Region distribution system was designed in radial distribution systems which are far from Strategic Business Unit (SBU) centres. Power distribution system losses depend on substation-to-load centre distance and system overloading. Due to the distance between sending and receiving centres, Offinso, Mampong, Bekwai, and other substations have low voltages. ECG attempts to address these problems by manually adjusting the tap settings of the station transformer and implementing localized load shedding in the surrounding area to match the consumption demand. However, these practices are not in line with professional standards for the country's development.

To enhance the performance of the distribution system (DS) and achieve objectives like reducing power losses, improving voltage profile, voltage stability margin, system reliability, and security, the implementation of a compensating device with cutting-edge technology is essential considered (Tsai-Hsiang Chena, Lung-Sheng Chiang & Nien-Che Yang, 2012; Huda &

Živanović, 2017). Shunt-connected DSTATCOMs (Distribution Static Compensators) offer advantages such as lower losses, minimal harmonic distortion, simplicity, and cost-effectiveness (Devabalaji Kaliaperumal Rukmani, Yuvaraj Thangaraj, Umashankar Subramaniam, Sitharthan Ramachandran, Rajvikram Madurai Elavarasan, Narottam Das, Luis Baringo & Mohamed Imran Abdul Rasheed, 2020). Properly sizing and placing DSTATCOM devices are crucial to effectively compensate for distribution system performance (Venkatesh B., Rakesh Ranjan, & Gooi H. B., 2004).

Various researchers such as (Venkatesh, Rukmani, Thangaraj, and others) have presented different optimization algorithms (Evolutionary Programming Algorithm, Bio-inspired Cuckoo Search Algorithm, Lightning Search Algorithm, etc.) to properly size and distribute the compensating device in the distribution system to increase performance (Rukmani et al., 2020; Thangaraj & Kuppan, 2017; Venkatesh et al., 2004).

This research used the Backward/Forward Sweep load flow method for analysing the ECG 33 kV distribution system in the Ashanti region. Additionally, Particle Swarm Optimization (PSO) was utilized to determine the optimal bus for DSTATCOM. The DSTATCOM cuts down both active and reactive losses and makes the primary distribution system more stable and with a better voltage profile.

1.2. Statement of the problem

The 33 kV distribution network of the Electricity Company of Ghana (ECG) in the Ashanti region has been chosen as a case study for this research. The distribution network has fifty (50) distribution buses and twenty-one (21) Strategic Business Unit (SBU) centres that provide energy to the Ashanti region. As a result of commerce, an ever-growing residential population, and the construction of various industrial facilities, the electrical load demand on the 33 kV distribution system has been gradually increasing in the Region. Overloading the distribution

network component causes power outages, voltage instability, and voltage drops (Hichem Nemouchi, Ahmed Tiguercha & Ahmed Amine Ladjici, 2020). The outgoing feeder of the SBU substations presently endures regular power disruptions because of the existing system's overloading. This research examined Ashanti's ECG 33 kV primary distribution network, which occasionally loses electricity due to system overloading. Hence, the fifty buses of the 33 kV distribution network have been chosen as a case study.

These problems can range from voltage fluctuations, harmonic distortions, and reactive power imbalances, which can adversely affect the reliability, stability, and overall performance of the distribution network (Chowdhury S., Chowdhury S. P. & Crossley P., 2009). Due to the expansion of commercial and industrial sectors in the Ashanti Region, the 33 kV distribution network does not meet the efficiency standards set by IET (ADJOA, 2014; Standard & Horizontale, 2009). As noted above, strategically deploying reactive compensating devices can reduce power losses and enhance the voltage profile of the distribution system (Ismail Bazilah, Noor Izzri Abdul Wahab, Mohammad Lutfi Othman, Mohd Amran Mohd Radzi, Kanendra Naidu Vijyakumar & Muhammad Mat Naain, 2020).

1.3. Aims and Objectives

The aim is to address power quality issues and minimize power losses (both active and reactive losses) while enhancing the voltage profile of the radial distribution network. The study utilized the Particle Swarm Optimization (PSO) technique to determine the optimal size and placement of the Distribution Static Compensator (DSTATCOM) in the Ashanti Region's distribution system. The thesis' objectives are:

1. to perform technical analyse of the 33 kV distribution system in the Ashanti region.
2. to optimize the placement and sizing of DSTATCOM based on the Particle Swarm Optimization algorithm.

3. to do a comparative analysis of the existing system and the optimize system.

1.4. The significance of the research

The thesis aims to enhance the power system's performance to meet the increasing demand for electricity and ensure a reliable power supply. Custom Power Devices are a great way to improve the performance of a distribution system by reducing system losses and increasing bus voltage level (Ismail et al., 2020). The optimal capacitor placement and sizing are important considerations for utility companies because it helps to improve the efficiency and stability of the power system and reduce power losses.

Strategically placing and sizing capacitors empowers the utility company (ECG) to deliver consistent and efficient electricity to its customers. The advantages of well-placed and sized capacitors extend beyond the utility company to benefit the entire country. A more efficient, reliable, and stable power system contributes to driving economic growth, attracting new businesses, and fostering the development of innovative technologies. Furthermore, it plays a crucial role in reducing the environmental impact of power generation and helps mitigate the effects of climate change. In essence, this thesis offers valuable academic contributions by providing comprehensive data on the Ashanti Region 33 kV Distribution System, facilitating learning, research, and innovation in the field of electrical engineering.

1.5. The organization of the research

The main parts of this research paper are broken up into five chapters. The first chapter introduces the thesis's key idea and guides its body. The second chapter covers FACTS devices and distribution system theory. It comprises a literature assessment of previous discoveries

related to power quality in the distribution system, particularly power loss reduction and distribution line voltage profile enhancement.

The third chapter presents the case study area, required data, data analysis, and optimization method. Chapter Four presents simulation findings and a cost-benefit analysis on the best Distribution Static Compensator size and allocation on the ECG 33 kV distribution system before and after DSTATCOM. Chapter five covered the thesis's conclusion and suggestions.

CHAPTER TWO

LITERATURE REVIEW

2.1. Electrical Distribution System

Electric power systems consist of generation, transmission, and distribution systems. Power plants are positioned far from end-users to generate electricity due to environmental effects (Abebe Bikila, 2021). Transmission lines play a crucial role in the transfer of substantial quantities of electrical energy from power generation sources to distribution substations. These high-capacity lines serve as the vital conduits through which electricity is transmitted over long distances with minimal losses. By efficiently transporting the power generated at various plants, transmission lines enable the energy to reach its intended destinations, ensuring a reliable and consistent supply. This infrastructure forms the backbone of the electrical grid, facilitating the interconnection and integration of diverse power sources, including renewable energy installations and conventional power plants.

The distribution system consists of both primary and secondary networks (Campbell Richard J., 2012). The primary distribution system receives power from the transmission substations, while the secondary distribution system delivers electricity to low voltage (LV) transformers serving customers. Ultimately, the distribution network distributes electricity to a wide range of residential, commercial, and industrial users. Through the use of low voltage transformers, the distribution network ensures that the voltage is reduced to a suitable level for residential consumption. A distribution network caters to both small and large consumers, ensuring that energy demand, efficiency, and power quality are met (Dan York, Grace Relf, & Corri Waters, 2019). Figure 2.1 shows a diagram of distribution system.

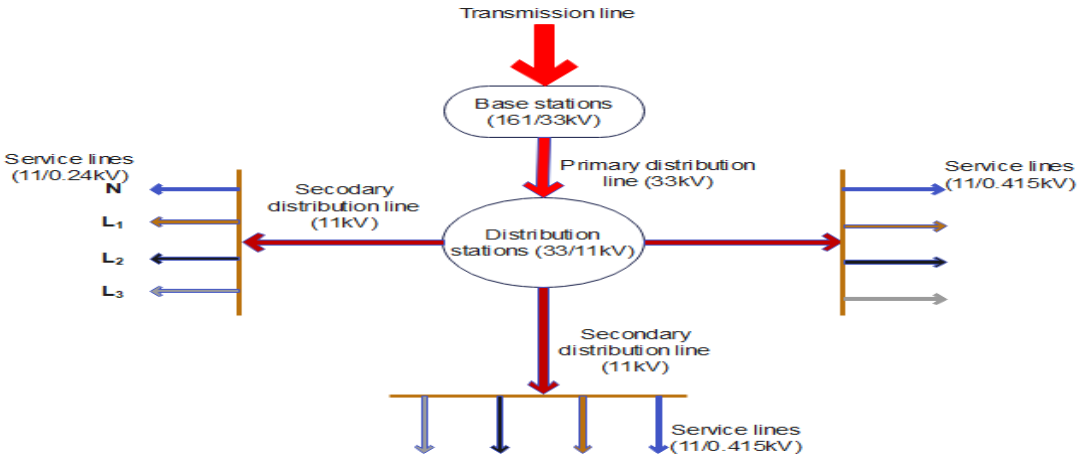

Figure 2. 1, A simple diagram of distribution system

The prominent components of the electrical distribution system include service lines, secondary distribution, and primary distribution. These elements play crucial roles in delivering electricity from the distribution substations to end-users efficiently and reliably. Service lines are responsible for directly connecting individual customers to the distribution network, providing electricity at their premises. Secondary distribution networks function as intermediaries, transporting electricity from the primary distribution system to various distribution transformers and further branching out to reach a larger number of consumers. The primary distribution system forms the foundation of the distribution network, receiving electricity from the transmission system and distributing it to the secondary distribution networks. These components collectively ensure the effective delivery of electricity to residential, commercial, and industrial users, meeting their diverse energy needs.

2.1.1. Classification of Distribution System

The classification of distribution systems provides a framework for understanding their characteristics, challenges, and design considerations. It helps in planning, designing, and operating distribution networks effectively to meet the diverse energy needs of consumers in

different settings. Figure 2.2 and 2.3 below shows the classification and radial distribution system respectively.

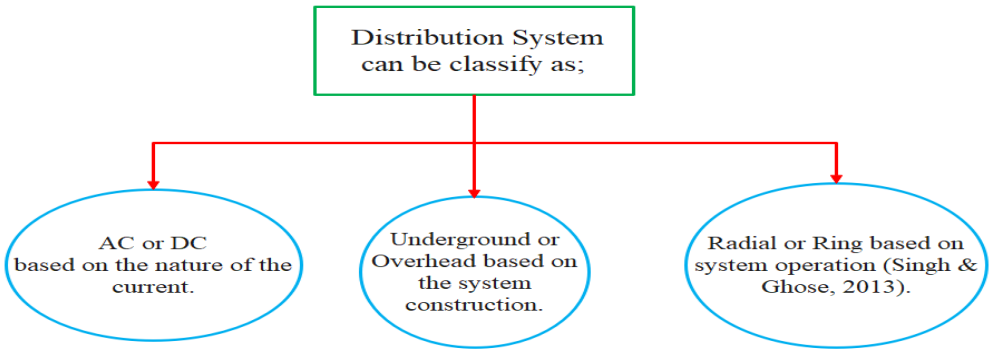

Figure 2. 2, Classification of distribution system

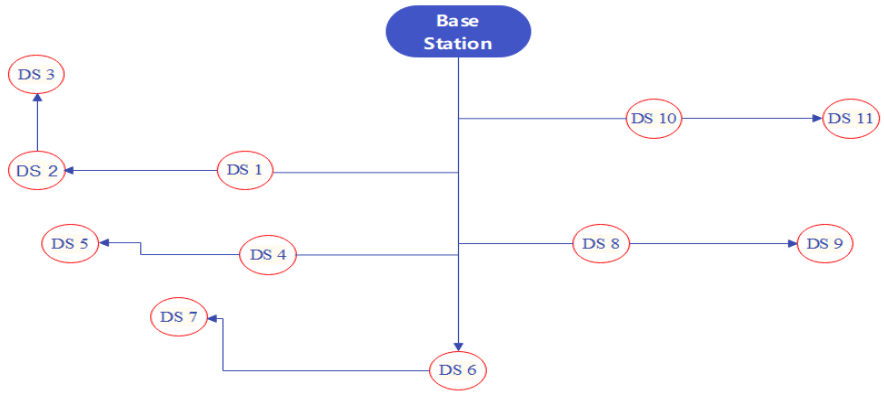

Figure 2. 3, Simple diagram of Radial distribution system.

2.1.2. Distribution System Power Loss and Voltage Drop

The distribution system needs a cost-effective system that distributes electrical energy at a minimum voltage drop and power loss. Technical and non-technical losses plague electrical power distribution networks. The energy distribution process is affected by technical losses, such as copper loss in the cable, transformer, switches, and generators. The customer service process causes non-technical losses, including erroneous meter activity and utility worker-assisted illegal use. Voltage drops and power losses occur due to the resistance and reactance of overhead cables in distribution systems. To mitigate these issues and enhance system

performance, various strategies can be employed, including network reconfiguration, the integration of Distributed Generation (DG), the installation of capacitors, and the use of Flexible AC Transmission System (FACTS) devices. These measures aim to minimize power losses and voltage drops, ensuring efficient power delivery throughout the distribution network.

2.1.2.1. Technical Losses

It is understood that electricity system losses negatively impact the economy. It is well known that not all energy delivered to a distribution system reaches the end-user. Most power sector technical and non-technical losses occur in the distribution system. (Chauhan & Rajvanshi, 2013).

Physical parts of the equipment in the power system are what cause technical losses in the power system. Technical losses are losses caused by internal power system activities and are commonly caused by power dissipation in electrical system components such as distribution lines, power transformers, power switches, measuring equipment, etc. If the power system contains known quantities of loads, technical losses can be computed and regulated. Technical losses that occur during transmission and distribution include substation, transformer, and feeder losses. Main feeder resistive losses, distribution transformer losses (resistive losses in windings and core losses), secondary network resistive losses, service drop resistive losses, and kWh meter losses are examples of technical losses.

Fundamental losses are inevitable in power delivery. Technical losses are caused by current flowing across an electrical network, including the I^2R losses inherent in all inductors due to conductors' finite resistance. Dielectric losses are caused by the heating of the dielectric material that separates conductors. The electromagnetic fields that surround conductors cause induction and radiation losses. In extreme weather conditions, improper functioning of distribution feeders may put the entire neighbourhood at risk because these wires may spark

and start a fire. Line losses in both primary and secondary feeders may occur in the distribution system. The square of the current traveling through the line's resistance (R) and reactance (X) determines the line losses:

$$P_{loss} = \sum_{ab=1}^{n} (i_{ab}^2 R_{ab}) \quad (2.1)$$

$$Q_{loss} = \sum_{ab=1}^{n} (i_{ab}^2 X_{ab}) \quad (2.2)$$

Where, P_{loss} is total active power loss, Q_{loss} is total reactive power loss, i_{ab} is branch current flowing from bus a to bus b, R_{ab} is line resistance between bus a and bus b and X_{ab} is line reactance between bus a and bus b.

2.1.2.2. Voltage Drop in a Distribution System

Distribution lines or electric circuits should have the same receiving and sending end voltages. In the real situation, sending and receiving voltages are usually different. The conducting devices' resistance and impedance produce voltage changes down the line.

Distribution system resistance and reactance reduce voltage. Despite the fact that all utility system equipment is designed for a specific function, it is practically impossible to offer each client with the same voltage (Alessandro Bosisio, Alberto Berizzi, Edoardo Amaldi, Cristian Bovo & Xu Andy Sun, 2020). Figure 2.4 simplifies distribution system voltage drop.

$$S = P_l + jQ_l \quad (2.3)$$

$$I = \left[\frac{S}{V_b}\right] = \frac{P_l + jQ_l}{V_b} \quad (2.4)$$

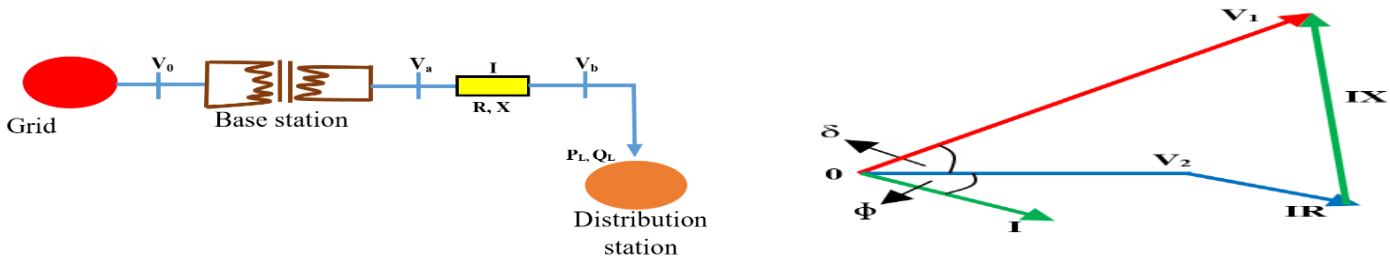

(a) (b)

Figure 2.4, A single line diagram (a) and a related phasor diagram (b) of voltage drop in a distribution system.

The voltage loss on the feeder is determined in the following manner:

$$V_a - V_b = I(R + jX) = IR\cos\theta + IX\sin\theta = RP_l + XQ_l - \frac{jXP_l - RQ_l}{V_b} \quad (2.5)$$

$$\Delta V = [V_a - V_b] \quad (2.6)$$

Where, **I** is Current through the Primary distribution lines, **θ** is Power-factor angle, **R** is Resistance of the feeder, **X** is Reactance of the feeder, $\mathbf{V_a}$ is sending end voltage, $\mathbf{V_b}$ is receiving end voltage, $\boldsymbol{P_l}$ is active load power, $\boldsymbol{Q_l}$ is reactive load power, **S** is apparent power, and $\Delta\boldsymbol{V}$ is the voltage drop.

As indicated by Equations (2.5) and (2.6), voltage drops typically occur on the load side, leading to a decrease in the voltage profile toward the end. These voltage drops and profiles play a crucial role in the regulation of voltage in distribution networks (Min-Hung Chou, Chun-Lien Su, Yung-Chi Lee, Hai-Ming Chin, Giuseppe Parise & Chavdarian P. B., 2017).

2.1.3. Performance Improvement of Distribution System

A distribution line losses and voltage variation can be reduced using several methods (Joel Egwaile, Kingsley Ogbeide & Austin Osahenvemwen, 2018). Power loss and voltage drop reduction

can be done by using network re-conducting (conductor grading), network reconfiguration, optimal distribution transformer location and sizing, highly effective transformers, high voltage distribution systems, distributed generation, building new substations and reactive power compensation.

2.1.3.1. Reactive Power Compensation

Reactive power compensation in the transmission and distribution system has several benefits, such as changing the voltage profile, increasing power flow capacity (by lowering feeder impedance), increasing system capacity (by controlling reactive power flow with capacitors), and reducing power losses (Abouzar Samimi, 2019). Reactive power compensation is a good way to improve the voltage profile and cut down losses when the size and location of the DSTATCOM are optimal. By putting in reactive compensating equipment like Flexible AC Transmission System (FACTS), the voltage profile can be stabilized.

Flexible AC Transmission System (FACTS) devices are advanced power electronic devices used in electrical power systems to enhance system stability. These devices are designed to regulate and control voltage, reactive power, and impedance in AC transmission and distribution systems. Reactive compensation devices are used to provide or absorb reactive power to maintain reactive power balance. FACTS devices are used for power flow management, enhanced distribution capabilities, voltage control, reactive power compensation, stability enhancement, power quality improvement, power conditioning, flicker abatement, renewable and distributed generation, and storage connections (Nasiru B. Kadandani & Yusuf A. Maiwada, 2018; Utkarsh Patel, 2012).

FACT's device can be built on thyristors, such as the Static VAr-compensator and the Thyristor Controlled Series Compensator (TCSC), or voltage source converters, such as the Static

Synchronous Series Compensator (SSSC), STATCOM, UPFC, and IPFC (Shobana S., Tamil Selvi K., Abirami P., Pushpavalli M. & Sivagami P., 2019). FACTS controllers interact with the power system in four ways: Series, Shunt, Series-Series, and Series-Shunt combinations (Abdulrazzaq, 2015; Sharad Chandra Rajpoot, Prashant Singh Rajpoot, Kishan Gupta & Rewati Raman Yadav, 2017).

2.1.3.2. FACTS Controllers in a Series

Series compensators use capacitors to reduce the equivalent reactance of a power line at rated frequency, raise load terminal voltage, and inject voltage in series with the line. Series controllers only produce or consume variable reactive power since the voltage and line current are in phase quadrature (Abebe Bikila, 2021; Alam et al., 2010). The most common series compensators are Static Synchronous Series Compensator (SSSC), Thyristor-Controlled Series Compensation (TCSC).

2.1.3.3. FACTS Controllers in a Shunt

Capacitors and reactors are shunt controllers that inject variable current into the line. As long as the injected current is in phase quadrature with the line voltage, the shunt Controllers only supply or consume variable reactive power (Abebe Bikila, 2021; Ismail et al., 2020). Shunt compensators include the SVC, SSG, TCR, and SVC (DSTATCOM). Distribution system shunt compensators serve these purposes:

i. To compensate for low load power factor, the source current would have a power factor close to unity. Harmonic suppression generates a sinusoidal source current from loads.
ii. To regulate loads that fluctuate supply voltage.

2.1.3.4. FACTS Controllers in Series-Series Combination

FACTS Controllers in Series-Series Combination, also known as Thyristor-Controlled Series Compensators (TCSCs) and they are static power controllers that are connected in series with a transmission line. They are designed to control the power flow along the line by injecting a variable impedance into the line. TCSCs are primarily used to improve the power transfer capability of a transmission line. TCSCs reduce the impedance of a transmission line by injecting a negative reactance into the line. This can increase the power flow through the line without causing voltage instability. They also help to increase voltage stability during periods of high load by injecting a positive reactance into the line (Abebe Bikila, 2021; Kadandani et al., 2018).

2.1.3.5. FACTS Controllers with a Series-Shunt Combination

Series-Shunt FACTS features, also known as Unified Power Flow Controllers (UPFCs), represent advanced static power controllers. They offer comprehensive control over real, reactive, and voltage parameters in a transmission line, regulating real power flow by adjusting series voltage or shunt current. UPFCs play a key role in damping oscillations, enhancing power system stability. Series-connected FACTS controllers manage voltage and power flow, injecting voltage to boost or buck at the receiving end, ensuring voltage stability during varying loads. Shunt-connected FACTS controllers focus on controlling reactive power flow, injecting current to absorb or generate reactive power, thereby preventing voltage fluctuations and improving overall system stability (Abebe Bikila, 2021; Kadandani et al., 2018).

2.1.3.6. Application of FACTS Devices

FACTS devices are a powerful tool for improving the performance of power systems. Their utilization spans a broad spectrum, encompassing tasks such as voltage control, power flow

optimization, grid stability improvement. With innovative solutions, FACTS devices adeptly tackle the dynamic challenges faced by contemporary power systems, making substantial contributions to the establishment of a more dependable, efficient, and sustainable electrical infrastructure. Table 2.1 offers an in-depth examination of the applications and functions of FACTS devices (Georgilakis & Vernados, 2011; Rajpoot et al., 2017).

Table 2. 1, Application of FACTS devices

Subject	Problem	Corrective action	Convention solution	FACTS devices
Voltage limit	Low voltage when a heavy load is applied	Supply reactive power	Shunt capacitor Series capacitor	SVC (DSTATCOM), TCSC
	High voltage at light load	Absorb reactive power	Switch EHV line and shunt capacitor	SVC (DSTATCOM), TCSC
	High voltage	Absorb reactive power	Add shunt reactor	SVC (DSTATCOM)
	Low voltage	Supply reactive power or prevent overload	Switch shunt capacitor, shunt reactor, series capacitor	SVC (DSTATCOM)
	Low voltage and overload	Supply reactive power and limit burden	Combination of more devices	DSTATCOM, UPFC, TCSC, SVC
Thermal limit	Line or transformer overload	Reduce overload	Add line or transformer or add series reactor	SVC, TCSC
	Tripping of parallel circuit (line)	Limit circuit (line) loading.	Add series reactor and capacitor	UPFC, TCSC

2.2. The Selected Compensative device

Voltage drops, power losses, and network instability pose challenges in radial distribution systems. Addressing these issues requires the incorporation of equipment that can mitigate these drawbacks to meet the load demand. To address power quality issues in distribution systems, reactive power injection is an effective solution. This is where Distribution Static Compensators (DSTATCOMs) play a crucial role, offering advantages such as low power losses, minimal harmonic output, automatic operation, strong regulatory capabilities, compact size, and cost-effectiveness. Distribution Static Compensator does not cause resonance or

harmonic distortion (Alam et al., 2010; Devabalaji et al., 2018; Mohsin Mahmood, Om Shivam, Pankaj Kumar & Gopal Krishnan, 2014; Stanelyte & Radziukynas, 2019). The DSTATCOM device enhances voltage regulation, voltage balancing, power factor collection, harmonics minimization, and power losses (Mahmood et al., 2014).

2.2.1. Distribution Static Compensator (DSTATCOM)

Distribution Static Compensator (DSTATCOM) is a type of Flexible AC Transmission System (FACTS) device used in power distribution systems. It is designed to improve the quality and efficiency of electrical power by compensating for reactive power and minimizing voltage fluctuations (Alam et al., 2010). Due to the excessive demand for power in radial distribution systems, the implementation of DSTATCOM becomes indispensable (Aadesh Kumar Arya1, Ashwani Kumar1 & Saurabh Chanana, 2019; Cholapandian V., Yuvaraj T. & Devabalaji K. R., 2018; Rukmani et al., 2020). Distribution Static Compensator (DSTATCOM) device control power flow and increase electrical power network transient stability.

In dense loading conditions, DSTATCOM injects or supplies the current needed to enhance the voltage profile at the load bus where it is connected and regulate it to appropriate reference levels. DSTATCOM's storage capacity prevents lengthy reactive power injection. As the synchronous voltage source, DSTATCOM controls and corrects bus voltages and power factor. DSTATCOM lowers voltage fluctuations by comparing the line waveform to the reference signal and injecting or absorbing reactive current to correct the inaccuracy. Figure 2.5 depicts DSTATCOM incorporated into system bus (Oloulade A., Moukengue Imano A., Viannou A. & Tamadaho H., 2018).

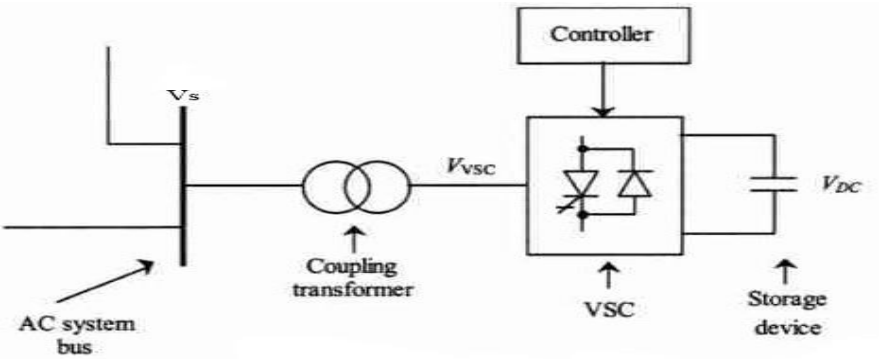

Figure 2.5, DSTATCOM connected to system bus (Oloulade et al., 2018).

2.2.1.1. Components of DSTATCOM

The DSTATCOM has a three-phase inverter (usually a PWM inverter using SCR, MOSFET, or IGBET), D.C capacitor to supply D.C voltages, link reactor to connect the inverter output to the AC supply, and filter to smooth out the high frequency caused by the PWM inverter. The DC side capacitor powers the inverter's three-phase voltage. The capacitor bank supplies a constant DC voltage that is transformed to three-phase AC. The radial distribution system's coupling transformer receives AC output voltage. Link reactors connect device voltage to AC voltage (Egwaile et al., 2018).

2.2.1.2. Operation of DSTATCOM

The DSTATCOM measures all voltages and currents in the AC power network where the voltage instability occurred and feeds them to the controller for comparison with reference orders. After feedback control, the controller sends switching signals to the power converter's primary semiconductor switches. DSTATCOM acts as an inductor and absorbs reactive power if the AC voltage magnitude (Vs) is greater than the Voltage Source Converter (VSC). DSTATCOM injects reactive power into the system as a variable capacitor if the AC voltage magnitude (Vs) is less than the magnitude of a Voltage Source Converter. The DSTATCOM activates no-load mode if VSC and Vs are equal (Hota et al., 2021; Reddy et al., 2012; Salkuti, 2021a). Figure 2.6 shows the operation modes.

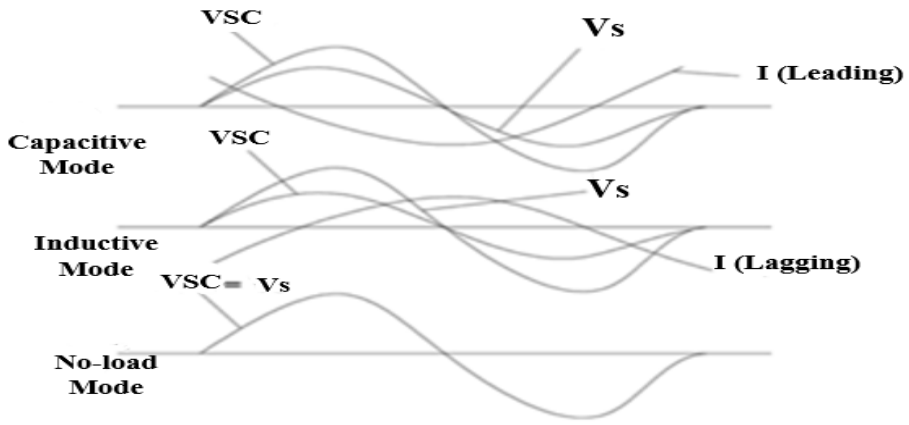

Figure 2.6, Operation mode of DSTATCOM (Salkuti, 2021)

2.3. Power Flow Methods for Radial Distribution System

Power flow analyses are crucial for the advancement and optimization of power systems, offering valuable insights into system behaviour and performance. Given the non-linear nature of load flow, addressing it requires iterative methods such as Gauss-Siedel, Newton-Raphson, Fast decoupling, and Backward/Forward Sweep (Murari & Padhy, 2020).

2.3.1. Backward/Forward Sweep Algorithm (BFS)

BFS Load flow method was considered among the other load flow methods due to its speed, convergence, simplicity, inexpensive memory, less computational power, and solution accuracy (Abebe Bikila, 2021; Lata & Vadhera, 2020; Limei Zhang, Yongfu Liu, Penghui Zhang, Wei Tang, Jing Lv, Lu Zhang & Dongming Li, 2017).

This research uses the convergence-potential Backward/Forward Sweep. BFS is tested under various loading situations, including R/X ratios, quick, simple, and static load on algorithm convergence characteristics, to produce exact results throughout the process (Bakhshideh Zad B., Hasanvand H., Lobry J. & Vallée F., 2015; Lata & Vadhera, 2020).

2.4. Power System Optimization Methods

In the field of power system engineering, optimization enhances operational dependability while also increasing system security and cost savings. Power systems have become enormous and complex, which means that in order to handle power system difficulties, optimization algorithms that consider a variety of fundamental limits are required.

2.4.1. Particle Swarm Optimization (PSO)

In 1995, Kennedy and Eberhart came up with the idea of using a meta-heuristic population-based optimization approach that called "Particle Swarm Optimization." PSO was developed to optimize nonlinear problems, and it was modelled by the social behaviour of several species of animal communities (Okwu & Tartibu, 2021). Each individual animal was referred to as a particle or agent, and collectively, the creatures were referred to as a population or swarm (Abebe Bikila, 2021).

The PSO optimization is based on the idea of simulating the movement of a group of individual animals to find the best solution to a mathematical problem, similar to how birds or fish search for food in a large space either dispersed or together. This is accomplished by simulating the movement of a group of individuals to find the optimal solution (Okwu & Tartibu, 2021).

The objective function is what decides the level of fitness possessed by each individual particle. This method is modelled after the behaviour of birds flocking together or fish schooling, which is an iterative search approach in which particles move across a broad area of search space based on the objective function. This concept forms the basis of this algorithm. Each particle investigates the entirety of the space by travelling in unpredictable ways while keeping track of the positions of its neighbouring particles and the best solutions it has discovered in the past based on its own experiences. The swarm shares information about its most advantageous

places depending on the dynamic changes in their location and speed (Kumarasundari P. & Sujatha Balaraman, 2019; Okwu & Tartibu, 2021).

2.5. Overview of Ghana's Electricity

Electricity is one of the most essential factors that determines the level of economic prosperity in each nation. It is essential to the day-to-day operations of every sector, from the domestic to the commercial to the industrial (Kumi, 2017; Oyedepo, 2012).

Electricity is essential for the growth of every area of a nation's economy, including but not limited to the following: education, quality healthcare, transportation, communication, mineral extraction, and serving as the foundation for economic development. It is possible to trace the origins of Ghana's power industry all the way back to the days when the Gold Coast was under colonial rule. During this time, the majority of the nation's energy needs were met by solitary diesel generator facilities. Most of these networks were owned by commercial enterprises like mines and factories, as well as municipal governments and other institutions like hospitals and schools (Kumi, 2017).

In 1914, the Gold Coast Railway Administration established the first public energy generation system in Sekondi to generate electricity for the activities of the railway sector. This was done to meet the needs of the railway sector. This was expanded to include Takoradi in the year 1928. On the other hand, in 1947 the Public Works Department and the Railways Administration handed over responsibility for the provision of power to the Electrical Department that was established by the Ministry of Works and Housing. During that time, diesel generator plants were the most common method for producing power. By the year 1955, the Public Works Department (PWD) of Ghana had successfully brought electricity to a few of the country's most significant cities, including Kumasi, Tema, Accra, Nsawam, Tamale, and Bolgatanga (Kumi, 2017).

The Akosombo Dam Project, which was finished in 1961 was responsible for providing a total capacity of 912 MW power (Kumi, 2017; VRA, n.d.). Even while the provision of energy for the aluminium sector was the primary objective of the project (VALCO), it also made it possible to switch from using diesel generators to using hydroelectricity to produce most of the electricity that was used.

The Volta Aluminium Company (VALCO) and the National Electricity Distribution Company (now called ECG) were the two companies that consumed the most electricity during this period. The Kpong Hydroelectric Power Station was finished in 1982, which added 160 MW to the total installed capacity of the producing facilities (Kumi, 2017). In 1984, Ghana encountered its initial electricity crisis despite an increased in its generation capacity. This was as a result of a severe drought that took place from 1982 to 1984, during this time the total inflow into the Akosombo Dam was less than 15% of what the long-term average would have been (Kumi, 2017). As a direct response to the crisis, Ghana's generating mix was augmented with the addition of thermal power plants.

The initial 550 MW facility of these thermal plants was located at the Takoradi Thermal Plant, which is operated by VRA (Tapco and Tico). At the close of the year 2015, Ghana's total installed capacity of thermal power plants reached 2,053 megawatts (MW) (Energy Commission, 2016; Kumi, 2017). The lack of reliable access to electrical power has permeated nearly every aspect of daily life in Ghana, leading to the invention of word "Dumsor" to describe the situation. The 400 MW Bui Hydroelectric Power Station was commissioned in December 2013 to provide power to sustain the peak load of the country, which has been consistently increasing over the previous few years (Energy Commission, 2016; Kumi, 2017).

Throughout the course of the last decade, Ghana's energy industry has been afflicted with problems related to power production, which has had a substantial impact on the country's

economic status. According to estimates provided by the World Bank, Ghana's economy lost 1.8% of its GDP due to a lack of electricity in 2007, which was ranked as the country's second most severe impediment to commercial activity (Kumi, 2017).

The National Electrification Scheme was founded in 1989, marking the beginning of Ghana's commitment to fulfil its goal of providing universal access to electricity by the year 2020 (Kumi, 2017; MoP, 2005). By a margin of 5%, Ghana did not meet its target of attaining universal access to electricity by the year 2020. If certain efforts are not done to accelerate the process, achieving universal access will not be possible (Kumi, 2017).

The World Bank-funded Ghana Energy Development and Access Project (GEDAP) began in 2007 to reduce distribution network losses, increase distribution system capacity, and increase access to electricity by introducing renewable energy (Kumi, 2017). Remember that having access to power means more than just being connected to the grid. It also means having a reliable, inexpensive supply of electricity (Gifty Serwaa Mensah, Francis Kemausuor & Abeeku Brew-Hammond, 2014). Ghana's power industry appears to be having power supply issues, which could impede universal access. Ghana had large power outages in 1983–1984, 1997–1998, 2003, 2006–2007, and 2011–present (Kumi, 2017; Serwaa Mensah et al., 2014). The distribution of electrical power in Ghana relies on a radial network, which is facing challenges in meeting the increasing load demands of the nation as it continues to grow. This situation necessitates improvements and upgrades to the distribution system to ensure reliable and efficient power supply.

2.5.1. ECG Distribution system in Ashanti Region, Ghana

Ghana is equipped with several of 33 kV distribution stations, the primary function of it, is to deliver electrical power to various regions in the country. Ashanti region is one of the sixteen (16) regions found in Ghana to receive electric power supply from ECG. Ashanti region is

placed at the geographical coordinates of 6.7470° North and 1.5209° West. Ashanti region is allocated in the south part of Ghana, West Africa. The Ashanti region is equipped with twenty-one (21) 33 kV distribution stations and a variety of protection devices. These protection devices include the current transformer, the voltage transformer, the circuit breaker, the bus bar, the earthling transformer, the surge arrester, the grounding, control systems and protection panel. Some of these protection devices can function automatically while others can be operated manually.

The Electricity Company of Ghana (ECG) operates two (02) base stations (Awomaso and Ridge) in the Ashanti Region, each receiving 161 kV from Ghana transmission company (GridCo). The two base stations provide a 33 kV distribution lines to the twenty-one (21) distribution stations within the region. The 33 kV distribution network in region has 50 buses. The Electricity Company of Ghana does not make use of any compensating equipment that provide reactive power in order to make up for severe voltage reductions and power losses. As a consequence of this, the objective of this thesis is to conduct research into the ECG 33 kV distribution network in order to improve the effectiveness and standard of power-driven systems in the Ashanti region of Ghana.

2.6. Related Research Studies

Numerous researchers are currently implementing a variety of strategies, such as distributed generation, network reconfiguration, synchronous condenser, and capacitor banks, to improve the effectiveness of distribution networks and find a solution to the issue of poor power quality that is caused by power distribution networks.

The following are review of the various pieces of published research on the incorporation of compensators on distribution networks. (Balamurugan et al., 2018) detail how to improve the performance of a distribution system by employing the Whale Optimization technique to

determine the optimal location and sizes for a DSTATCOM device. The objective of the work was to reduce total power losses. The voltage stability index was utilized to ascertain the optimal placement of the DSTATCOM while Whale Optimization method was utilized in order to ascertain the ideal size for the DSTATCOM. The proposed work has been evaluated in India using a standard IEEE 69-bus distribution system as well as a radial distribution system with 28 buses.

Devabalaji et al., 2018 propose a bio-inspired Cuckoo Search Algorithm (CSA) for radial distribution networks with distributed generation and distribution static compensator. The suggested method assigns DG and DSTATCOM using the voltage stability index and loss sensitivity factor. CSA determines radial distribution network DG and DSTATCOM sizes. This article calculates load flow using the BFS algorithm. The method reduces power losses and boosts bus voltages. The proposed mechanism is tested on a famous IEEE 33-bus and a massive 136-bus (Devabalaji et al., 2018).

Prasad et al., 2020 describes a two-stage fuzzy and Shuffled Frog Leaping Algorithm (SFLA) for DSTATCOM placement in distribution networks. Power loss and voltage profile are the major goals. Frog prey behaviour inspired the SFLA meta-heuristic search approach. The SFLA uses metaheuristic shuffling for global information interchange and frog leaping for local search. Fuzzy determines the ideal DSTATCOM placement, while SFLA determines the size. The proposed method has been tested on IEEE 15-bus, 33-bus, and 69-bus systems (Ambika Prasad Hota, Sivkumar Mishra, Debani Prasad Mishra & Surender Reddy Salkuti, 2020).

Amin et al., 2019 presented an efficient hybrid Analytical Coyote Optimization technique for discovering the ideal placement and sizing of DSTATCOM in the radial distribution system to minimize active power loss and improve voltage profiles while remaining operationally

constrained. The coyote optimization approach is used to establish the optimal allocation of DSTATCOM in the distribution system, while analytical techniques are used to estimate the ideal size of DSTATCOM. The proposed method has been validated using the IEEE 33 and 69 bus systems (Amal Amin, Salah Kamel, Ali Selim & Loai Nasrat, 2019).

A new technique for appropriate size and position of distributed generation and distributed static compensator in radial distribution systems was developed to reduce real power losses and improve voltage profile. The loss sensitivity factor and voltage stability index indicate the appropriate placement for DG and DSTATCOM, respectively. The Artificial Fish Swarm Optimization Algorithm (AFSOA) calculates distributed generation and static compensator sizes. A conventional IEEE 33 and 69 bus radial distribution system (RDS) were tested the proposed approach (Salkuti, 2021).

Thangaraj & Kuppan, 2017 proposed a new approach for radial distribution network DG and DSTATCOM placement. The proposed work reduces power loss, under-voltage, and voltage stability index within limits. Lightning Search Algorithm (LSA) solved the multi-objective function. The approach moved user loads linearly from light to heavy with a 1% phase size. LSA sizes DSTATCOMs and DGs for each load phase. Two test systems, IEEE 33-bus and 69-bus were used (Thangaraj & Kuppan, 2017).

Kumarasundari & Balaraman, 2008 develops a mechanism to reduce losses and improve voltage profiles in an active radial distribution network. Estimating the DG's optimal position uses the Decouple Load Flow (DLF) approach and the loss sensitivity factor with voltage variance. To maintain a steady bus voltage profile, DSTATCOM is strategically located in the system network to deliver reactive power. The suggested solution is validated using MATLAB simulation of an IEEE 69-bus radial distribution network (Kumarasundari & Balaraman, 2008).

Arya et al., 2019 recommended locating and scaling DSTATCOM in the distribution system to improve performance. Reducing system losses and improving power quality are the main objectives. The Gravitational Search Method, a new algorithm, locates devices for power loss reduction, voltage profile improvement, and annual energy savings for the distribution operator. A Forward/Backward algorithm calculates load flow analysis. The suggested system was tested using IEEE 33 and IEEE 69 bus systems (Arya et al., 2019).

Fuzzy and PSO enhanced distribution network voltage profiles and power losses reduction. The researcher reduced power losses and improved voltage profile by optimizing 25 DSTATCOM position and sizing. IEEE 33-bus and IEEE 69-bus were tested the technique. The four best areas for power loss and voltages are prioritized. This article includes overloads of 125, 150, and 175 percent (Ali & Devi, 2015).

Yuvaraj et al., 2015 used a Harmonic Search Technique to find DSTATCOM's placement and dimensions. Optimization functions include power loss minimization. Work was tested on the IEEE 33-bus system. It analyses load flow using a direct bus injection to branch current (BIBC) matrix. Before and after DSTATCOM installation, the suggested study compares RDS yearly total loss. 28.97% and 28.67% reductions were achieved in active and reactive power losses (Yuvaraja T., Devabalajia K.R. & Ravi K., 2015).

Rukmani et al., 2020 suggested a bio-inspired Cuckoo Search Algorithm (CSA) approach to allocate the DSTATCOM in a radial distribution system (RDS) to minimize power loss and improve voltage profile. This study uses the loss sensitivity factor to determine device placement and the CSA algorithm to calculate DSTATCOM size. Load flow analysis uses the efficient backward/forward method, and the work was tested on the IEEE 33-bus and 69-bus system (Rukmani et al., 2020).

2.7. Summary and Research Gaps

According to the literature review above, an optimization algorithm can allocate and size DFACTs devices in the distribution network to reduce system losses and optimize the radial distribution network voltage profile. To solve the distribution network's power quality issue, researchers have focused on compensating devices using optimization methods. DSTATCOM placement maximizes load capability, power loss reduction, voltage stability enhancement, and power performance improvement. Incorrect allocation may limit advantages and endanger system performance.

Nevertheless, electric utilities face a challenge in determining the most suitable location and size of devices, which can potentially lead to increased power loss and a deteriorated voltage profile. Regrettably, certain researchers have neglected to consider these crucial aspects while addressing the issue. Evaluations related to real and reactive power, voltage profile, and cost. Moreover, some optimization strategies employed by researchers exhibit long simulation times and insufficient convergence, which have not been duly considered in solving the problem.

All the researchers evaluated their methods on the IEEE distribution system; hence their conclusions are not applicable to real-world distribution system applications. This thesis optimally located and sized the capacitor bank (DSTATCOM) using Particle Swarm Optimization (PSO). Real power loss, reactive power loss, voltage profile, and energy cost were considered in this research.

In this Research, the effective load flow analysis approach (Backward/Forward Sweep), which is better for radial distribution systems, was used. The DSTATCOM, which affects the distribution network as a reactive power compensator, has been installed. The work for the research was centred on an active radial distribution network known as the ECG 33 kV

distribution network. This network is currently responsible for providing customers in the Ashanti region of Ghana with electric power.

CHAPTER THREE

MATERIAL AND METHODS

A simulation model technique was used to obtain and evaluate data as well as the solutions needed to fix the issue that was detected on the 33 kV distribution buses. This was done to accomplish the objectives of the thesis and bring it closer to completion. The information gathered included the quantity of active and reactive power that was present on the buses, as well as the length of the network impedance (resistance and reactance) for each segment.

Case study was done on the fifty distribution buses on the Electricity Company of Ghana (ECG) 33 kV distribution network. The thesis stared at load flow analysis to look at how an existing system works and optimization techniques for locating and sizing the appropriate reactive power compensation device.

3.1. Data Collection

The ECG 33 kV distribution network is configured in a ring in some parts but operates in a radial system. The researcher gathered 33 kV distribution network data from ECG with the assistance of two ECG control engineers and substation technicians. The data covers a picture of the network line diagram with its parameters, power demand in each substation, and system bus voltages. The data collected from ECG are presented in Appendix I, II & III. The Electrical Transient Analyzer Program (ETAP) was used to model the Ashanti Region's 33 kV distribution network based on the data collected and Figure 3.1 below shows the model network. Line and bus data were extracted from ETAP, and the MATLAB program was also used as a platform for Particle Swarm Optimization (PSO) to determine the perfect size and location of distribution static compensators (DSTATCOM) in a 33 kV distribution network. The ECG 33

kV distribution network in Ghana's Ashanti region serves as the model network for this research.

3.2. ECG 33 kV Distribution Network in Ashanti Region

The diagram in Figure 3.1 illustrates the ECG 33 kV network in the Ashanti region, comprising fifty (50) bus bars. This includes one (01) main bus bar dedicated to GridCo, eight (08) bus bars serving as base stations (bulk supply points), and forty-one (41) bus bars allocated to Sub-strategic Business Unit (SBU) centers. The network receives power from incoming transmission lines operating at 161 kV, supplying electricity to two base stations. Subsequently, these base stations distribute electric power to nearby 33 kV distribution stations within the region.

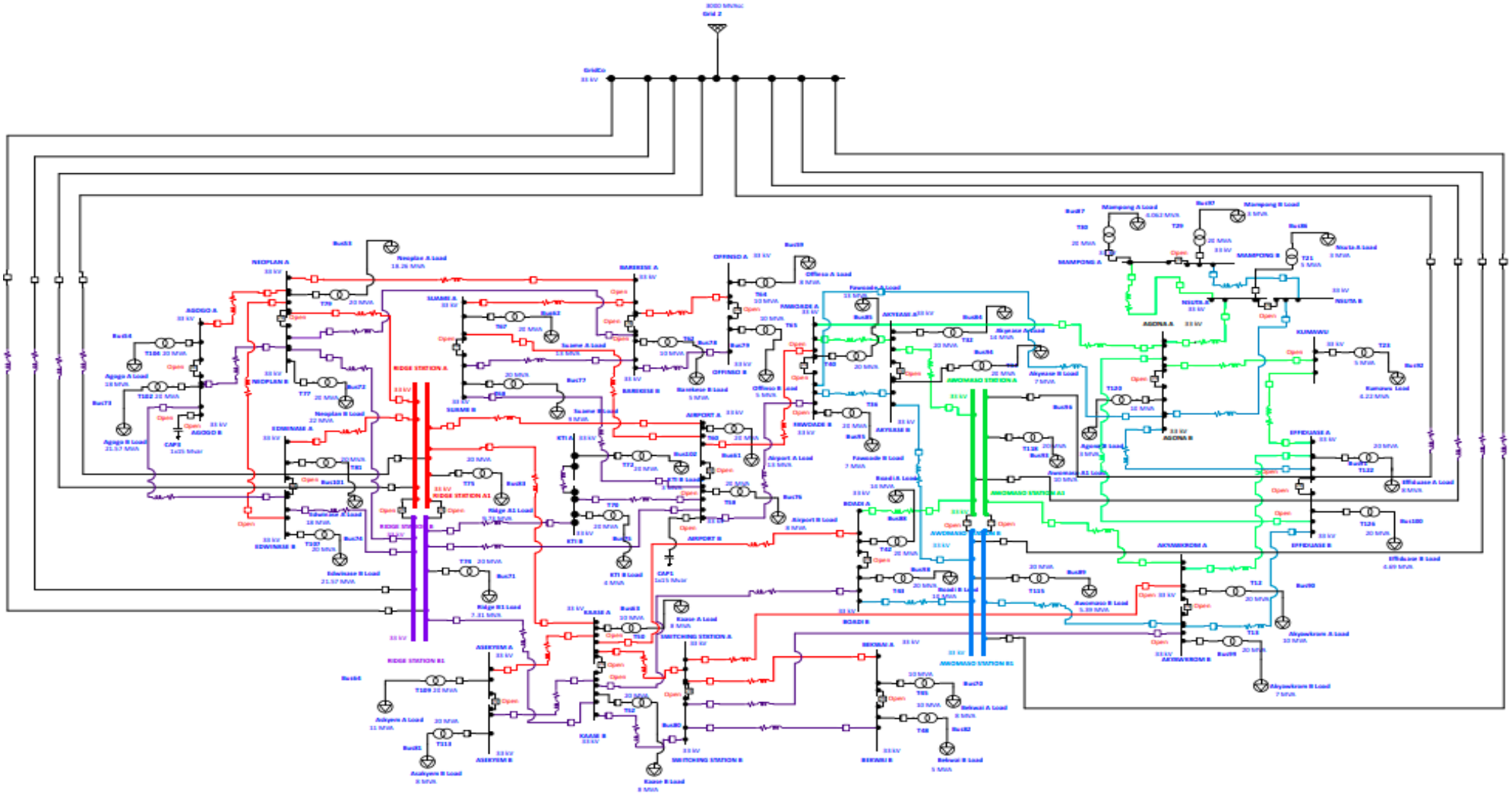

Figure 3. 1, Ashanti region 33 kV primary distribution network

The 33 kV network is interlinked and receives supply from two primary base stations, namely Awomaso and Ridge stations. Each of these base stations is equipped with four supply buses, distributing power to twenty-one distribution stations (SBU) across the region. The Awomaso and Ridge stations receive a high voltage level of 161 kV from the Ghana Grid Company (GridCo). The incoming 161 kV grid lines are connected to the same bus bars in the two base stations. Each base station is equipped with four step-down transformers, each with a capacity of 66 MVA and operating at 161/33 kV. Additionally, the two base stations are interconnected through the twenty-one distribution stations, utilizing outgoing lines with a voltage level of 33 kV. These distribution stations include Neoplan (A & B), Airport (A & B), Kaase (A & B), and others, as illustrated in Figure 3.1.

The secondary transmission lines that distribute electric power to twenty-one primary distribution stations in the region are categorized into different parts such as Abuakwa, Kaase, Airport, KTI, Edwinase, Neoplan, Akyease, Boadi, Offinso, etc. which has 15 outgoing feeders (secondary transmission lines). All outgoing feeders from twenty-one primary distribution stations are operated in a radial system. The bus graph view of the ECG 33kV distribution system is shown in Figure 3.2. The bus graph view shows several buses connected to each other by arrows. The buses represent the different substations buses in the ECG 33 kV distribution network. The arrows represent the network feeders between the buses.

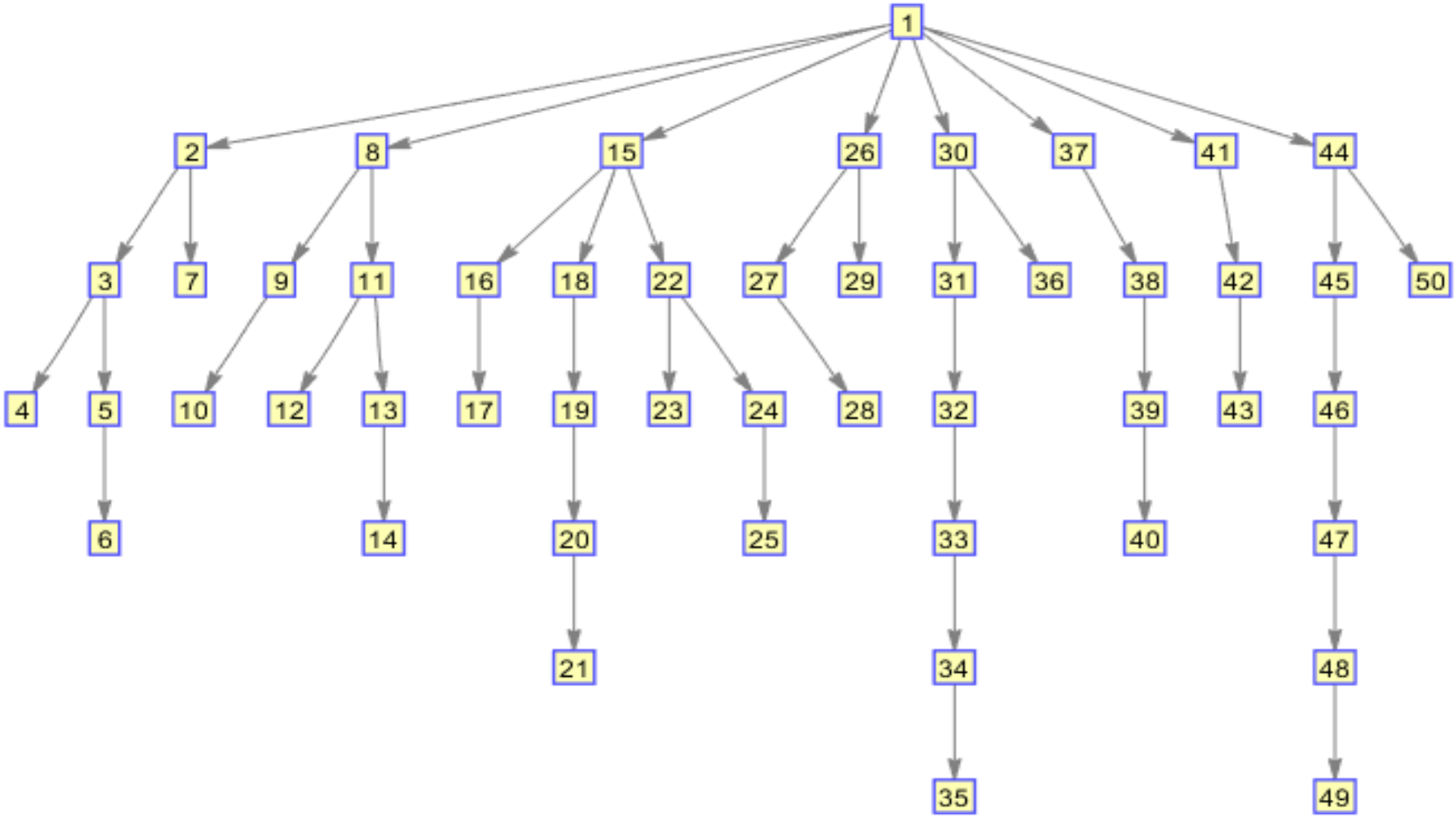

Figure 3.2, Ashanti region 33 kV network bus graph view

Bus 1 represents the GridCo bus that supplies electricity at a voltage of 161 kV to eight base station buses (buses 2, 8, 15, 26, 30, 37, 41, and 44). The base station buses then distribute electricity at a voltage of 33 kV to forty-one other buses in the Ashanti region. The diagram (Figure 3.2) provides a useful overview of the 33 kV distribution network in the Ashanti region. It can be used to understand the flow of electricity in the network, to identify potential bottlenecks, and to plan for future upgrades.

3.2.1. The 33 kV system Layout

The substation centres (SBU) provide the voltage of 33 kV, 11 kV, 0.415 kV and 0.24 kV to a variety of consumers, including residential, commercial, and industrial loads. There are no separate feeders for industrial, commercial, or residential use. The following are the list of the substation centres (SBU) as shown in Figure 3.1 above.

- GridCo: the incoming transmission line from Ghana Grid Company with 161 kV voltage level
- Ridge station (A, A1, B, B1) and Awomaso station (A, A1, B, B1): base station buses that supplies power to twenty-one (21) substation centres (SBU) in the region.
- Agogo (A & B): It is distribution station buses which supply power to the Atwima Nwabiagya District of the Ashanti Region via two transformers which rated 20 MVA for each.
- Neoplan (A & B): It is distribution station buses, which supply power to the Kumasi Metropolitan Assembly (Batanma, North Suntreso, South Suntreso, part of Kwadaso etc.) of the Ashanti Region via two transformers, which rated 20 MVA for each.
- Edwinase (A & B): It is distribution station buses which supply power to the Kwadaso Municipal Assembly of the Ashanti Region via two transformers which rated 20 MVA for each.

- Suame (A & B): It is distribution station buses which supply power to the Suame Municipal assembly of the Ashanti Region via two transformers which rated 20 MVA for each.
- Barekese (A & B): It is distribution station buses which supply power to the Atwima Nwabiagya North District of the Ashanti Region via a transformer which rated 10 MVA.
- KTI (A & B): It is distribution station buses, which supply power to the Kumasi Metropolitan Assembly (Amokom, Asafo, Oforikrom, Fante-Newtown etc.) of the Ashanti Region via two transformers, which rated 20 MVA for each.
- Asekyem (A & B): It is distribution station buses, which supply power to the Atwima Kwanwoma district of the Ashanti Region via two transformers, which rated 20 MVA for each.
- Kaase (A & B): It is distribution station buses, which supply power to the Kumasi Metropolitan Assembly (Kaase, Kowait, Ahodwo, Atonsu etc.) of the Ashanti Region via two transformers, which rated 20 MVA and 10 MVA.
- Offinso (A & B): It is distribution station buses, which supply power to the Offinso Municipal Assembly of the Ashanti Region via two transformers, which rated 10 MVA for each.
- Airport (A & B): It is distribution station buses, which supply power to the Asokore Mampong Municipal Assembly of the Ashanti Region via two transformers, which rated 20 MVA for each.
- Switching station (A & B): It is switching station that located at Kuntenase to supply 33 kV network to Bekwai and Akyawkrom distribution stations.
- Bekwai (A & B): It is distribution station buses, which supply power to the Bekwai Municipal Assembly of the Ashanti Region via two transformers, which rated 10 MVA for each.

- Fawoade (A & B): It is distribution station buses, which supply power to the Kwabre East district of the Ashanti Region via two transformers, which rated 20 MVA for each.
- Boadi (A & B): It is distribution station buses, which supply power to the Ayigya district of the Ashanti Region via two transformers, which rated 20 MVA for each.
- Akyease (A & B): It is distribution station buses, which supply power to the Achiase District of the Ashanti Region via two transformers, which rated 20 MVA for each.
- Mampong (A & B): It is distribution station buses, which supply power to the Mampong Municipal Assembly of the Ashanti Region via two transformers, which rated 20 MVA for each.
- Agona (A & B): It is distribution station buses, which supply power to the Sekyere South District of the Ashanti Region via a transformer, which rated 10 MVA.
- Nsuta: It is distribution station buses, which supply power to the Sekyere Central District of the Ashanti Region via a transformer, which rated 5 MVA.
- Kumawu: It is distribution station buses, which supply power to the Sekyere Kumawu District of the Ashanti Region via a transformer, which rated 5 MVA.
- Effiduase (A & B): It is distribution station buses, which supply power to the Sekyere East District of the Ashanti Region via two transformers, which rated 20 MVA for each.
- Akyawkrom (A & B): It is distribution station buses, which supply power to the Ejisu Municipal Assembly of the Ashanti Region via two transformers, which rated 20 MVA for each.

3.2.2. Substation Transformer Parameter

The distribution system uses various transformer capacities and voltages. High voltage is stepped down by the two base station transformers. These transformers decrease 161 kV to 33

kV. Twenty-one SBU centres transformers convert 33 kV to 11 kV. Twenty-seven transformers have capacity of 20 MVA, while seven have 10 MVA and two have 5 MVA. The Appendix I provides a summary of the data regarding the total number of transformers at SBU centres, together with its capabilities.

3.2.3. Transmission line parameters of ECG 33 kV distribution network

The primary reason for power loss and voltage issues in an electrical distribution system are network distance and the excessive load on the distribution line, which are constrained by its limited capacity. The ECG 33 kV system experiences this problem due to the enormous distance between substation centres (SBU). The extensive network length has led to decreased power delivery capability, resulting in power losses and voltage drop. To assess the system's current condition, the load flow analysis considers the distance covered by the system as a crucial factor. Appendix II provides detailed information about the secondary transmission lines within the Ashanti region's 33 kV distribution network. This data includes the cable type, size, length, and destination of each line.

3.2.4. Estimated Load on Existing Network

To carry out an analysis of the distribution network for the power system, it is necessary to understand the value of the load that is being placed on the network. It is vital to do this to establish the underlying cause of power loss (both active and reactive) in addition to a weak voltage profile. The researcher modelled the existing 33 kV network in the Ashanti region by using ETAP 19.0.1C (refer to Figure 3.1 for more information) and then estimated the loads that were being carried by the network. This allowed the researcher to evaluate the current state of the network. The estimated loads that were put on the network in each SBU centre are presented in Appendix III. The loads were estimated based on the capacities of substation transformers and the consumption capability in the area.

3.2.5. Single Line Diagram of the ECG 33 kV network

When analysing distribution line performance, it is essential to have a comprehensive understanding of each distribution feeder parameter. These parameters include resistance, reactance, segment distance, active power, and reactive power. A variety of approaches can be taken to acquire these. When calculating the positive sequence impedance of each branch, the distance of the conductor as well as the type of conductor that is stated in Appendix II are taken into consideration.

The research work focuses on ECG 33 kV distribution network which distribute power to Ashanti region. The network has fifty (50) buses, forty-nine (49) branches and thirty-six (36) transformers with a total length of 574.4km. The single line diagram of the ECG 33kV network is drawn by Visio Professional 2016 software as shown in Figure 3.3 below.

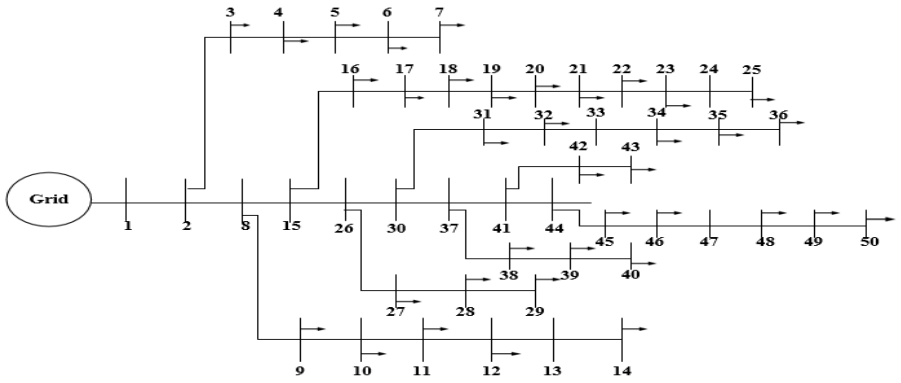

Figure 3.3, ECG 33kV distribution network line diagram

3.2.6. Line and Bus Data of the ECG 33 kV Distribution Network

Assessing the effectiveness of a distribution system requires a thorough understanding of various transmission line parameters, such as resistance, reactance, active power, and reactive power. The positive sequence impedance for each branch was determined by considering factors such as conductor size, conductor type, and the distance between conductors. The network was modelled and data on lines and buses were gathered using ETAP software. Thus,

the impedance (resistance and reactance) values were computed based on distance and distribution system conductor type. Appendix IV display bus and line data.

3.3. Mathematical Modeling of DSTATCOM

The static model (Figure 3.4) analysed the distribution system. Reactive power at the attached bus raises the device's bus voltage profile. As a result, the DSTATCOM has an impact on the voltages on surrounding buses. The receiving voltages on the candidate bus are V_{m+1}, whereas the transmitting voltages on the previous bus are V_m.

The current (I_{m+1}) is the result of combining I_m and I_{DS}. Where I_m is sending current and I_{DS} is DSTATCOM's injection current, and it is in quadrature with the voltage. Figure 3.4 shows a simple two-bus radial distribution system (Guwaeder & Ramakumar, 2019).

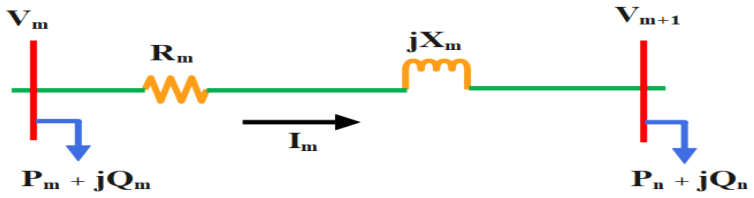

Figure 3.4, Two bus radial distribution system.

The voltage equation of the two-bus system is as follows,

$$V_{m+1} = V_m < \theta_m - (R_m - jX_m)I_m < \delta \qquad 3.1$$

In a traditional radial system, voltages at the buses are often less than 1p.u. Supposing the voltage on receiving bus (V_{m+1}) is less than 1p.u, DSTATCOM installed on bus would improve the voltage profile.

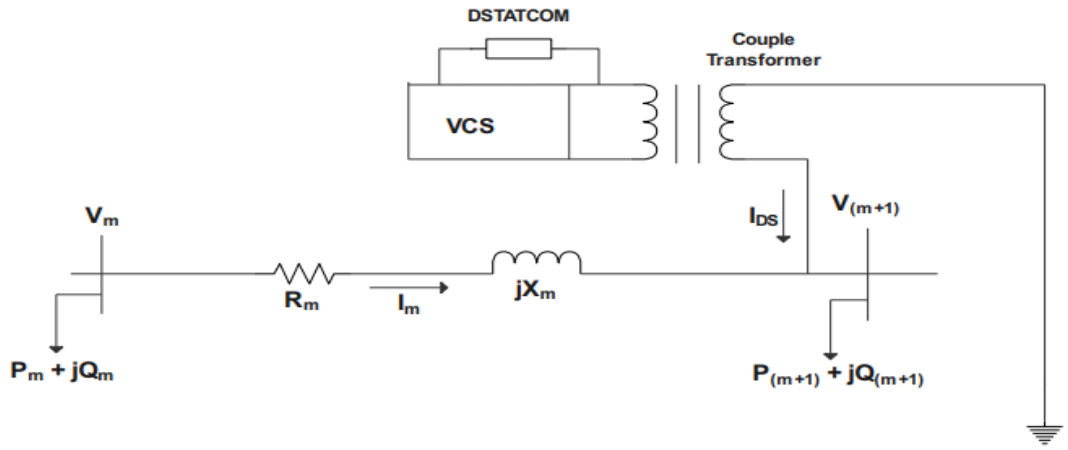

Figure 3.5, Two bus radial distribution system with DSTATCOM.

The new voltage after installed DSTATCOM (Figure 3.5) is express as (Egwaile et al., 2018);

$$V_{m+1}^{\sim} = V_m^{\sim} < \theta_m^{\sim} - (R_m - jX_m)I_m^{\sim} < \delta + I_{DS} < \left(\frac{\pi}{2} + \theta_{m+1}^{\sim}\right) \qquad 3.2$$

Where $\theta_{m+1}^{\sim}$, $\theta_m^{\sim}$, δ and $\left(\frac{\pi}{2} + \theta_{m+1}^{\sim}\right)$ are the phase angle of $V_{m+1}^{\sim}$, $V_m^{\sim}$, $I_m^{\sim}$ and I_{DS} respectively.

When the real and imaginary parts of the above equations parted, we develop,

$$V_{m+1}^{\sim} cos\theta_{m+1}^{\sim} = Rea(V_m^{\sim} < \theta_m^{\sim}) - Rea(Z_m I_m^{\sim} < \delta) - R_m I_{DS} cos\left(\frac{\pi}{2} + \theta_{m+1}^{\sim}\right)$$
$$+ X_m I_{DS} sin\left(\frac{\pi}{2} + \theta_{m+1}^{\sim}\right) \qquad 3.3$$

$$V_{m+1}^{\sim} sin\theta_{m+1}^{\sim} = Ima(V_m^{\sim} < \theta_m^{\sim}) - Ima(Z_m I_m^{\sim} < \delta) - X_m I_{DS} cos\left(\frac{\pi}{2} + \theta_{m+1}^{\sim}\right)$$
$$+ R_m I_{DS} sin\left(\frac{\pi}{2} + \theta_{m+1}^{\sim}\right) \qquad 3.4$$

Where, R_m, X_m and Z_m represent line resistance, inductance, and impedance respectively, Rea and Ima are real and imaginary parts of the system.

Therefore, if d = $V_{m+1}^{\sim}$, $u_1 = Rea(V_m^{\sim} < \theta_m^{\sim}) - Rea(Z_m I_m^{\sim} < \delta), u_2 = Ima(V_m^{\sim} < \theta_m^{\sim}) - Ima(Z_m I_m^{\sim} < \delta)$, $u_3 = -X_m$, $u_4 = -R_m$, $u_5 = X_m$, $u_6 = R_m$, w_1 and $w_2 = I_{DS}$, k = $\theta_{m+1}^{\sim}$ and b = $\frac{\pi}{2} + \theta_{m+1}^{\sim}$.

Therefore, the Equation (3.3) and (3.4) will be;

$$dcosk = u_1 - u_4 w_1 cosb + u_5 w_1 sinb \quad 3.5$$

$$dsink = u_2 - u_3 w_2 cosb + u_6 w_2 sinb \quad 3.6$$

From Equation (3.5)

$$w_1 = \frac{dcosk - u_1}{-u_4 cosb + u_5 sinb} \quad 3.7$$

From Equation (3.6)

$$w_2 = \frac{dsink - u_2}{-u_3 cosb + u_6 sinb} \quad 3.8$$

Therefore, from Equation (3.7) and (3.8)

$w_1 = w_2 = \frac{dcosk - u_1}{-u_4 cosb + u_5 sinb} = \frac{dsink - u_2}{-u_3 cosb + u_6 sinb}$

By rewriting both side equation, it can be written as.

$$du_4 + sinb(-u_5 + u_6) + cosb(-u_3 - u_4) = 0 \quad 3.9$$

Therefore, let $sinb = t, cosb = \sqrt{(1 + t^2)}$, $(-u_5 + u_6) = y_1$ and $(-u_3 - u_4) = y_2$.

So, Equation (3.9) change to,

$$du_4 + y_1 t - y_2 \sqrt{(1 - t^2)} = 0 \quad 3.10$$

By squaring both side of Equation (3.10), the expression become,

$$(y_1^2 + y_2^2)t^2 + 2du_4 y_1 t + d^2 u_4^2 - y_2^2 = 0 \quad 3.11$$

therefore,

$$t = \frac{-B \pm \sqrt{B^2} - 4AC}{2A} \quad 3.12$$

Were,

$$A = y_1^2 + y_2^2 = (-u_5 + u_6)^2 + (-u_3 - u_4)^2 \quad 3.13$$

$$B = 2du_4y_1 = 2(-u_5 + u_6) + (V_n^{\sim}) \quad 3.14$$

$$C = d^2u_4^2 - y_2^2 = (V_n^{\sim} * R_m)^2 - (-u_3 - u_4)^2 \quad 3.15$$

Therefore, let $V_{m+1}^{\sim} = V_{m+1}$, $I_{DS} = 0$ and $\theta_{m+1}^{\sim} = \theta_{m+1}$

For determining the correct value of root, the boundary consideration can be expressed as,

$$t = \frac{-B \pm \sqrt{B^2} - 4AC}{2A}$$

However, the bus voltage phase angle can be expressed as,

$$\theta_{m+1}^{\sim} = sin^{-1}\left(\frac{-B \pm \sqrt{d}}{2A}\right) \quad 3.16$$

The Equation of (3.17 and 3.18) can be expressed as DSTATCOM current angle and magnitude respectively.

$$< I_{DS} = \frac{\pi}{2} + k = \frac{\pi}{2} + sin^{-1}t \quad 3.17$$

$$|I_{DS}| = w_1 = \frac{V_{m+1}^{\sim} cos\theta_{m+1}^{\sim} - u_1}{-u_4 sin\theta_{m+1}^{\sim} - u_3 cos\theta_{m+1}^{\sim}} \quad 3.18$$

Therefore, the reactive power injection can be expressed as

$$jQ_{DS} = (V_{m+1}^{\sim} < \theta_{m+1}^{\sim}) * \left(I_{DS} < \left(\frac{\pi}{2} + \theta_{m+1}^{\sim}\right)\right) \quad 3.19$$

3.4. Power Flow Analysis on ECG 33 kV Radial Distribution System

Power flow analysis is crucial in the controlling, planning and operation of the power system to ensure the efficiency of the system. Power flow study focuses on many aspects of AC power characteristics such as active and reactive losses, voltage magnitude and voltage angle.

Power flow analyses on existing distribution systems are necessary before determining DSTATCOM installation and sizing. Most distribution systems are radial, with a high resistance and reactance ratio (R/X) value that hinders load flow algorithm convergence. The BFS algorithm is a popular power flow analysis method due to its speed, robust convergence, simplicity, low memory, and solution accuracy.

Kirchhoff's current and voltage laws are the basis of the BFS algorithm's iterative steps. This algorithm calculated twice per step.

To begin, a Backward Sweep is performed using the existing computations. This sweep calculates current at the last node and works its way backwards to the initial node.

Forward Sweep calculates voltage from the first node to the last. When the voltage gap is exceedingly low, iterations stop (Bakhshideh Zad et al., 2015; Sarkar & Bhattacharyya, 2012). This research uses Backward/Forward Sweep load flow for distribution load flow for system accuracy and computational efficiency.

The Equivalent Current Injection (ECI), Bus Injection to branch Current matrix (BIBC) and Branch Current to the Bus Voltage matrix (BCBV) were used in this method.

The complex power (S_i) for bus-i is written as,

$$S_i = P_i + jQ_i \qquad 3.20$$

Were, $i = 1,,2,3,4,5 \dots \dots \dots \dots \dots \dots n$

3.4.1. Equivalent Current Injection

The equivalent current injection (ECI) values play a critical role in load flow analysis as they represent the current injections at each node (Hota & Mishra, 2021). In a fundamental load flow analysis, the ECI values are iteratively transformed using the ECI equation, which computes the equivalent current injection based on the updated voltage, active power, and reactive power at each node. By iteratively updating the voltage and power values and recalculating the ECI values at each iteration, the load flow analysis converges to a solution that satisfies power balance and voltage constraints within the system. The computation of ECI values typically involves utilizing the voltage differences between nodes and the admittance matrix, which represents the network's connectivity and impedance. From Equation 3.20, the ECI is expressed as,

$$Ii = I_i^r(V_i) + jI_i^i(V^{\mathrm{k}}i) = \left(\frac{P_i + jQ_i}{V_i^k}\right) \qquad 3.21$$

The ECI at the k^{th} iteration at the i^{th} node in the load flow solution is expressed as,

$$I^{\mathrm{k}}i = I_i^r\left(V_i^k\right) + jI_i^i\left(V_i^k\right) = \left(\frac{P_i + jQ_i}{V_i^k}\right) \qquad 3.22$$

Where S_i is the complex power at the i^{th} bus, P_i is the active power at the i^{th} bus, jQ_i is the reactive power at the i^{th} bus, V^{k} is the bus voltage at the k^{th} iteration for i^{th} bus, I^k is the Equivalent Current Injection at the k^{th} iteration for i^{th} bus, I^r is the real part of Equivalent Current Injection at the k^{th} iteration for i^{th} bus and I^i is the imaginary part of the Equivalent Current Injection at the k^{th} iteration for i^{th} bus.

3.4.2. Backward Sweep (Formation of BIBC Matrix)

Backward Sweep moves from the last node to the origin. Kirchhoff's Current Law (KCL) was applied to the distribution network to calculate branch currents as a function of bus injected

currents (Figure 3.6). Bus injection to branch current (BIBC) is a mathematical representation that relates the currents injected at each bus in a power system to the currents flowing through the branches (Pathak & Prakash, 2018; Raj & Kumar, 2020). It is a fundamental matrix used in power flow analysis and fault analysis to determine the currents flowing through different branches based on the injections at the buses The branch currents B1, B2, B3, B4, and B5 were calculated from the Equivalent Current Injections at each bus using Equation (3.21).

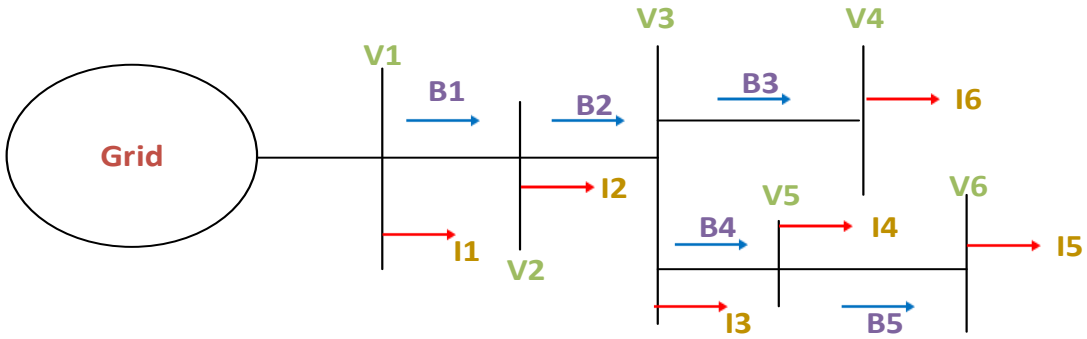

Figure 3.6, Simple radial distribution network

$$B_1 = I_2 + I_3 + I_4 + I_5 + I_6 \qquad 3.23$$

$$B_2 = I_3 + I_4 + I_5 + I_6 \qquad 3.24$$

$$B_3 = I_6 \qquad 3.25$$

$$B_4 = I_4 + I_5 \qquad 3.26$$

$$B_5 = I_5 \qquad 3.27$$

Therefore, the Bus Injection to Branch Current (BIBC) matrix can be expressed from the above Equations (3.23 – 3.27) as,

$$\begin{vmatrix} B_5 \\ B_4 \\ B_3 \\ B_2 \\ B_1 \end{vmatrix} = \begin{vmatrix} 0 & 0 & 0 & 1 & 0 \\ 0 & 0 & 1 & 1 & 0 \\ 0 & 0 & 0 & 0 & 1 \\ 0 & 1 & 1 & 1 & 1 \\ 1 & 1 & 1 & 1 & 1 \end{vmatrix} \begin{vmatrix} I_6 \\ I_5 \\ I_4 \\ I_3 \\ I_2 \end{vmatrix} \qquad 3.28$$

The general form of Equation 3.28 can be written as,

$$|B| = |BIBC||I_{i+1}| \qquad 3.29$$

Therefore, BIBC for the given simple network (Figure 3.6) can be expressed as,

$$|BIBC| = \begin{vmatrix} 1 & 1 & 1 & 1 & 1 \\ 0 & 1 & 1 & 1 & 1 \\ 0 & 0 & 0 & 0 & 1 \\ 0 & 0 & 1 & 1 & 0 \\ 0 & 0 & 0 & 1 & 0 \end{vmatrix} \qquad 3.30$$

3.4.3. Forward Sweep (Formation of BCBV Matrix)

The Branch Current to Bus Voltage (BCBV) matrix is the relationship of branch currents and bus voltages of the radial distribution system that can be obtained by applying Kirchhoff's Voltage Law (KVL). The voltages of bus $1, 2, 3, 4, 5\ and\ 6$ as shown in Figure 3.6 can be expressed as,

$$V_6 = V_5 - (Z_{56}B_5) = V_1 - (Z_{12}B_1) - (Z_{23}B_2) - (Z_{35}B_4) - (Z_{56}B_5) \qquad 3.31$$

$$V_5 = V_3 - (Z_{35}B_4) = V_1 - (Z_{12}B_1) - (Z_{23}B_2) - (Z_{35}B_4) \qquad 3.32$$

$$V_4 = V_3 - (Z_{34}B_3) = V_1 - (Z_{12}B_1) - (Z_{23}B_2) - (Z_{34}B_3) \qquad 3.33$$

$$V_3 = V_2 - (Z_{23}B_2) = V_1 - (Z_{12}B_1) - (Z_{23}B_2) \qquad 3.34$$

$$V_2 = V_1 - (Z_{12}B_1) \qquad 3.35$$

Therefore, Z_{ij} is the line impedance between bus i and j and V_i is the voltage at bus i. By Equation (3.31 -3.35), the bus voltage of the system can be represented as,

$$\begin{vmatrix} V_6 \\ V_5 \\ V_4 \\ V_3 \\ V_2 \end{vmatrix} = \begin{vmatrix} V_1 \\ V_1 \\ V_1 \\ V_1 \\ V_1 \end{vmatrix} - \begin{vmatrix} Z_{12} & Z_{23} & Z_{35} & Z_{56} & 0 \\ Z_{12} & Z_{23} & Z_{35} & 0 & 0 \\ Z_{12} & Z_{23} & Z_{34} & 0 & 0 \\ Z_{12} & Z_{23} & 0 & 0 & 0 \\ Z_{12} & 0 & 0 & 0 & 0 \end{vmatrix} \begin{vmatrix} B_5 \\ B_4 \\ B_3 \\ B_2 \\ B_1 \end{vmatrix} \qquad 3.36$$

$$|BCBV| = \begin{vmatrix} V_1 \\ V_1 \\ V_1 \\ V_1 \\ V_1 \end{vmatrix} - \left| \begin{matrix} 1 & 1 & 1 & 1 & 0 \\ 1 & 1 & 1 & 0 & 0 \\ 1 & 1 & 1 & 0 & 0 \\ 1 & 1 & 0 & 0 & 0 \\ 1 & 0 & 0 & 0 & 0 \end{matrix} \right| \left| \begin{matrix} 0 & 0 & 0 & Z_{56} & 0 \\ 0 & 0 & Z_{35} & 0 & 0 \\ 0 & 0 & Z_{34} & 0 & 0 \\ 0 & Z_{23} & 0 & 0 & 0 \\ Z_{12} & 0 & 0 & 0 & 0 \end{matrix} \right| \quad 3.37$$

$$|BCBV| = |V_1| - |BIBC||Z_d| \quad 3.38$$

Equation (3.38) can be written as,

$$\begin{vmatrix} V_1 \\ V_1 \\ V_1 \\ V_1 \\ V_1 \end{vmatrix} - \begin{vmatrix} V_6 \\ V_5 \\ V_4 \\ V_3 \\ V_2 \end{vmatrix} = \begin{vmatrix} Z_{12} & Z_{23} & Z_{35} & Z_{56} & 0 \\ Z_{12} & Z_{23} & Z_{35} & 0 & 0 \\ Z_{12} & Z_{23} & Z_{34} & 0 & 0 \\ Z_{12} & Z_{23} & 0 & 0 & 0 \\ Z_{12} & 0 & 0 & 0 & 0 \end{vmatrix} \quad 3.39$$

$$\begin{vmatrix} V_1 \\ V_1 \\ V_1 \\ V_1 \\ V_1 \end{vmatrix} - \begin{vmatrix} V_6 \\ V_5 \\ V_4 \\ V_3 \\ V_2 \end{vmatrix} = \left| \begin{matrix} 1 & 1 & 1 & 1 & 0 \\ 1 & 1 & 1 & 0 & 0 \\ 1 & 1 & 1 & 0 & 0 \\ 1 & 1 & 0 & 0 & 0 \\ 1 & 0 & 0 & 0 & 0 \end{matrix} \right| \left| \begin{matrix} 0 & 0 & 0 & Z_{56} & 0 \\ 0 & 0 & Z_{35} & 0 & 0 \\ 0 & 0 & Z_{34} & 0 & 0 \\ 0 & Z_{23} & 0 & 0 & 0 \\ Z_{12} & 0 & 0 & 0 & 0 \end{matrix} \right| \left| \begin{matrix} B_5 \\ B_4 \\ B_3 \\ B_2 \\ B_1 \end{matrix} \right| \quad 3.40$$

$$\Delta V = |BCBV||B| \quad 3.41$$

$$\Delta V = |BIBC||Z_d||B| \quad 3.42$$

The universal form for the bus voltage at $(k+1)^{th}$ iteration from Equation (3.36) can be written as,

$$|V_{k+1}| = |V_1| - |BCBV||B| \quad 3.43$$

The relationship between node current injections (3.29) and bus voltages (3.41) could be written as,

$$|\Delta V| = |BCBV||BIBC||I_{i+1}| \quad 3.44$$

$$\Delta V = |BIBC||Z_d||B||I_{i+1}| \quad 3.45$$

The Distribution Load Flow matrix (DLF) is expressed as,

$$|DLF| = |BCBV||BIBC| = |BIBC||Z_d||BIBC| \quad 3.46$$

By substituting Equation (3.45) into Equation (3.46), can be expressed as,

$$|\Delta V| = |DLF||I_{i+1}| \quad 3.47$$

The result for the load flow in the distribution system can be expressed as,

$$|\Delta V_{k+1}| = |DLF||I_k| \quad 3.48$$

$$|V_{k+1}| = |V_1| + |\Delta V_{k+1}| \quad 3.49$$

3.4.4. Algorithm of Backward/Forward Sweep for Power Load Flow

The Backward/Forward Sweep load flow algorithm may have the following steps:

Step 1: Read the line and bus data of the distribution network.

Step 2: Calculate each node current injections matrix.

Step 3: Calculate the BIBC matrix and determine the branch current.

Step 4: Formulate the BCBV matrix.

Step 5: Calculate the distribution load flow (DLF) matrix.

Step 6: Set Iteration $k = 0$.

Step 7: Iteration $k = k + 1$.

Step 8: Update voltages.

Step 9: If max ($|V^{k+1}|$ - $|V^{k}|$) $> tolerance$, go to step 5.

Step 10: Calculate each branch current and power losses from final bus voltage.

Step 11: Print the magnitudes and angles of bus voltages, branch currents, and power losses.

Step 12: Stop/end.

3.5. Mathematical module of Particle Swarm Optimization (PSO)

The possible solutions involve the coordination of two vectors, represent the position (X) and Velocity (V) of a particle. At the end of each iteration, the particle with the best solution shares its location coordinates (P_{gb}) with the swarm (Okwu & Tartibu, 2021). The PSO algorithm variables are defined as follow,

The location of the particle (i^{th}) at time (t) is represented by the dimensional vector (D).

$$X_{id}(t) = (X_{i1}, X_{i2}, \dots X_{id}) \in S \tag{3.50}$$

The velocity of the particle (i^{th}) at time (t) is represented by the dimensional vector (D).

$$V_{id}(t) = (V_{i1}, V_{i2}, \dots V_{id}) \in S \tag{3.51}$$

The best previous position of each particle at time $'t'$ is a point in $'S'$ and designated by,

$$P_{lbd}(t) = (P_{i1}, P_{i2} \dots, P_{id}) \in S \tag{3.52}$$

The global best position attained among entire particles is a point in $'S'$ and designated by,

$$P_{gbd} = \left(P_{gb1}, P_{gb2} \dots, P_{gbd}\right) \in S \tag{3.53}$$

Particles change their coordinates based on their best searching knowledge (P_{lbd} and P_{gbd}). Update velocity and location equations are shown by,

$$V_{id}^{t+1} = w * V_{id}^{t} + C_1 * r_1 * (P_{lbd}^{t} + X_{id}^{t}) + C_2 * r_2 * \left(P_{gbd}^{t} - X_{id}^{t}\right) \tag{3.54}$$

$$X_{id}^{t+1} = X_{id}^{t} + V_{id}^{t+1} \qquad 3.55$$

Where, $i = 1, 2 \ldots n$ (The number of particles in the swarms), $d = 1, 2 \ldots m$ (A particle's number of members in the searching space), C_1, C_2 = Acceleration coefficient, r_1, r_2 = uniformly spread random numbers in the range $[0, 1]$ added in the model to introduce stochastic nature, V_{id}^{t} is Current velocity of the particle $('i')$, V_{id}^{t+1} is updated velocity of the particle $('i')$, P_{lbd} is the particle best position value, P_{gbd} is the group of the particle best position value, X_{id}^{t} is Current search point of a particle, X_{id}^{t+1} is the updated searching point of a particle and w is inertial weight.

The inertia weight function can be expressed as,

$$w = w_{max} - \frac{w_{max} - w_{min}}{t_{max}} * t \qquad 3.56$$

Where, w_{min} and w_{max} are the minimum and maximum inertia weights respectively and t and t_{max} are the present and maximum iteration. Each particle is represented in the diagram as shown in Figure 3.7 (Abdulrazzaq, 2015; Rajpoot et al., 2017).

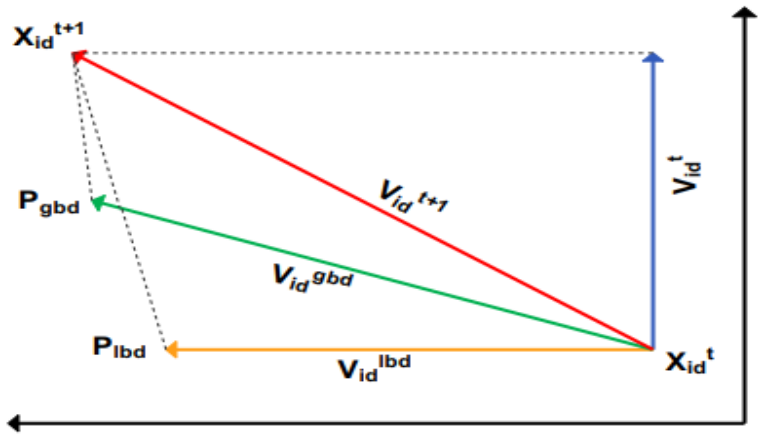

Figure 3.7, PSO search mechanism in multidimensional search space illustration.

3.5.1. PSO Parameters

The basic parameters of the PSO algorithm are particle velocity, random number, weighting coefficients, inertial weight, and expiry criterion. The particle velocity is one of the methods in PSO algorithm which restricted to the bounds. The fitness function is determined by the parameters of $V_{\max}$ and $V_{\min}$, which indicates the search region between the current and target positions. The particles take longer to enter desired solutions if they are few (Shobana et al., 2019). Random values (numbers) are in the range of $0\ and\ 1$, which helps to achieve the stochastic behavior of the PSO.

Social and cognitive accelerations represent stochastic weighting coefficients. High-value outcomes cause unexpected movement toward target zones. Low levels let particles go far before being brought down. The parameters can be set in the range of 1-2. An inertia weight improved local and global searches. The inertia weight started high and decreased during optimization. Equation (3.56) adjusts inertia weight (w) to 0.2 and 0.9. Iterations and objective function tolerances are used to meet the termination condition. For solution correctness, the end condition requires a maximum number of iterations.

3.5.2. PSO Procedure implementation

Each PSO particle has a real-valued vector. Each optimized parameter was a problem space dimension. Below are the PSO steps,

Step 1: Initialization

Set the iteration counter to 1 to generate a random n-particle dimension. The objective functions are calculated by randomly generating each particle's starting velocity and setting lower and upper limits.

Step 2: Set the iteration count $(iter = 1)$.

Step 3: Set the tolerance ($maxiter > iter$).

Step 4: Formulation of objective function

Step 5: Upgrading of both local minimum and the global minimum of particles.

Step 6: Update particle velocity and position of each particle using equation (3.54) and (3.55) respectively.

Step 7: Update the iteration counter ($iter = iter + 1$).

Step 8: If criteria are satisfied, go to step 7 else go to step 2.

Step 9: Stop/end if the particle generated optimal solution.

The system process plays a crucial role in evaluating the operational characteristics and performance of the network. The system process of this research is represented by flow chart in Figure 3.8. The flow chart below outlines the sequential procedure adopted to accomplish the objective of this research.

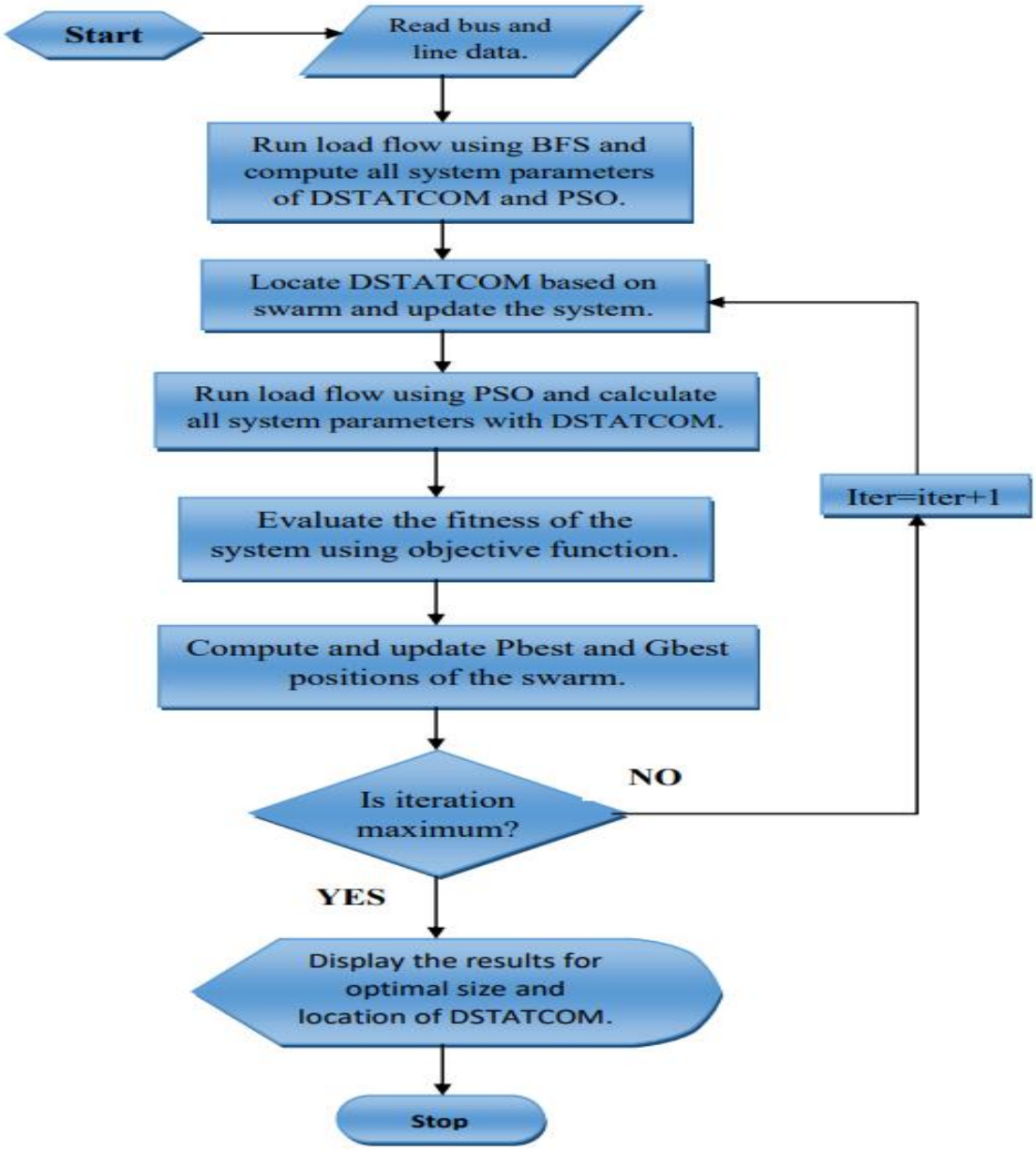

Figure 3.8, Flow Chart of System Process

The flow chart above shows the step-by-step approach to achieve the aim of this research. Firstly, it initialized by reading the load and line data values from the network provided and run load flow using Backward/Forward Sweep method and recorded as base case. After the base case, the parameters of PSO would initialize to locate the DSTATCOM on the vulnerable buses base on swarm update and run load flow using PSO algorithm and calculated the system parameters with DSTATCOM. The iteration is set to maximum number of 100 to know the optimal location and size of DSTATCOM on system buses.

3.6. Formulation of Problem

The research considered power loss minimization, voltage profile enhancement and economical aspect of the distribution system. Two conditions are used to determine the search space: voltage sensitivity factor and particle swarm optimization. The first criterion was the use of the voltage sensitivity factor to allocate buses for optimal DSTATCOM placement. The second condition was to determine the best optimal DSTATCOM sizing. Finally, the system is expected to meet several constraints inside the distribution system's objective function.

In this optimization problem, the three objects were considered in the objective function. The research aims were to reduce power losses (active and reactive), improve the voltage profile and reduce total annual cost. The concept of each were formulated separately and the objective function was applied to all the three objects.

3.6.1. Power Loss

The total distribution system losses can be formulated as,

$$f_1 = P_{loss} \tag{3.57}$$

$$f_1 = Q_{loss} \tag{3.58}$$

$$P_{loss} = \sum_{i=1}^{NBr} R_i I_i^2 \tag{3.59}$$

Where, f_1 is first objective function related to system losses, $P_{loss}\ is$ active power loss, I_i is line i current, R_i is resistance of i^{th} line, NBr is the number of system branches.

$$Q_{loss} = \sum_{i=1}^{NBr} X_i I_i^2 \tag{3.60}$$

Where, Q_{loss} is reactive power loss and X_i is reactance of i^{th} line.

The total power losses can be formulated as,

$$total\ loss\ \% = \frac{total\ loss\ without\ DSTATCOM - total\ loss\ with\ DTSATCOM}{total\ loss\ with\ DSTATCOM} * 100 \qquad 3.61$$

Where, total loss without DSTATCOM and total loss with DSTATCOM were the total line losses in the system.

3.6.2. Voltage Profile Improvement

Compensating the system with DSTATCOM increased voltage. The target function for voltage improvement can expressed as,

$$f_2 = V_{imp} \qquad 3.62$$

$$V_{imp} = \sum_{i=1}^{NBr} (V_n - V_i)^2 \qquad 3.63$$

Where, $f_2\ is$ second objective function of voltage profile improvement, V_n is the nominal voltage of the system which is equal to 1 per unit (1p.u), V_i is the voltage of the i^{th} bus, NBr is the number of system buses.

3.6.3. Economical Aspect of Energy

One of the goals of this research was cost analysis of the compensating device which related to system power losses. The cost analysis of this research includes the cost of energy loss, cost of DSTATCOM and total annual cost saving with payback period.

3.6.3.1. Cost of Energy loss

The cost of energy loss can be expressed as,

$$CE_{loss} = P_{loss} * (E_c * T) \qquad 3.64$$

Where, CE_{loss} = cost of energy loss, E_c = energy rate $(0.06\$/kWh)$, and T = time duration $(8760h)$.

3.6.3.2. Cost of DSTATCOM

The cost of DSTATCOM can be expressed as,

$$DSTATCOM_{cost/year} = DSTATCOM_{cost}\frac{(1+B)^{nDSTATCOM} * B}{(1+B)^{nDSTATCOM} - 1} \quad 3.65$$

Where, $DSTATCOM_{cost/year}$ is the annual cost of DSTATCOM, $DSTATCOM_{cost}$ is the cost of investment in the year of allocation ($50\$/Kvar$), B is the asset rate of return ($B = 0.1$), , and $nDSTATCOM$ is the longevity of DSTATCOM ($nDSTATCOM = 30years$).

3.6.3.3. Total Annual Saving Cost

The total annual saving cost can be expressed as,

$$f_3 = T_{cs} = kp(T * P_{Tloss}) - kp\left(T * P_{Tloss}^{with\ DSTATCOM}\right) - (kc * DSTATCOM_{cost/year}) \quad 3.66$$

Where, $kp, kc\ and\ T$ indicate the cost of energy losses, duration proportion and hour/year respectively, P_{Tloss} is total power loss before DSTATCOM integration, and $P_{Tloss}^{with\ DSTATCOM}$ is total power loss after the incorporation of DSTATCOM.

The payback period can be precise as,

$$payback\ period = \frac{capital\ cost}{saving\ cost} \quad 3.67$$

The three objective functions above can be expressed as,

$$\min\{f\} = (w_1 * f_1) + (w_2 * f_2) + (w_3 * f_3) \quad 3.68$$

Where, w_1, w_2 and w_3 are weighting values which determined the essential of three objective functions. The summation of these weighing values must be equal to 1 (Abebe Bikila, 2021). The Table 3.1 below shows the individual weighting values.

Table 3. 1, Representation of weighting value

No.	Objective functions	Weighting value
1	Power loss (w_1)	0.4
2	Voltage profile improvement (w_2)	0.3
3	Total annual saving cost	0.3

3.7. Constraints

3.7.1. DSTATCOM Constraints

3.7.1.1. DSTATCOM Placement Constraints

The constraint in this contest, is to reduce the number of DSTATCOM placement. Therefore, the optimum number of DSTATCOM must be less than or equal to maximum number of bus locations. DSTATCOM constraint can be expressed as,

$$N_{DSTATCOM} \leq N_{DSTATCOM}^{max} \quad 3.69$$

3.7.1.2. DSTATCOM Size Constraint

The size of DSTATCOM in the distribution system should not be either small or too large than load value to achieve the appropriate solution. The size constrain of DSTATCOM can be expressed as,

$$Q_{min} \leq Q_{DSTATCOM} \leq Q_{max} \quad 3.70$$

3.7.2. Total Reactive Power Injection Constraint

The total reactive power injection must be less than or equal to the total load reactive power which can be articulated as,

$$Q_{DSTATCOM}^{total} \leq Q_L^{Total} \quad 3.71$$

3.7.3. Operational Constraints

3.7.3.1. Bus voltage Constraint

All distribution system buses voltages should be within acceptable limit. The equation can be expressed as,

$$V_{min} \leq V_i \leq V_{max} \quad 3.72$$

$$0.95 \leq V_i \leq 1.05$$

Where V_i is the voltage of i^{th} bus.

3.7.3.2. Load Current Constraint

The load current should be less than or equal to the maximum rating.

$$I_{ij} \leq I_{ijmax} \quad 3.73$$

3.7.3.3. Power Flow Constraint

The power flow through the distribution lines was limited by the thermal capacity of the lines. It can be expressed as,

$$S_{ij} \leq S_{ijmax} \quad 3.74$$

Where, S_{ijmax} is the maximum capacity of the line between bus i and j. Power flow through the distribution lines were limited to 100MVA ($S_{ijmax} = 100MVA$).

3.7.3.4. Active Power Losses Constraint

The active power loss after integration of DSTATCOM should be less than or equal to the active power loss before the installation of DSTATCOM.

$$P_{total\ loss}^{with\ DSTATCOM} \leq P_{total\ loss}^{without\ DSTATCOM} \quad 3.75$$

3.8. Verification of Real data and Simulated result.

In the power distribution system analysis, the value of the monthly peak, average, and minimum voltage of the system must be recorded to determine the authentication of simulated data with real data. However, the real data on the average voltages of each distribution bus were recorded from October 2021 to September 2022. The findings of the simulation data are compared to the real data that was received at the various buses in the real system. The error margins fall within the permissible ranges of -0.1–2.8. Appendix V presents the error margins for both the simulated and the real data. A value of 0.878 was obtained when the real data were compared to the simulated data using the Pearson correlation. The results from the simulation demonstrate a confidence level of 95%. The real and simulated voltages of the study were compared to the IEC 60038-2009 standard, and the bus voltages were found to be within the allowable range of 5%. Because the IEC standard requires an error margin of 10%, the study's margin of error is significantly better (Standard & Horizontale, 2009a). Appendix V shows the existing system voltages as compared to the ETAP system model voltages.

3.9. Study Cases Definitions

The selection of study cases was guided by existing literature, aimed at supporting the outcomes of the proposed method. Most researchers have utilized both fixed and switched DSTATCOM (Abebe Bikila, 2021; Adel Ali Abou El-Ela, Ragab A. El-Sehiemy, Abdel-Mohsen Kinawy & Mohamed Taha Mouwafi, 2015; Amara et al., 2019; El-Fergany & Abdelaziz, 2014). These two types of DSTATCOM (fixed and switched) were chosen to verify the distinctions in compensation between them concerning distribution system performance. The study cases encompass a range of scenarios that were simulated to analyze the effectiveness of the solution which is presented in Table 3.2 below.

Case 0 involves the load flow study which was performed to analyze the distribution system's behavior under normal operating conditions without the DSTATCOM's intervention. This initial assessment provides a foundation for comparing and evaluating the impact of the DSTATCOM in subsequent cases. By examining the system's performance without the DSTATCOM, researchers can effectively assess the effectiveness and benefits of integrating the DSTATCOM technology in the distribution system. The findings from Case 0 serve as a crucial reference point for understanding the improvements and advantages brought about by the proposed DSTATCOM solution in the subsequent study cases.

Case 1 implemented fixed DSTATCOM technology on the ECG 33 kV distribution system in the Ashanti region. The case focused on optimal allocation and sizing of only fixed DSTATCOM technology on the base case. The primary objective of this integration was to enhance the voltage profile of each bus while minimizing power losses. Economic analysis on energy losses was also considered in this section.

In **Case 2**, switched DSTATCOM technology was applied to the ECG 33 kV distribution system in the Ashanti region. The main focus was on determining the best allocation and size of switched DSTATCOM technology in the reference case (Case 0). The primary goal of this integration was to improve the voltage profile of each bus while also minimizing power losses. Additionally, an economic analysis of energy losses was conducted as part of this investigation.

Table 3.2, Study cases description

Scenario	Technology	Remark
Case 0	-	Existing system without DSTATCOM integration.
Case 1	Fixed DSTATCOM	Integrated fixed DSTATCOM into the ECG 33 kV distribution system in Ashanti region.
Case 2	Switched DSTATCOM	Utilized switched DSTATCOM technology in the ECG 33 kV distribution system in Ashanti region.

CHAPTER FOUR

RESULT AND DISCUSSION

In this chapter, the findings of the ECG 33 kV distribution system are presented. To evaluate the effectiveness of the proposed approach, three cases were examined: the system without DSTATCOM (used as the base case or Case 0), with fixed DSTATCOM integration (used as the Case 1), and with switched DSTATCOM integration (used as the Case 2). The Backward/Forward Sweep power flow analysis technique was utilized to investigate the voltage profile, power losses (active and reactive), and energy cost with and without DSTATCOM integration. The system results of the ECG 33 kV distribution system are presented based on ECG 33 kV primary distribution feeders (refer from Figure 3.3). The optimization procedure was carried out to know the optimal placement and sizing of DSTATCOM using MATLAB R2021a software. These results provide insight into the potential benefits of integrating DSTATCOM in the ECG 33 kV distribution system.

4.0. CASES

4.1. Case 0: Existing Network Results

To assess the performance of the ECG 33 kV distribution system, a load flow study was carried out on existing system, which served as the base case (Case 0), and DSTATCOM integration was not included in this study. The evaluation of both the active and reactive power losses, as well as the voltage profile of the buses, was conducted in this section. The findings of this investigation showed that the ECG 33 kV distribution system suffers from substantial losses, with the total active power loss amounting to 14.530 MW and the total reactive power loss amounting to 67.005 Mvar. Furthermore, the voltage level at bus 35 was found to be the lowest at 0.817 p.u. These results suggest that there is a significant amount of energy wasted in the

Ashanti region's ECG 33 kV distribution system each year, which could potentially be avoided by implementing more effective strategies.

4.1.1. Power Loss of Case 0

After evaluating the provided data from the power system, the active power losses, and reactive power losses at lines 2, 3, 4, 5, 6 and 7 within the system can be observe in Figure 4.1 below.

At Line 2, the active power loss is 0.01629 MW, indicating a relatively low power dissipation at this location. The reactive power loss is 0.05385 Mvar, which suggests a moderate level of reactive power consumption. Moving to Line 3, we observe a significantly higher active power loss of 1.2127 MW. This indicates a substantial amount of power being dissipated as losses at this line due to heavily loaded distribution lines connected to it. The corresponding reactive power loss is 5.8607 Mvar, further emphasizing the magnitude of power consumption at this line.

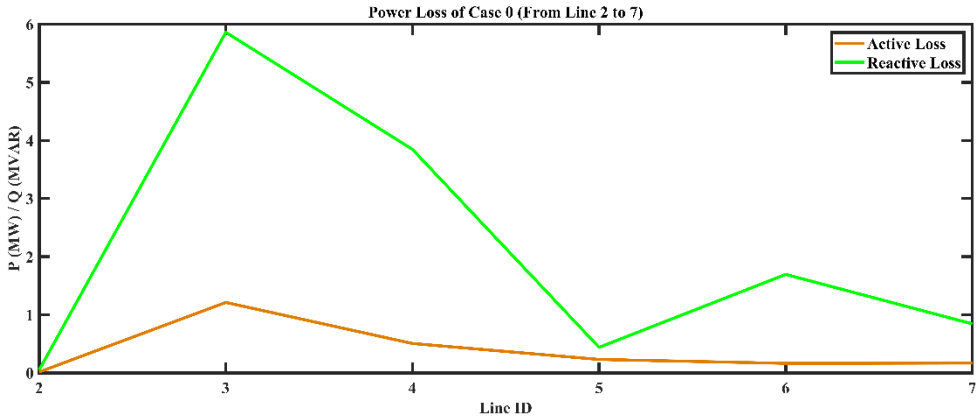

Figure 4.1, Active and reactive power loss of Case 0 (Line 2 to 9).

In figure 4.1 above, Line 4 displays notable power dissipation and consumption, with an active power loss of 0.5064 MW and a reactive power loss of 3.8464 Mvar. In contrast, Line 5 demonstrates relatively lower active and reactive power losses, indicating efficient power transmission. Line 6 and Line 7 have lower power dissipation, with moderate levels of reactive

power consumption. Evaluating the data helps identify areas for improvement and optimization in the power system, such as enhancing equipment efficiency, optimizing voltage levels, and implementing reactive power compensation techniques. Understanding these power losses contributes to overall system efficiency and reliability enhancement. Figure 4.2 below provide the active and reactive power losses between line 8 to 14.

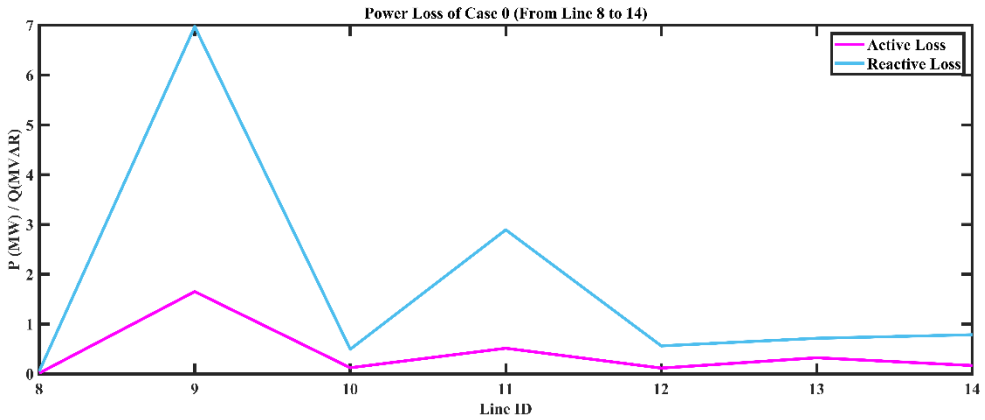

Figure 4.2, Active and reactive power loss of Case 0 (Line 8 and 14)

In Figure 4.2 above, the data discloses varying levels of power losses at lines 8, 9, 10, 11, 12, 13, and 14. Line 9 experiences the highest power losses because of commercial and industrial load demand in the vicinity, while lines 8, 10, 12, 13, and 14 have relatively lower losses. Analysing these losses helps identify areas for improvement and optimization within the power system.

The active and reactive power losses for lines 15, 16, 17, 18, 19, 20, 21, 22, 23, 24 and 25 are depicted in Figure 4.3 below. This figure illustrates the levels of power losses at each line, providing valuable insights into power dissipation and consumption within the power system.

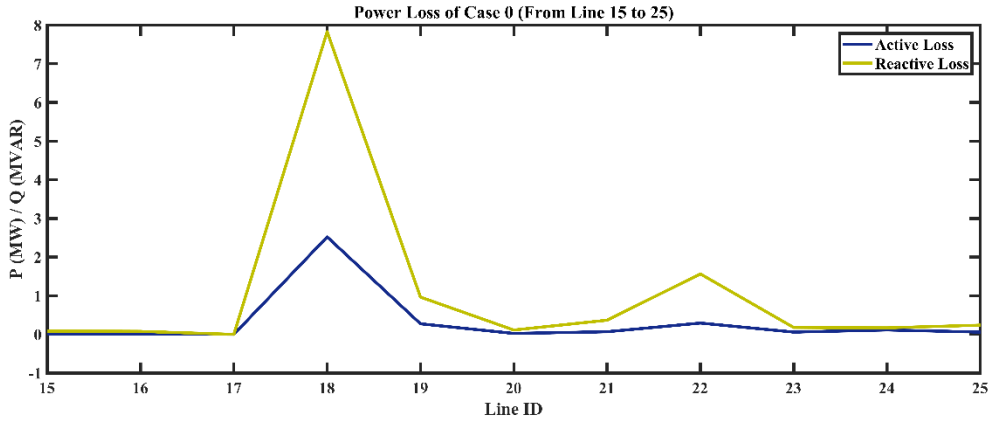

Figure 4.3, Active and reactive power loss of Case 0 (Line 15 to 25).

The provided data shows the active and reactive power losses at lines 15, 16, 17, 18, 19, 20, 21, 22, 23, 24, and 25. Lines 18 and 22 experience the highest power losses, while lines 17, 20, 23, and 24 have negligible losses. Examining these power losses facilitates the identification of areas within the power system that can be enhanced and optimized. The provided data in Figure 4.4 below presents the active and reactive power losses for lines 26, 27, 28, and 29.

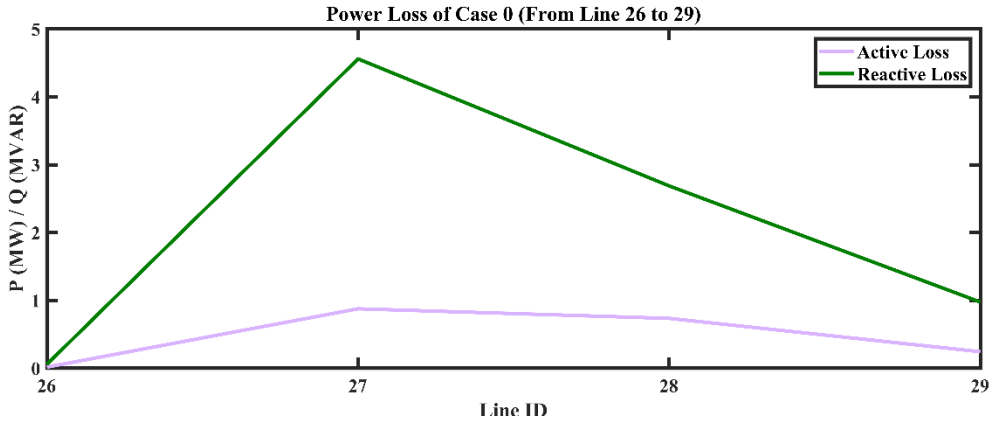

Figure 4.4, Active and reactive power loss of Case 0 (Line 26 to 29).

Line 26 demonstrates efficient power distribution with low losses, while Line 27 experiences high power dissipation due to commercial loads. Similarly, Line 28 shows notable losses, and Line 29 exhibits relatively efficient distribution. Evaluating these losses provides insights for optimizing power distribution and reducing losses in the system.

The active and reactive power losses for line 30 to 36 are depicted in Figure 4.5. Analysing these losses provides valuable information about the power dissipation and consumption along these lines.

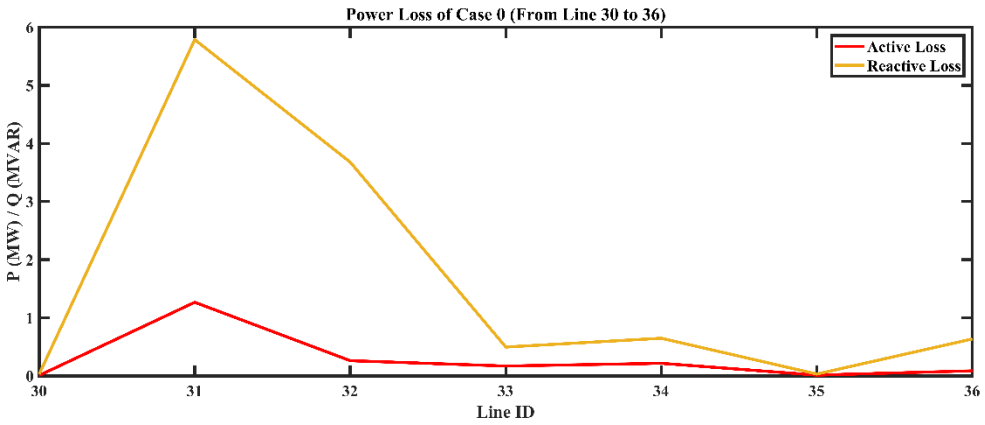

Figure 4.5, Active and reactive power loss of Case 0 (Line 30 to 36).

Different levels of power losses are seen at lines 30, 31, 32, 33, 34, 35, and 36, according to the data in Figure 4.5. Due to the proximity of industrial load demand, Line 31 stands out among these lines as having the biggest power losses, while the other lines show relatively smaller losses. In order to increase the power system's efficiency and performance, it is helpful to analyse these power losses in order to spot potential improvement and optimization opportunities. Figure 4.6 illustrates the active and reactive power losses associated with lines 37 to 40.

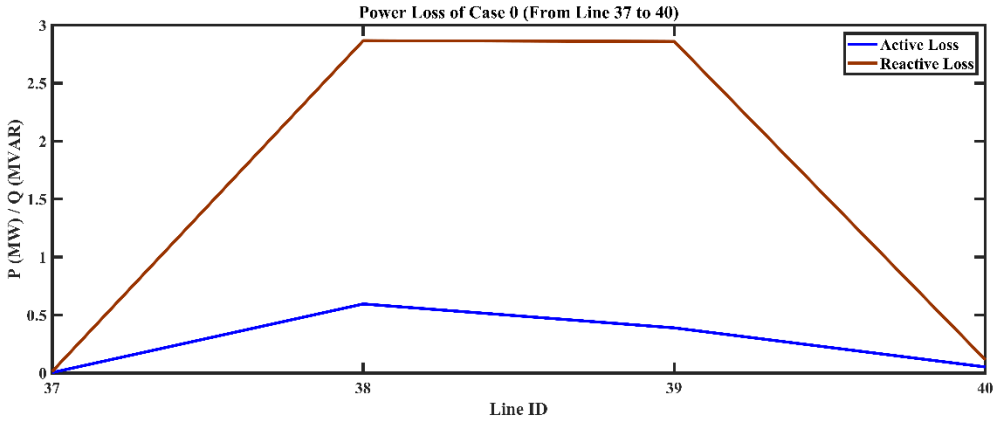

Figure 4.6, Active and reactive power loss of Case 0 (Line 37 to 40).

According to these power losses for lines 37 to 40: Reactive power loss on Line 37 is small at 0.01391 Mvar and comparatively low at 0.00424 MW. Comparatively, Line 38 suffers from greater power losses, with an active power loss of 0.5957 MW and a reactive power loss of 2.8663 Mvar. The active and reactive power losses for lines 41 to 43 are depicted in Figure 4.5.

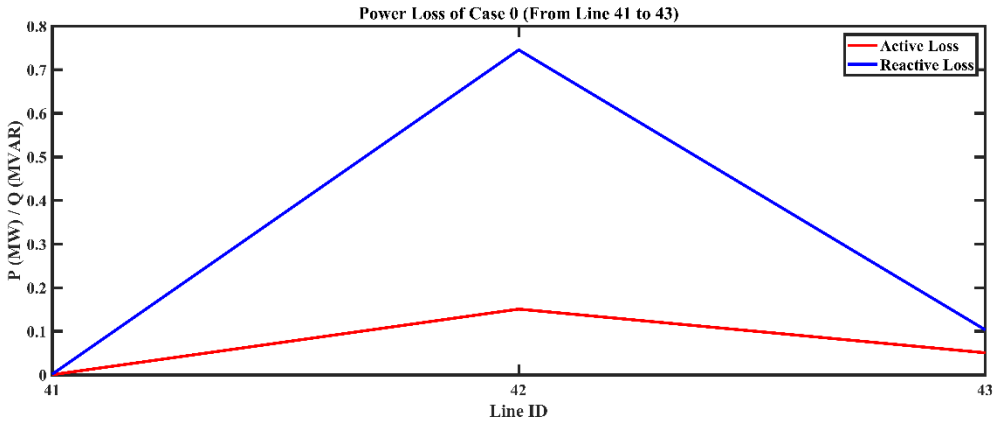

Figure 4.7, Active and reactive power loss of Case 0 (Line 41 to 43).

The data provided presents the active and reactive power losses for lines 41 to 43. Line 41 demonstrates a minimal active power loss of 0.000536 MW and a modest reactive power loss of 0.00165 Mvar, indicating efficient power distribution and consumption. On the other hand, Line 42 experiences higher power losses, with an active power loss of 0.151 MW and a reactive power loss of 0.7456 Mvar.

The active and reactive power losses for lines 44 to 50 are shown in Figure 4.8. This figure provides a visual representation of the power losses for these lines, which can be helpful for understanding the distribution of power losses.

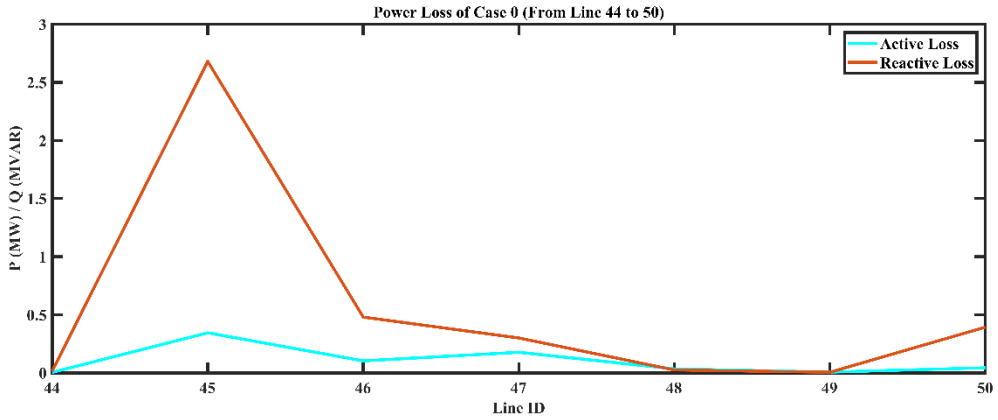

Figure 4.8, Active and reactive power loss of Case 0 (Line 44 to 50).

The provided data in Figure 4.8, reveals the active and reactive power losses for lines 44 to 50 in the ECG distribution system. Line 44 exhibits a relatively low active power loss of 0.0049 MW and a reactive power loss of 0.01611 Mvar. Line 45 experienced higher power losses, with an active power loss of 0.3451 MW and a reactive power loss of 2.6794 Mvar. These values indicate significant power dissipation and consumption at this line, potentially due to various factors such as high load demand or system inefficiencies.

It can be concluded that Lines 3, 9, 18, 27, 28, 31, 38, 39, 42 and 45 in the ECG 33 kV distribution network have the highest power losses. These lines demonstrate significant levels of power dissipation and consumption, indicating areas where improvements in efficiency and power loss reduction measures are required. Assessing these particular lines can offer valuable observations for optimizing the distribution network and improving its overall efficiency and dependability.

4.1.2. Voltage Profile of Case 0

The data in Figure 4.9 represents the voltages at different bus (bus 2 to 7) in Case 0 of the ECG 33 kV distribution system. The bus 1 in the ECG distribution system serve as reference bus.

Bus 2 has a voltage of 0.99948 p.u., indicating that it is close to the nominal voltage level and experiencing minimal deviation.

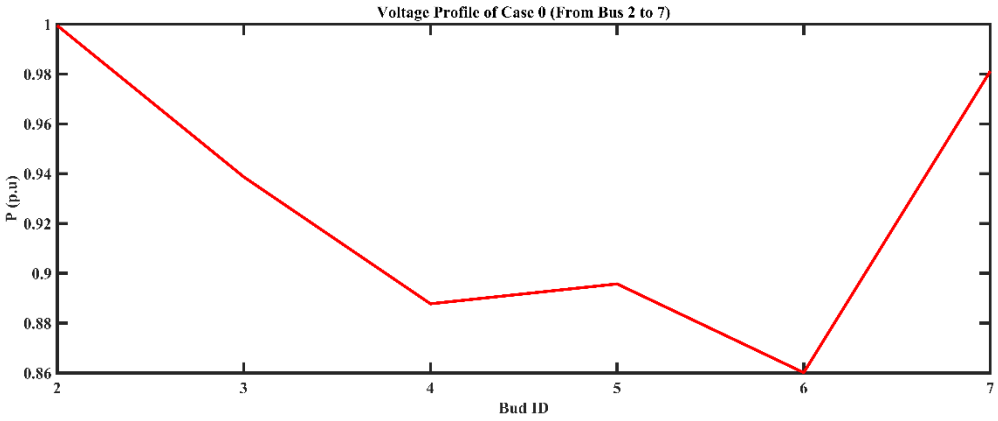

Figure 4.9, Voltage profile of Case 0 (From Bus 2 to 7).

However, buses 3, 4, and 6 exhibit lower voltages, suggesting potential voltage drop or regulation issues that require attention. Bus 7 maintains a voltage close to the nominal value. Addressing lower voltages at buses 4, 5, and 6 is crucial for reliable and efficient power system operation. Voltage regulation techniques, such as reactive power compensation, can be employed to mitigate voltage drop and maintain stability.

The voltage profile for buses 8 to 14 is presented in Figure 4.10. This profile showcases the voltage levels at each bus within the power system. Analyzing the voltage profile provides insights into the voltage stability and conditions experienced at these specific buses.

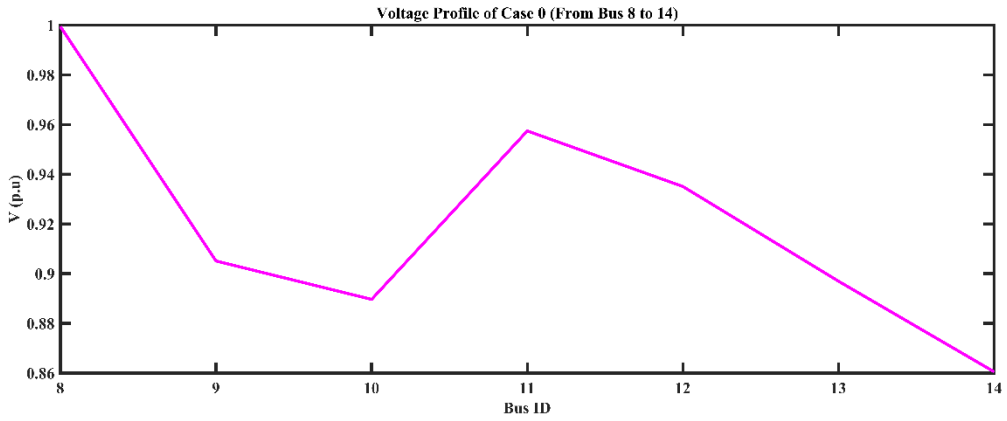

Figure 4.10, Voltage profile of Case 0 (From Bus 8 to 14).

Bus 8 operates at a voltage close to the nominal level, indicating a stable condition. However, Bus 9, Bus 10, Bus 13, and Bus 14 exhibit lower voltages, suggesting potential voltage drop or regulation issues. These deviations from the nominal voltage need to be addressed to maintain reliable power supply. The data highlights the importance of investigating and resolving voltage-related challenges at these buses. Measures such as transformer upgrades and reactive power compensation can be implemented to mitigate voltage drop and ensure voltage stability within acceptable limits. Figure 4.11 displays the voltage profile of buses 15 to 25, revealing the voltage levels at each bus in the power system.

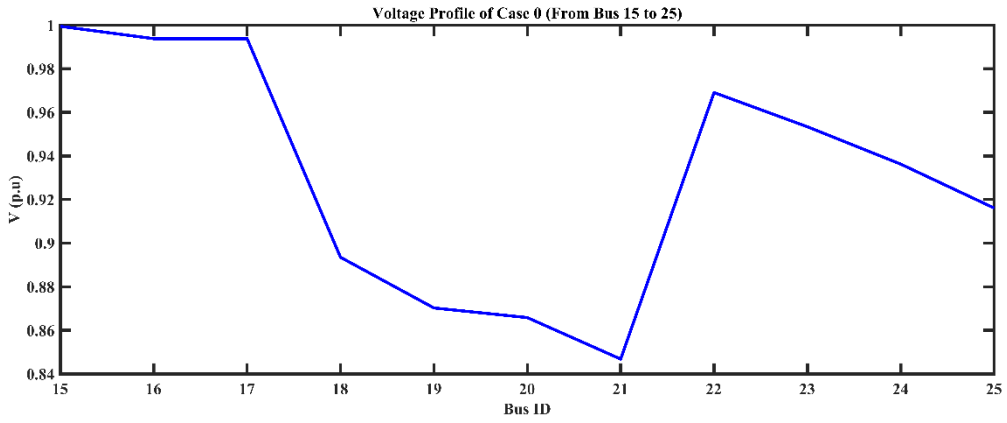

Figure 4.11, Voltage profile of Case 0 (From Bus 15 to 25).

Buses 15, 16, and 17 have relatively stable voltages, while Bus 18, 19, 20, and 21 experiences a significantly lower voltage. Addressing the lower voltages at Buses 18, 19, 20, 21, 24, and 25 is crucial for ensuring a reliable and efficient power system. The provided data in Figure 4.12, represents the voltage levels at buses 26 to 29 in Case 0 of the power system.

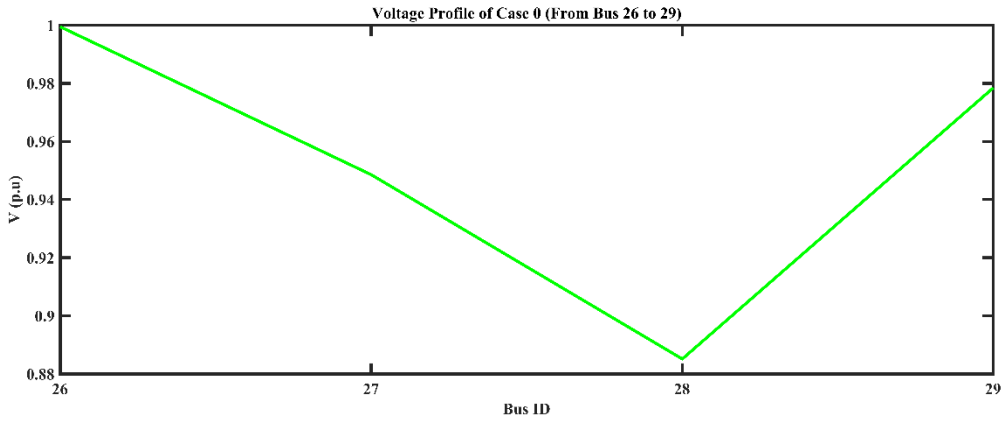

Figure 4.12, Voltage profile of Case 0 (From Bus 26 to 29).

The Figure 4.12, highlights voltage variations among the buses, emphasizing the need to address the lower voltages observed at buses to ensure reliable and efficient power system operation. The voltages at Buses 26, 27, and 28 vary significantly. Bus 26 has a relatively stable voltage, while Buses 27 and 28 have lower voltages that may impact the performance of the system. Figure 4.13 provides a visualization of the voltage profile associated with buses 30 to 36 in the power system. This voltage profile showcases the voltage levels at each of these buses, allowing for a comprehensive analysis of their voltage conditions.

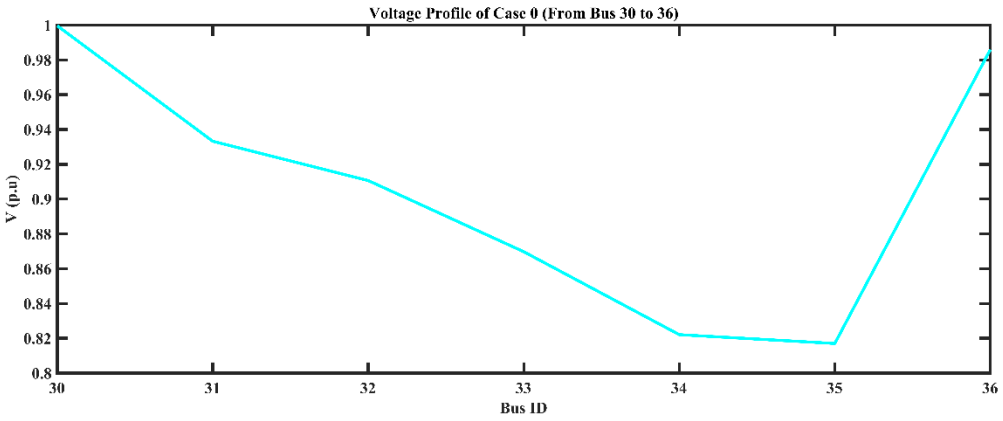

Figure 4.13, Voltage profile of Case 0 (From Bus 30 to 36).

Bus 30 operates at a stable voltage level, while Buses 31, 32, 33, 34, and 35 experience lower voltages that need to be addressed. Analyzing the data reveals voltage variations among the buses, highlighting the importance of resolving voltage-related issues at Buses 31-35. Voltage regulation techniques can be used to mitigate voltage drop and ensure stable voltage levels.

The voltage levels at buses 37 to 40 in Case 0 of the ECG 33 kV distribution system are depicted in Figure 4.14. This data provides insights into the voltage conditions experienced at these specific buses.

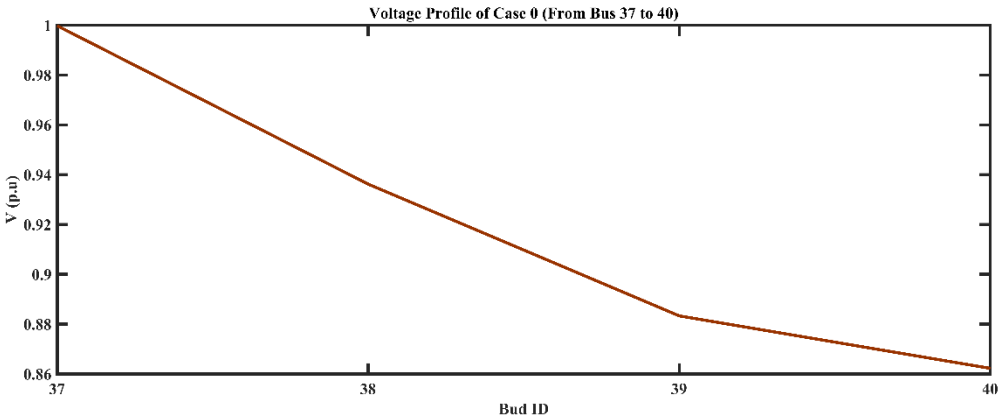

Figure 4.14, Voltage profile of Case 0 (From Bus 37 to 40).

Bus 37 maintains stable voltage close to nominal, while Bus 38, Bus 39 and Bus 40 show lower voltages indicating voltage drop issues. Bus 40 has the lowest voltage, indicating high voltage drop. Analyzing the data highlights voltage variations among the buses in Case 0. Addressing lower voltages at Buses 38, 39, and 40 is crucial for reliable power system operation.

Figure 4.15 illustrates the voltage profile across buses 41 to 43 in the distribution system. This voltage profile provides valuable information about the voltage levels at these specific buses.

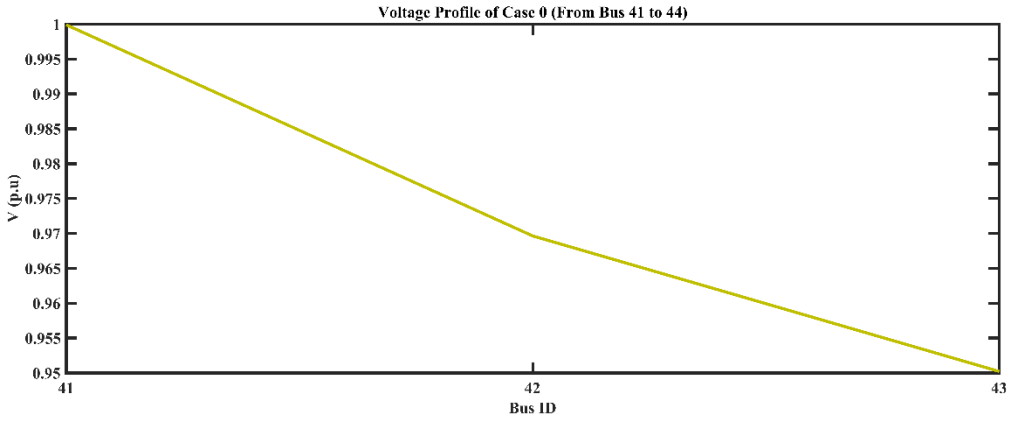

Figure 4.15, Voltage profile of Case 0 (From Bus 41 to 43).

Bus 41 operates at a voltage very close to the nominal level, indicating a stable and reliable power supply. Bus 42 exhibits a slightly lower voltage, but it is still within an acceptable range, suggesting stable voltage conditions. Similarly, Bus 43 has a further decrease in voltage, but it is still within acceptable limits. Overall, the voltage levels at these buses in Case 0 of the distribution system are within acceptable ranges, indicating stable voltage conditions. It is important to monitor and maintain these voltage levels to ensure the reliable operation of connected loads and the overall performance of the power system.

Figure 4.16 illustrates the voltage profile of buses 44 to 50 in Case 0 of the ECG 33 kV distribution system. The data presented represents the voltage levels at these buses within the system.

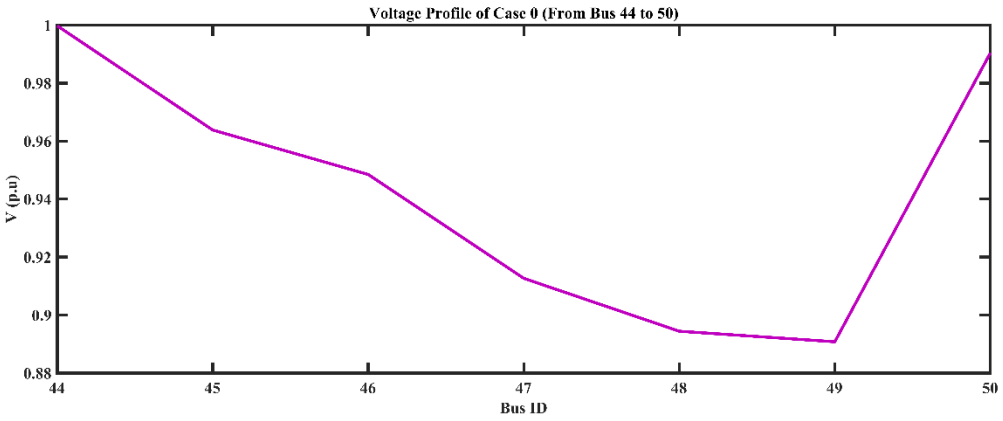

Figure 4.16, Voltage profile of Case 0 (From Bus 44 to 50).

Bus 44 operates at a voltage close to the nominal level, indicating a stable voltage condition and reliable power supply. Bus 45 and Bus 46 experience slightly lower voltages but within an acceptable range as compared to the IEC 60038-2009 standard (Ackermann & Knyazkin, 2002; Standard & Horizontale, 2009). However, Bus 47, Bus 48, and Bus 49, exhibit lower voltages, indicating potential voltage drop that should be addressed to ensure a reliable power supply. Overall, monitoring and maintaining voltage levels across these buses are crucial for the reliable operation performance of the distribution system.

In Case 0, the voltage profiles of different buses show distinct characteristics. Buses 2, 8, 15, 26, 30, 37, 41, and 44, which serve as bulk supply stations, exhibit voltages close to the nominal level, indicating stable voltage conditions with minimal deviation. This suggests a reliable and efficient power supply at these buses.

On the other hand, buses 3, 9, 11, 16, 17, 27, 31, 38, 42, and 45 experience slightly lower voltages compared to the nominal level. Although these voltages deviate from the nominal value, they are still within an acceptable range (Ackermann & Knyazkin, 2002; Standard & Horizontale, 2009), indicating relatively stable voltage conditions.

However, buses 4, 5, 6, 10, 12, 13, 14, 18, 19, 20, 21, 28, 33, 34, 35, 39, 40, 43, 47, 48, and 49 exhibit the lowest voltages. These buses are located far from the bulk supply stations and cater to residential, commercial, and industrial loads. The lower voltages observed in these buses indicate potential voltage drop challenges. Comparing the results to the IEC 60038-2009 standard revealed that many bus voltages fell below the limit of 10% for system bus voltage (Ackermann & Knyazkin, 2002; Standard & Horizontale, 2009). This voltage profile indicates that the network experiences a significant amount of loss, as the required margins fall within a 10% range.

The results of the base case (Case 0), which did not involve the integration of DSTATCOM, have been summarized in Table 4.1. This table presents a comprehensive overview of the total active and reactive power losses in the system and the voltage profile after conducting a power flow analysis. It gives a clear picture of the state of the ECG 33 kV distribution system in the Ashanti region. The information provided in the table is vital in identifying the key areas that require attention and improving the system's overall performance.

Table 4. 1, The Summary Results of Case 0

Parameters	**Case 0**
Total active power loss (MW)	14.530
Total reactive power loss (Mvar)	67.005
Minimum voltage (p.u.)	0.817 at bus 35
Maximum voltage (p.u.)	1 at bus 1
High active and reactive power losses lines	3, 9, 18, 27, 28, 31, 38, 39, 42 and 45

4.2. Case 1: Fixed DSTATCOM Results

In this section, the integration of a fixed DSTATCOM on the ECG 33 kV distribution system in the Ashanti region is discussed, with the aim of improving the voltage profile of each bus and minimizing power losses. Fixed DSTATCOMs are designed to have a constant capacitance value that remains unchanged over time or under normal operating conditions. The analysis of

active and reactive losses and voltage profiles of the distribution system is presented in this section.

The main goal of this research is to reduce power losses and enhance the voltage profile at each bus to improve the overall system performance. To achieve this, a fixed DSTATCOM was optimal at bus 36 with capacity of 1200 kvar in the ECG 33 kV system in the Ashanti region. The integration was successful in maintaining the voltages within the range specified by the IEC 60038-2009 voltage drop standard (Ackermann & Knyazkin, 2002; Standard & Horizontale, 2009).

As a result of the integration, there was a significant reduction in both active and reactive power losses by 58.88% and 58.72%, respectively. This reduction in power losses was achieved by the fixed DSTATCOM compensating for the reactive power in the system. The voltage profile was also improved, which will ultimately lead to a reduction in losses and enhanced system performance.

4.2.1. Power Loss of Case 1

The integration of a fixed DSTATCOM into the ECG 33 kV distribution system resulted in a significant decrease in total active power loss. Figure 4.17 provides a visual representation of the power losses of lines 2, 3, 4, 5, 6 and 7 after the integration of fixed DSTATCOM. The reduction in power losses is a positive development as it leads to a more efficient distribution system, which can translate into cost savings for the power company and improved service for consumers.

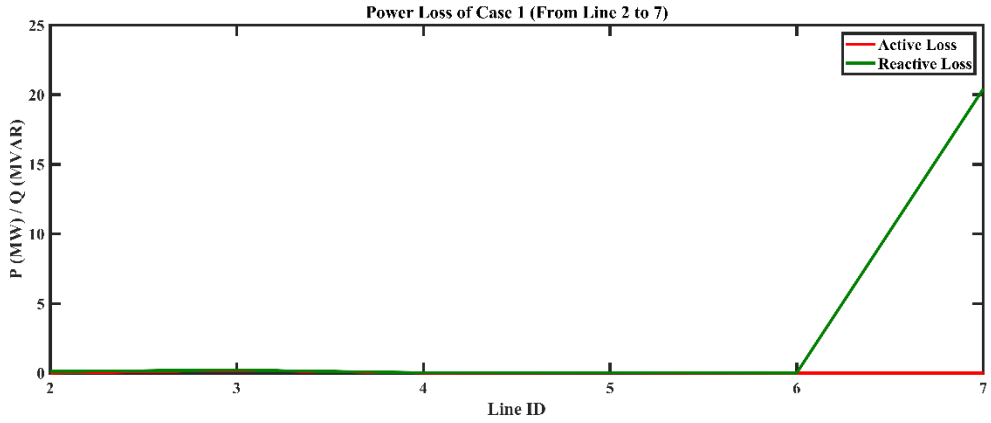

Figure 4.17, Active and reactive power loss of Case 1 (Line 2 to 7).

Line 2 demonstrates efficient power distribution and consumption, with a low active loss of 0.002 MW and a modest reactive loss of 0.041 Mvar. In contrast, Line 3 experiences higher losses, with an active loss of 0.195 MW and a reactive loss of 0.165 Mvar, likely due to inadequate voltage regulation. Lines 4 to 7 have relatively low losses, indicating effective management. Overall, evaluating power losses provides insights into system efficiency. Minimizing losses is vital for improving overall efficiency and reducing energy wastage.

Figure 4.18 below illustrates the power losses through lines 8 to 14 in the ECG 33kV distribution system. This power losses provides valuable information about the energy wasted levels at these specific lines.

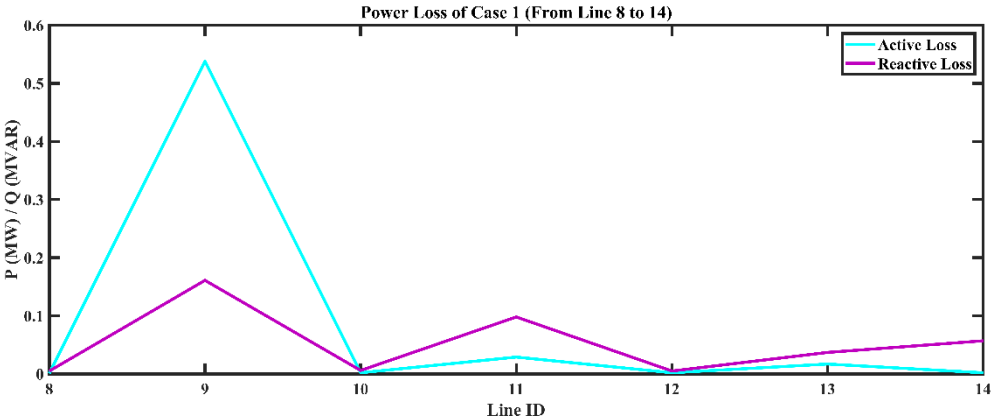

Figure 4.18, Active and reactive power loss of Case 1 (Line 8 to 14).

Line 8 demonstrates a relatively low active loss of 0.001 MW and a small reactive loss of 0.005 Mvar, indicating efficient power distribution along this line. In contrast, Line 9 experiences a slightly higher active loss of 0.002 MW, but it has a significant reactive loss of 0.161 Mvar. Lines 10, 11, 12, 13, and 14 all exhibit moderate power losses, with active losses ranging from 0.001 MW to 0.005 MW and reactive losses ranging from 0.005 Mvar to 0.098 Mvar. These losses attributed to the presence of reactive loads. Overall, the data highlights the varying power losses across different lines in Case 1. Figure 4.19 below illustrates the power losses associated with lines 15 to 25.

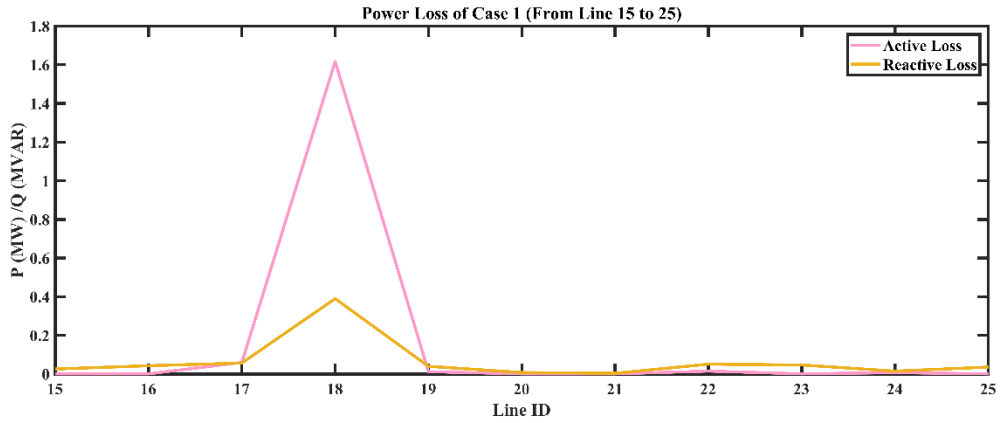

Figure 4.19, Active and reactive power loss of Case 1 (Line 15 to 25).

Line 15 and 16 demonstrate efficient power distribution with minimal losses, while Line 17 and 18 shows higher losses indicating potential issues. Lines 19 to 25 exhibit low losses, indicating efficient distribution. Analyzing the power losses in Case 1 emphasizes the need to minimize losses for improved efficiency. Figure 4.20 depicts the power losses occurring across lines 26 to 29 in the ECG 33kV distribution system. This visual representation offers important insights into the levels of losses occurring at these particular lines.

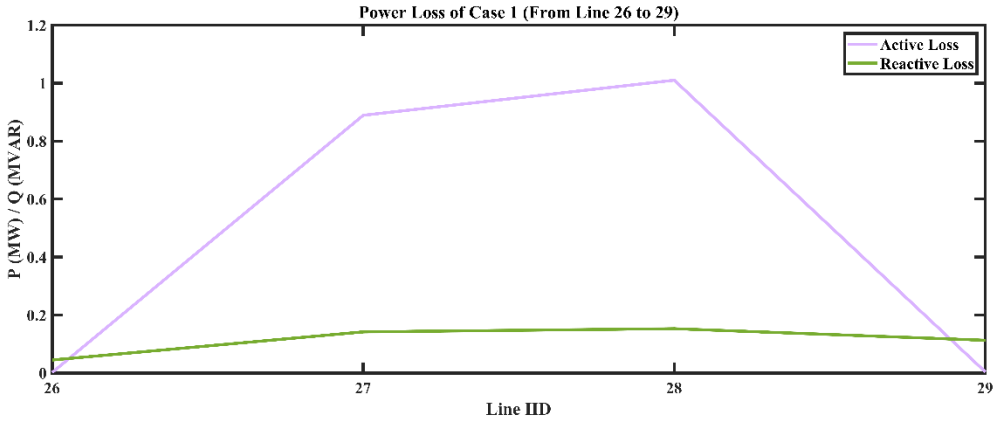

Figure 4.20, Active and reactive power loss of Case 1 (Line 26 to 29).

The power loss data for lines 26 to 29 in Case 1 of the ECG 33kV distribution system shows that Line 26 has relatively low losses, while Lines 27 and 28 have significantly higher losses. Addressing the higher losses in Lines 27 and 28 will be crucial to improve the efficiency and reliability of the power distribution network. Figure 4.21 below shows the power losses between lines 26 to 29 in the ECG 33kV distribution system.

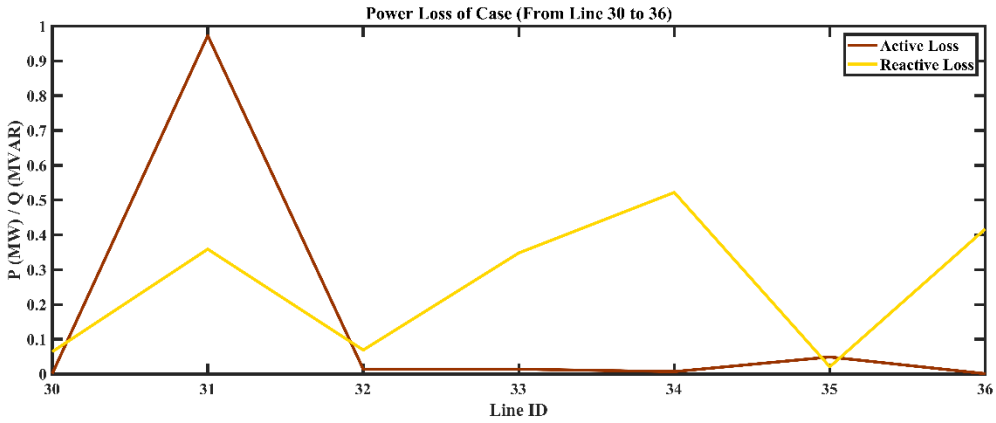

Figure 4.21, Active and reactive power loss of Case 1 (Line 30 to 36).

The Figure 4.21 shows that the active losses for lines 30, 32, 35, and 36 are relatively low, while the active losses for lines 31, 33, and 34 are significantly higher.

The low active losses for lines 30, 32, 35, and 36 suggest that these lines are relatively efficient.

The high active losses for lines 31, 33, and 34 suggest that these lines may be experiencing

some inefficiencies. These inefficiencies could be due to a excessive load demand on the system. Line 35 demonstrates a relatively higher active loss of 0.049 MW but a low reactive loss of 0.021 Mvar because of less reactive power along the line. The power losses (active and reactive) of 37 to 40 are depicted in Figure 4.22.

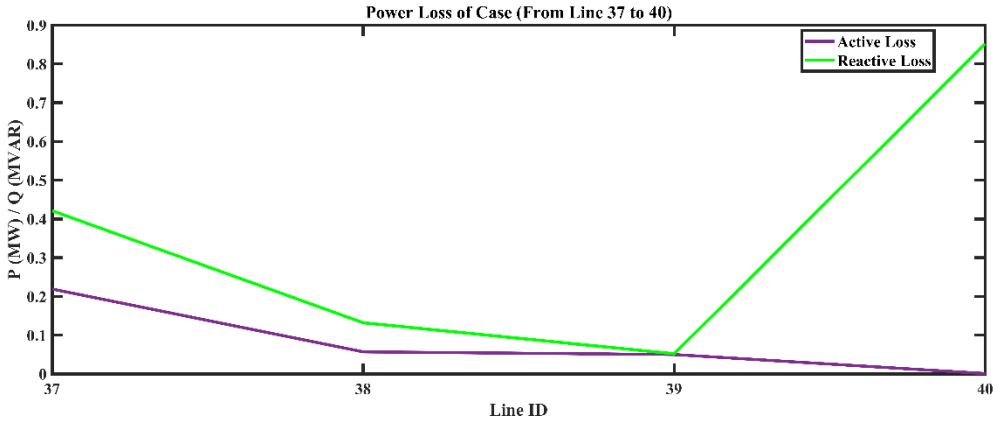

Figure 4.22, Active and reactive power loss of Case 1 (Line 37 to 40).

Line 37 has higher active and reactive losses, suggesting power distribution inefficiencies due to impedance. Line 38 has moderate losses, while Line 39 demonstrates efficient power distribution. Line 40 has low active loss but significant reactive loss, indicating issues with reactive power management and voltage regulation that need to be resolved for enhanced system performance. Figure 4.23 below shows the power losses associated with lines 41 to 43 of the ECG 33 kV distribution system.

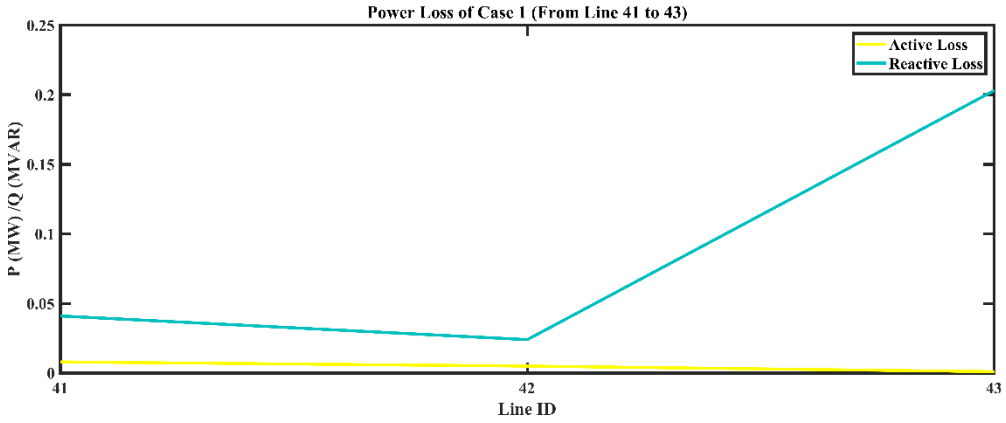

Figure 4.23, Active and reactive power loss of Case 1 (Line 41 to 43).

Line 41 shows moderate active loss and relatively low reactive loss, indicating acceptable power distribution efficiency. Line 42 demonstrates lower active loss and minimal reactive loss, suggesting efficient power distribution. However, Line 43 has very low active loss but significant reactive loss, indicating potential issues with reactive power management and voltage regulation. Figure 4.24 shows the power losses for lines 44 to 50 in the ECG 33 kV distribution system.

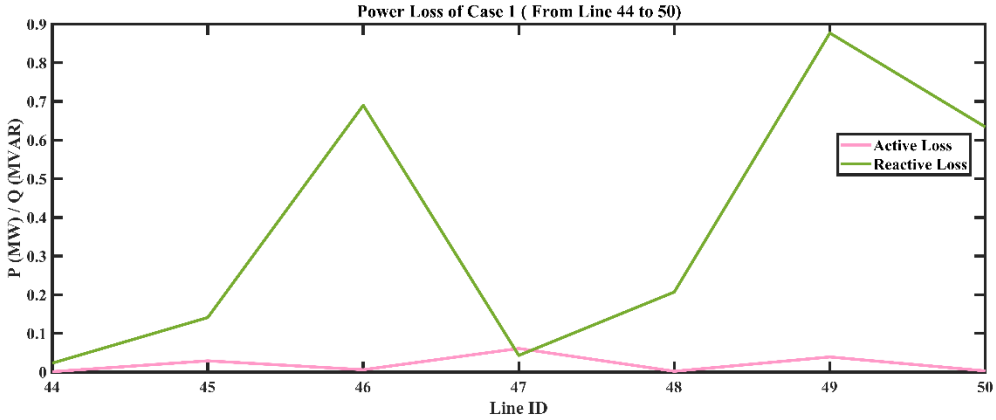

Figure 4.24, Active and reactive power loss of Case 1 (Line 44 to 50).

Line 44 demonstrates efficient power distribution with minimal active and reactive losses. In contrast, Line 45 experiences moderate losses in both active and reactive power. Line 46 has low active loss but significant reactive loss, indicating potential issues with reactive power

management. Line 47 has higher active loss but relatively low reactive loss, while Line 48 exhibits very low active loss but significant reactive loss. Similarly, Lines 49 and 50 have minimal active loss but significant reactive loss.

It can be concluded in Case 1 that Lines 3, 9, 18, 27, 28, and 31 in the ECG 33 kV distribution network have the moderate power losses which are within acceptable range (Ackermann & Knyazkin, 2002; Standard & Horizontale, 2009). These lines demonstrate less significant levels of power dissipation. Assessing these lines can offer valuable observations for optimizing the distribution network and improving its overall efficiency and dependability.

4.2.2. Voltage Profile of Case 1

To improve the voltage profile, a fixed DSTATCOM with a capacity of 1200 kvar was optimally located on the 33 kV distribution system bus 36 in the Ashanti Region using the Particle Swarm Optimization (PSO) technique. After the integration of the fixed DSTATCOM, the voltage profile was analyzed and the results of buses 2 to 7 were presented in Figure 4.25.

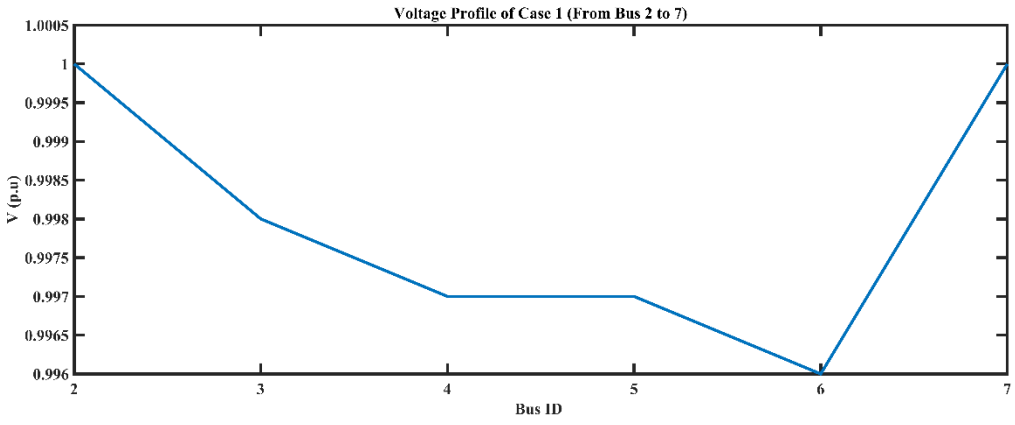

Figure 4.25, Voltage profile of Case 1 (From Bus 2 to 7).

From the Figure 4.25 above, it can be observed that Bus 2 and Bus 7 operates at the nominal voltage level of 1 per unit (p.u.), indicating a stable voltage condition. Buses 3 to 6 exhibit slightly lower voltage levels, ranging from 0.998 p.u. to 0.996 p.u. These deviations from the

nominal voltage indicate a small drop in voltage but are still within an acceptable range (Ackermann & Knyazkin, 2002; Standard & Horizontale, 2009). Figure 4.26 shows the voltage profile between bus 8 to 14 in the ECG 33kV distribution system. Examining the voltage data of bus 8 to 14 provides insights into the voltage levels and conditions at these specific buses in the power system.

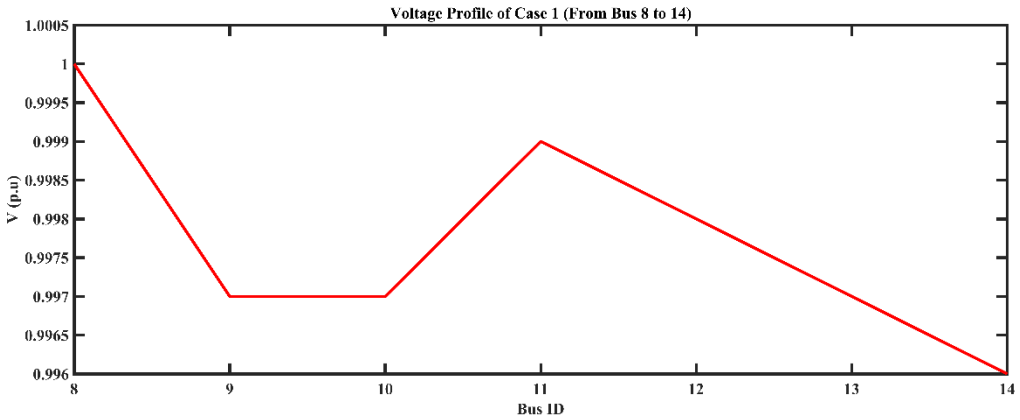

Figure 4.26, Voltage profile of Case 1 (From Bus 8 to 14).

Bus 8 operates at the nominal voltage level of 1 per unit (p.u.), indicating a stable voltage condition. This suggests that the voltage at Bus 8 is within an acceptable range and reflects efficient power supply.

Buses 9 to 14 exhibit slightly lower voltage levels, ranging from 0.997 p.u. to 0.996 p.u. These deviations from the nominal voltage indicate a small drop in voltage but are still within a tolerable range (Ackermann & Knyazkin, 2002; Standard & Horizontale, 2009). It is important to maintain these voltage levels to ensure reliable power supply to connected loads. The voltage levels at buses 15 to 25 in the ECG 33kV distribution system can be observed in Figure 4.27.

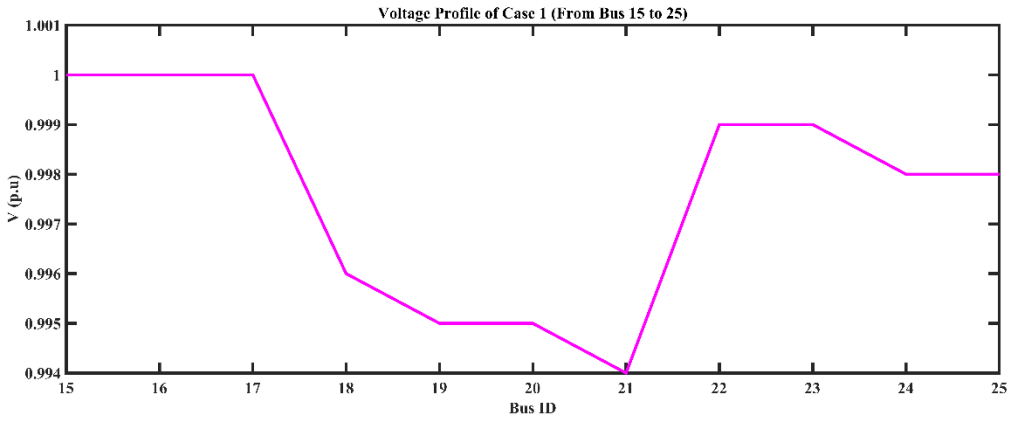

Figure 4.27, Voltage profile of Case 1 (From Bus 15 to 25).

Buses 15, 16, and 17 all exhibit a voltage of 1 p.u., indicating that they operate at the nominal voltage level. This suggests stable voltage conditions at these buses. Bus 18, 19, 20, 21, 24, and 25 has a slightly lower voltage, ranging from 0.995 p.u. to 0.998 p.u. , indicating a small deviation from the nominal voltage. Although lower than the nominal value, the voltage level is still within an acceptable range (Ackermann & Knyazkin, 2002; Standard & Horizontale, 2009), suggesting relatively stable voltage conditions at this buses. Figure 4.28 below shows the voltage levels at buses 26 to 29 in the ECG 33kV distribution system.

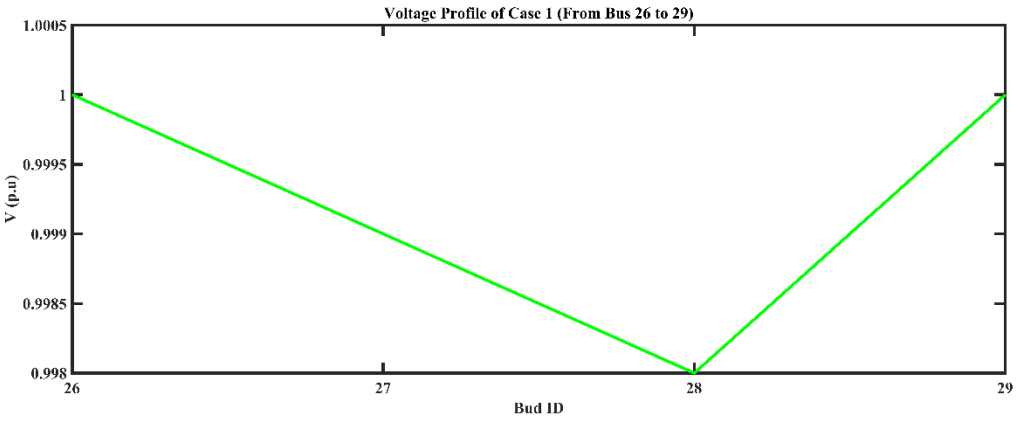

Figure 4.28, Voltage profile of Case 1 (From Bus 26 to 29).

Bus 26 maintains the nominal voltage level of 1 p.u., indicating stable voltage conditions. Similarly, buses 27 and 29 are very close to the nominal voltage level. This recommends stable

voltage conditions with minimal deviation, ensuring reliable power supply. Bus 28, however, has a slightly lower voltage of 0.998 p.u., indicating a small deviation from the nominal voltage. The voltage levels at buses 30 to 36 in the ECG 33kV distribution system are illustrated in Figure 4.29 below.

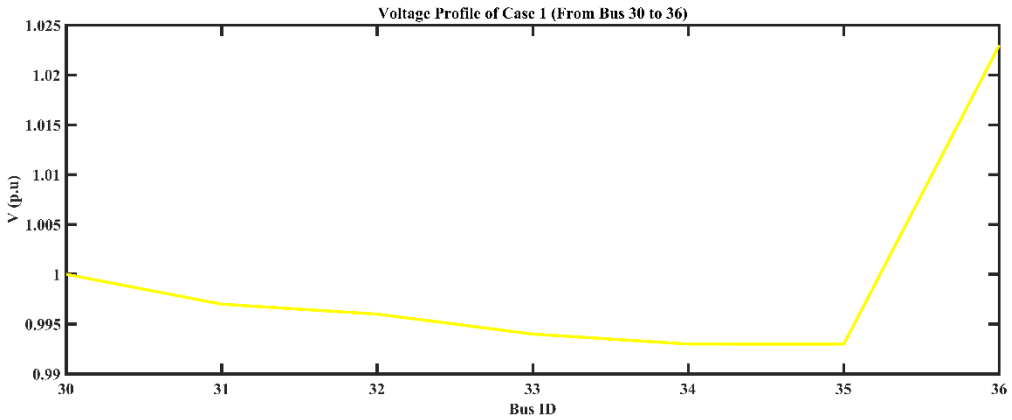

Figure 4.29, Voltage profile of Case 1 (From Bus 30 to 36).

Bus 30 operates at a voltage of 1 p.u., indicating that it maintains the nominal voltage level. Bus 31 to 35 operate at voltages ranging from 0.993 p.u. to 0.997 p.u., which are slightly lower than the nominal voltage level but still within an acceptable range. These buses exhibit stable voltage conditions with minor deviations. However, Bus 36 operates at a voltage of 1.023 p.u. due to the DSTATCOM on that bus as a optimal place, which is a little bit more than the nominal voltage level. The Figure 4.30 below, shows the voltage profile of buses 37 to 40 in the ECG 33kV distribution system.

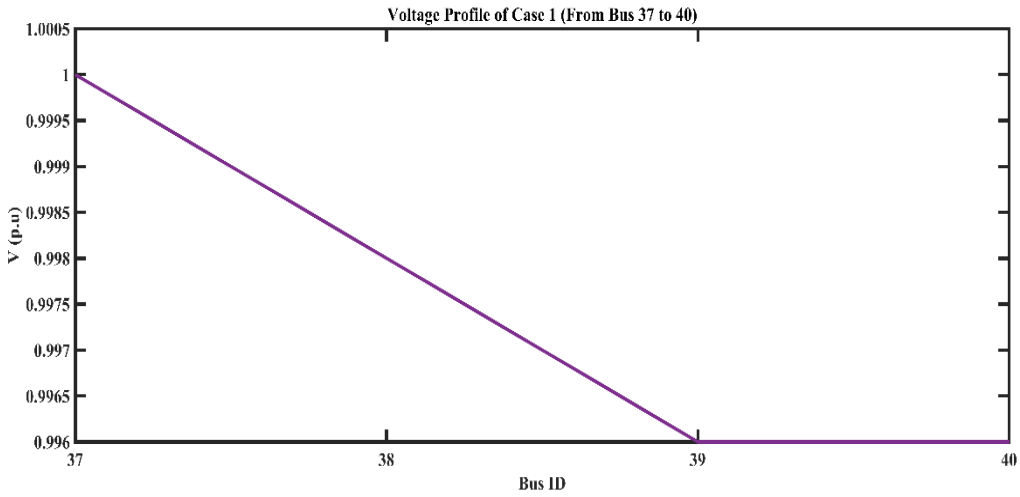

Figure 4.30, Voltage profile of Case 1 (From Bus 37 to 40).

Bus 37 maintains the nominal voltage level of 1 p.u. This suggests stable voltage conditions at this bus. Similarly, Bus 38 to 40 operate at voltages ranging from 0.996 p.u. to 0.998 p.u., which are marginally below the nominal voltage level but still within acceptable bounds. These buses exhibit stable voltage conditions with minor deviations. The voltage profile of buses 41 to 43 in the ECG 33kV distribution system are shown in Figure 4.31.

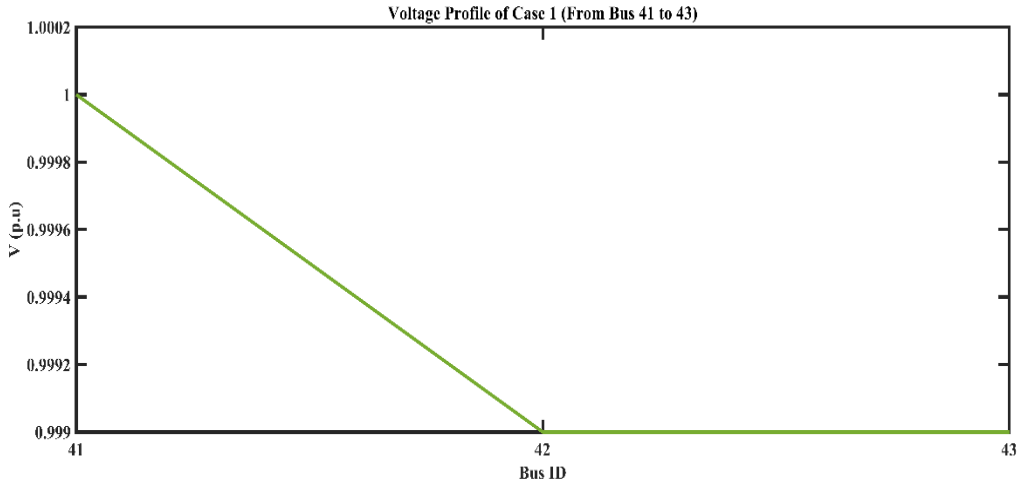

Figure 4.31, Voltage profile of Case 1 (From Bus 41 to 43).

In Case 1, Bus 41 serve as reference bus of this distribution feeder and operates at a voltage of 1 p.u., indicating that it maintains the nominal voltage level. Bus 42 and Bus 43 operate at

voltages of 0.999 p.u., which are very close to the nominal voltage level. These buses also exhibit stable voltage conditions with minimal deviation. Overall, the voltage profile of buses 41 to 43 in Case 1 indicates reliable and stable power supply. The voltage profile of buses 44 to 50 are depicted in Figure 4.32.

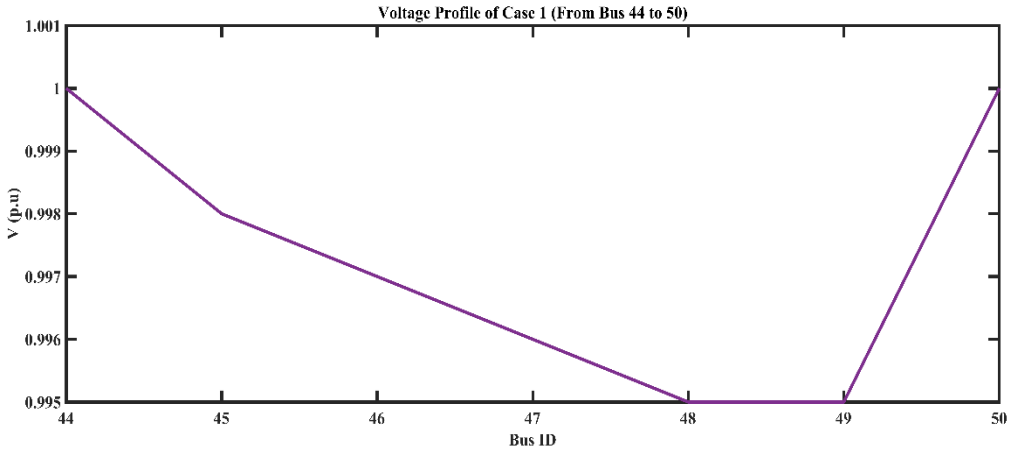

Figure 4.32, Voltage profile of Case 1 (From Bus 44 to 50).

Bus 44 and 50 maintain the nominal voltage level and proposes stable voltage conditions. Bus 45 to Bus 49 exhibit slightly lower voltages ranging from 0.995 p.u. to 0.998 p.u. These buses still demonstrate relatively stable voltage conditions. Overall, power losses and voltage profile of Case 1 generally proposes stable conditions (Ackermann & Knyazkin, 2002; Standard & Horizontale, 2009).

The Table 4.2 below, is a summary results obtained after carrying out the power flow analysis in Case 1. The table provides a comprehensive overview of the total active and reactive power losses experienced in the section, as well as the maximum and minimum voltage profile that was observed on the buses during the analysis.

Table 4. 2, The Summary Results of Case 1

Performance Measurement	Case 1
Minimum Bus Voltage (p.u.)	0.993
Maximum Bus Voltage (p.u.)	1.023
Total Active Power Loss (MW)	5.9752
Total Reactive Power Loss (Mvar)	28.4925
DSTATCOM Power Injection (kvar) and Location	1200 at bus 36
Number of DSTATCOM	1
Active Power Loss Percentage	41.12%
Reactive Power Loss Percentage	41.15%

4.3. Case 2: Switched DSTATCOM Results

Case 2 involved the installation of two switched DSTATCOMs, both having a size of 150 kvar. This section discusses how the line losses and voltage profile of each bus were improved through the integration of a switched DSTATCOM on the ECG 33 kV distribution system in the Ashanti region. The switched DSTATCOM works as a variable capacitance that can be adjusted to optimize system performance. The main goal of this research was to decrease the amount of power losses and enhance the voltage profile at each bus. In order to achieve this, two switched DSTATCOMs were installed on Bus 26 and Bus 30 in the ECG 33 kV system in the Ashanti Region, which helped to maintain the voltage within acceptable limits and minimize power losses of the distribution system (Ackermann & Knyazkin, 2002; Standard & Horizontale, 2009). As a result of this integration, both active and reactive power losses decreased by 41.28% and 3.31%, respectively. This shows that the integration of switched DSTATCOM was effective in enhancing the performance of the system and improving its efficiency.

4.3.1. Active Power Loss of Case 2

The Figure 4.33 below provides a visual representation of the power loss of Buses 2 to 7. The graph clearly shows the significant drop in power loss after incorporating the switched DSTATCOM, which confirms the effectiveness of this solution in reducing power losses.

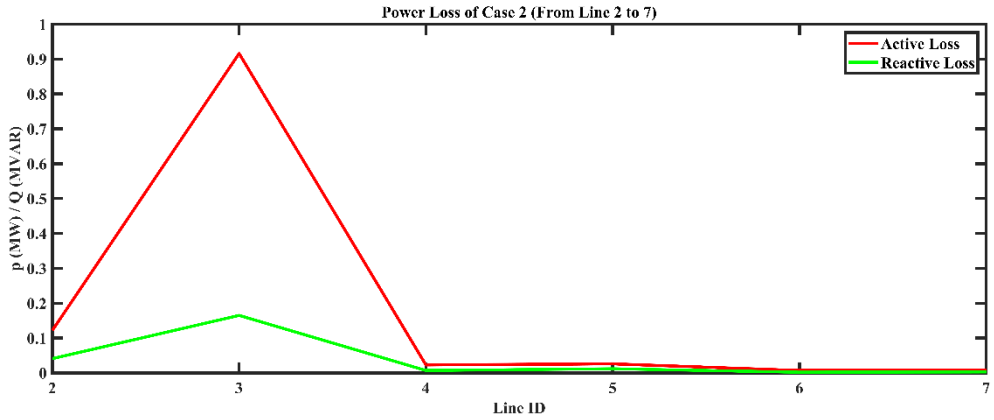

Figure 4.33, Active and reactive power loss of Case 2 (Line 2 to 7).

Line 2 experiences a moderate level of power loss, with an active loss of 0.122 MW and a reactive loss of 0.041 Mvar, indicating some power dissipation during distribution. On the other hand, Line 3 shows higher losses, with an active loss of 0.916 MW and a relatively higher reactive loss of 0.165 Mvar, suggesting potential inefficiencies and challenges in power distribution that need to be addressed. Lines 4, 5, 6, and 7 exhibit relatively low power losses, indicating more efficient power distribution. Figure 4.34 below illustrates the power losses for lines 8 to 14 of the distribution system.

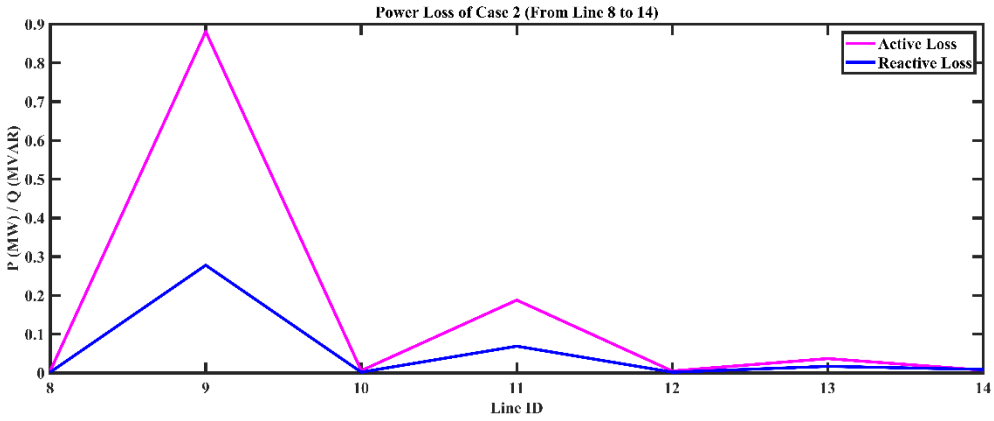

Figure 4.34, Active and reactive power loss of Case 2 (Line 8 to 14).

After the integration of switched DSTATCOM, Lines 8, 10, 12 and 14 exhibits a relatively low active losses and a very low reactive loss, signifying efficient power distribution with minimal

energy wastage. In contrast, Lines 9, 11 and 13 experiences moderate losses for both active and reactive. Figure 4.35 below illustrates the power losses through lines 15 to 25 in the ECG 33kV distribution system.

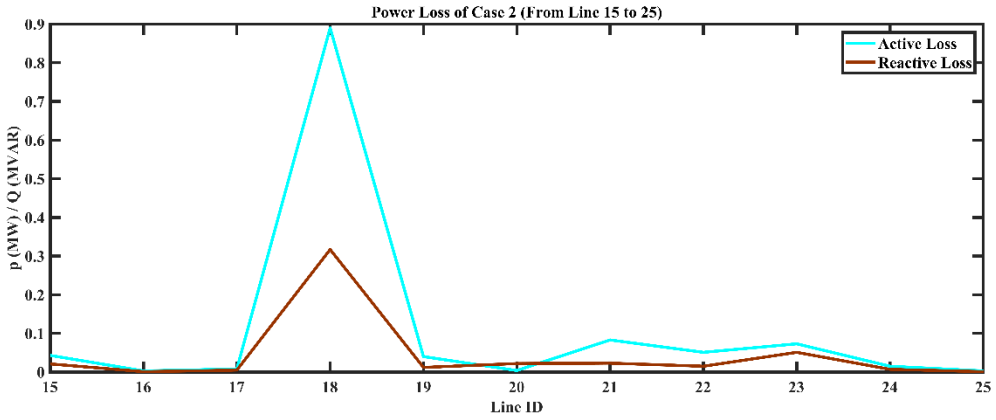

Figure 4.35, Active and reactive power loss of Case 2 (Line 15 to 25).

Lines 16, 17, 24 and 25 demonstrates very low losses, indicating efficient power distribution and minimal energy wastage. Lines 15, 19, 20, 21, 22 and 23 has moderate power losses, indicating power dissipation along the line. Line 18 experiences higher losses, which attributed to commercial and industrial load demand. The power losses incurred on lines 26 to 29 in the ECG 33kV distribution system are depicted in Figure 4.36 below.

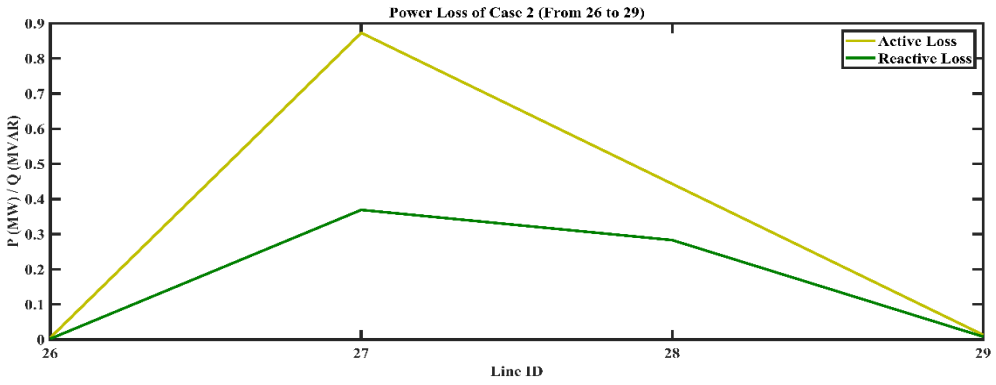

Figure 4. 36, Active and reactive power loss of Case 2 (Line 26 to 29).

Lines 26 and 29 exhibits a relatively low active loss and a minimal reactive loss, indicating efficient power distribution along this line after switched DSTATCOM integrated on neighbouring buses. Lines 27 and 28 experiences a higher active loss and a significant reactive loss. These losses occurred due to the load demand on these vicinities. Figure 4.37 displays the power losses experienced on lines 30 to 36 in the ECG 33kV distribution system.

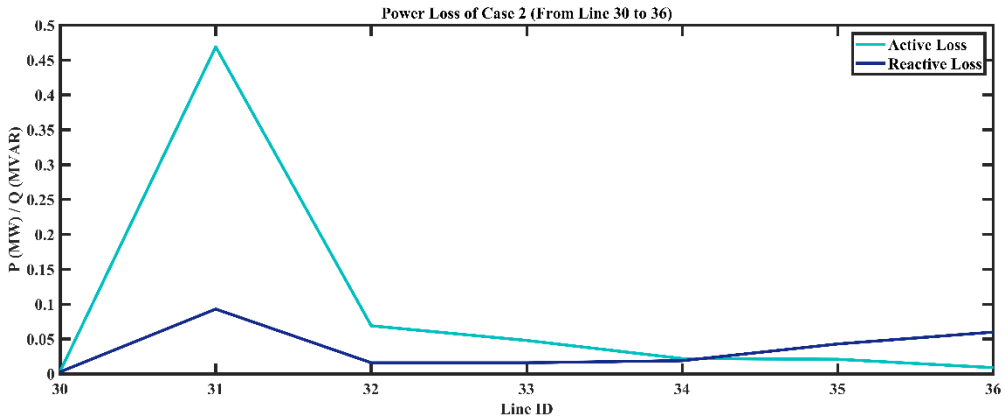

Figure 4.37, Active and reactive power loss of Case 2 (Line 30 to 36).

Line 30 demonstrates efficient power distribution with a relatively low active loss of 0.004 MW and a small reactive loss of 0.003 Mvar, due to the integration of DSTATCOM. This integration helps minimize energy dissipation along this line. On the other hand, Lines 32 to 36 exhibit different levels of power losses, ranging from moderate to low in both active and reactive components. In contrast, Line 31 experiences higher active losses of 0.469 MW and moderate reactive losses of 0.093 Mvar. The power losses on lines 37 to 40 in the ECG 33kV distribution system are illustrated in Figure 4.38 below.

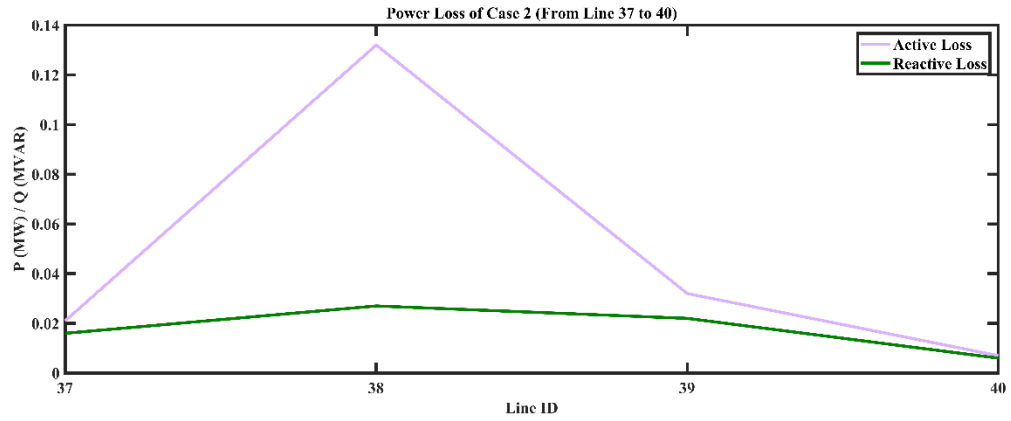

Figure 4.38, Active and reactive power loss of Case 2 (Line 37 to 40).

Lines 37, 39, and 40 demonstrate minimal active and reactive losses due to the integration of switched DSTATCOM. These losses indicate efficient power distribution with minimal energy dissipation. In contrast, Line 38 shows a moderate active loss of 0.132 MW and a modest reactive loss of 0.027 Mvar. Figure 4.39 below provides a visual representation of the power losses occurring on lines 41 to 43 in the ECG 33kV distribution system.

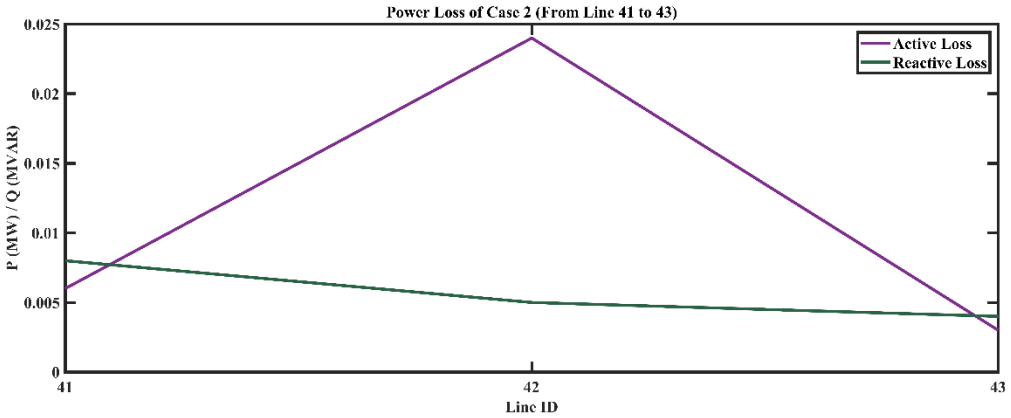

Figure 4.39, Active and reactive power loss of Case 2 (Line 41 to 43).

Line 41 and Line 43 demonstrate relatively low losses in both active and reactive power. In contrast, Line 42 displays a moderate active loss of 0.024 MW and a modest reactive loss of 0.005 Mvar. These losses propose efficient power distribution with minimal energy dissipation

along this line. The power losses experienced on lines 44 to 50 in the ECG 33kV distribution system are represented in Figure 4.40 below.

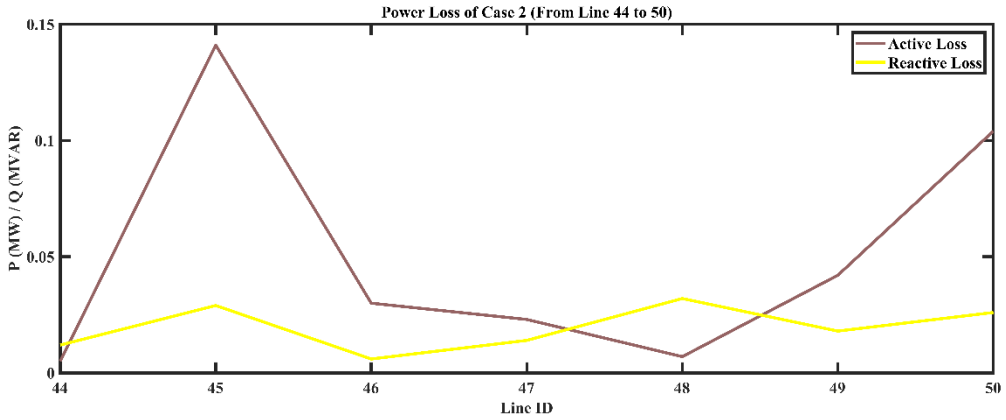

Figure 4.40, Active and reactive power loss of Case 2 (Line 44 to 50).

Line 44 exhibits a relatively low active loss of 0.005 MW and a moderate reactive loss of 0.012 Mvar. Line 45 experiences a higher active loss of 0.141 MW and a modest reactive loss of 0.029 Mvar. Lines 46 to 50 exhibit varying levels of power losses. They demonstrate moderate to low active and reactive losses, indicating relatively efficient power distribution with effective loss management.

Overall, minimizing power losses is crucial for improving the overall system efficiency and reducing unnecessary energy wastage. In Case 2 of the ECG 33 kV distribution network, several lines, specifically Lines 3, 9, 18, 27, 28, 31, 38, 42, and 45, exhibit moderate power losses that fall within an acceptable range according to the standards set by (Ackermann & Knyazkin, 2002; Standard & Horizontale, 2009). These lines demonstrate relatively lower levels of power dissipation. Analyzing these specific lines can provide valuable insights for optimizing the distribution network and enhancing its overall efficiency and reliability.

4.3.2. Voltage Profile of Case 2

Figure 4.41 presents the voltage profile analysis of the ECG 33 kV distribution system after integrating the switched DSTATCOMs. The voltage profiles were examined to evaluate the effectiveness of the switched DSTATCOMs in improving the voltage stability of the system. After the integration of the switched DSTATCOM, the voltage profile of buses 2 to 7 was examined and the findings were shown in Figure 4.41.

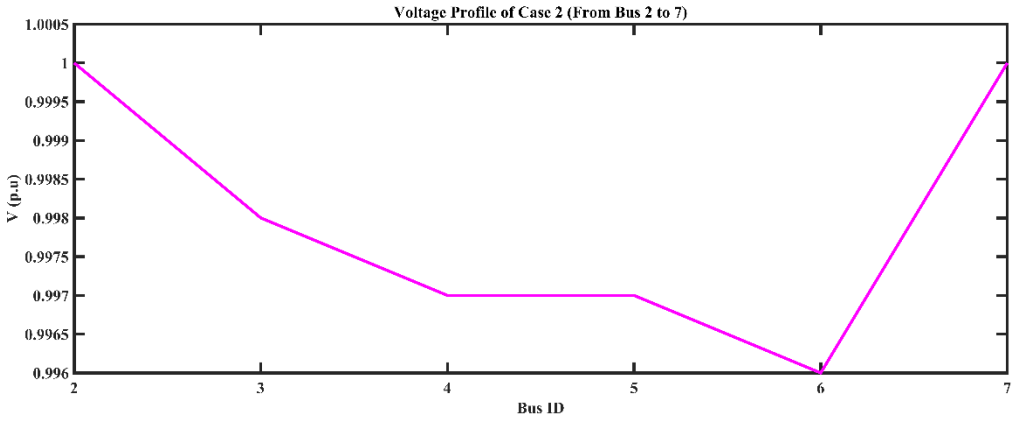

Figure 4.41, Voltage profile of Case 2 (From Bus 2 to 7).

The voltage profile of buses 2 to 7 in Case 2 indicates that Bus 2 operates at a voltage of 1 per unit (p.u.), while Buses 3, 4, and 5 operate at slightly lower voltages of 0.998 p.u., which are within an acceptable range. Bus 6 operates at a voltage of 0.996 p.u., slightly lower than the nominal level. However, Bus 7 maintains a voltage of 1 p.u. Overall, these findings demonstrate stable voltage conditions with minor deviations from the nominal voltage, indicating effective voltage regulation and reliable power supply through the integration of the switched DSTATCOM. The analysis of the voltage profile for buses 8 to 14 was conducted, and the results were illustrated in Figure 4.42.

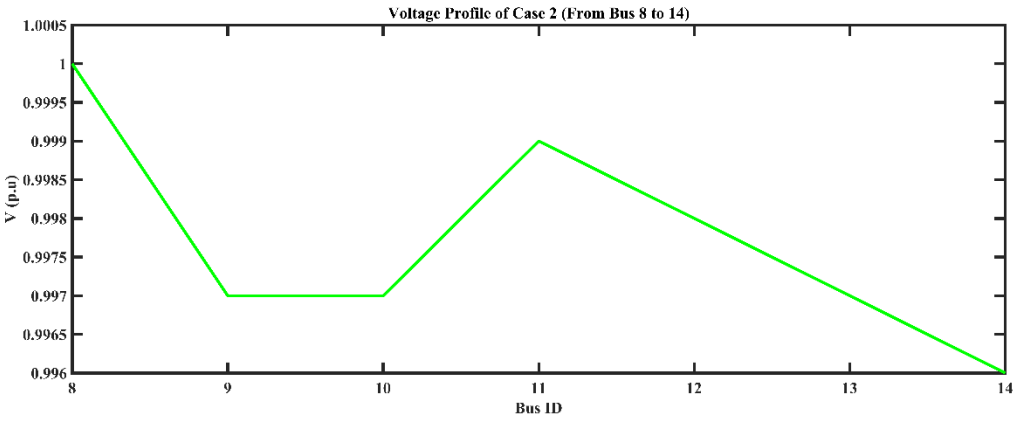

Figure 4.42, Voltage profile of Case 2 (From Bus 8 to 14).

Bus 8 operates at the nominal voltage level of 1 per unit (p.u.), while buses 9, 10, 11, 12, 13, and 14 have voltage levels slightly below the nominal voltage, ranging from 0.996 p.u. to 0.999 p.u. These findings signify that the voltage levels at these buses in Case 2 are within a tolerable range (Ackermann & Knyazkin, 2002; Standard & Horizontale, 2009), signifying stable voltage conditions in the ECG 33kV distribution system. The voltage profile of buses 15 to 25 was examined, and the findings were presented in Figure 4.43 below.

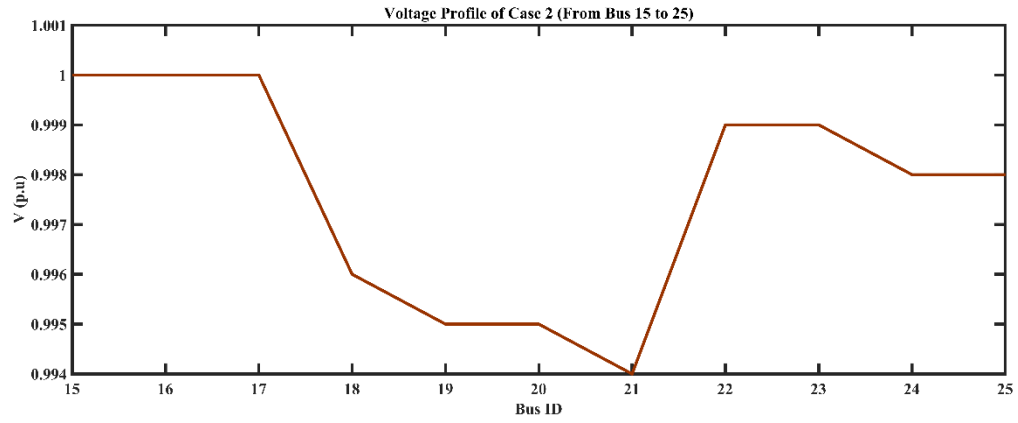

Figure 4.43, Voltage profile of Case 2 (From Bus 15 to 25).

In Case 2, the voltage levels of buses 15 to 25 in the ECG 33kV distribution system were assessed. Buses 15 to 17 operated at the nominal voltage level of 1 p.u., ensuring stable and reliable power supply. Buses 18 to 25 had slightly lower voltages ranging from 0.994 p.u. to

0.999 p.u., indicating minor deviations from the nominal level but remaining within an acceptable range. This analysis confirms the system's stable voltage conditions, enhancing the reliability and efficiency of the ECG 33kV distribution network. The voltage levels observed on buses 26 to 29 in the ECG 33kV distribution system are shown in Figure 4.44 below.

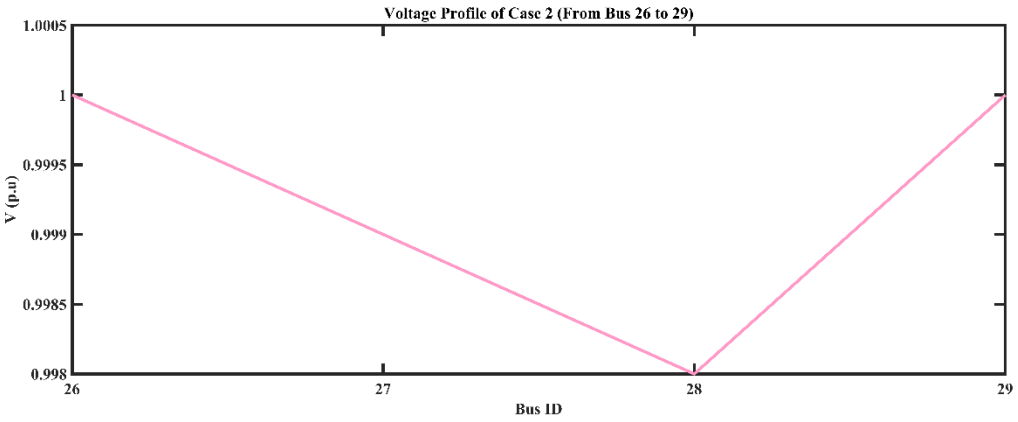

Figure 4.44, Voltage profile of Case 2 (From Bus 26 to 29).

Buses 26 and 29 maintain a voltage of 1 per unit (p.u.), while buses 27 and 28 operate at voltages very close to the nominal voltage level. This proposes stable voltage conditions with minimal deviation, indicating reliable power supply at these buses. The voltage profiles of buses 30 to 36 in the ECG 33kV distribution system are depicted in Figure 4.45 below.

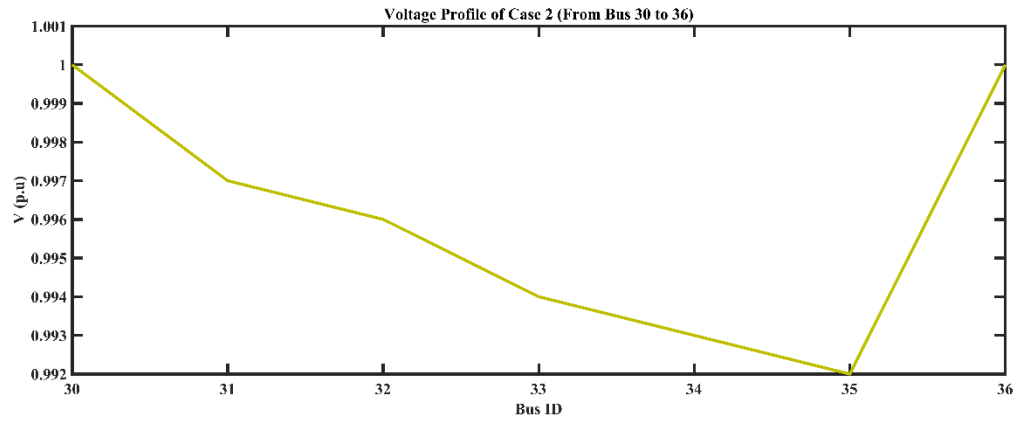

Figure 4.45, Voltage profile of Case 2 (From Bus 30 to 36).

Buses 30 and 36 in the ECG 33kV distribution system operate at the nominal voltage level of 1 per unit (p.u.) while the voltages in buses 31 to 35, range from 0.992 p.u. to 0.997 p.u., which are almost below the nominal level. These buses exhibit slight voltage variations from the nominal value, but they fall within acceptable bounds (Ackermann & Knyazkin, 2002; Standard & Horizontale, 2009), signifying steady voltage conditions. The voltage levels observed on buses 37 to 40 in the ECG 33kV distribution system are illustrated in Figure 4.46 below.

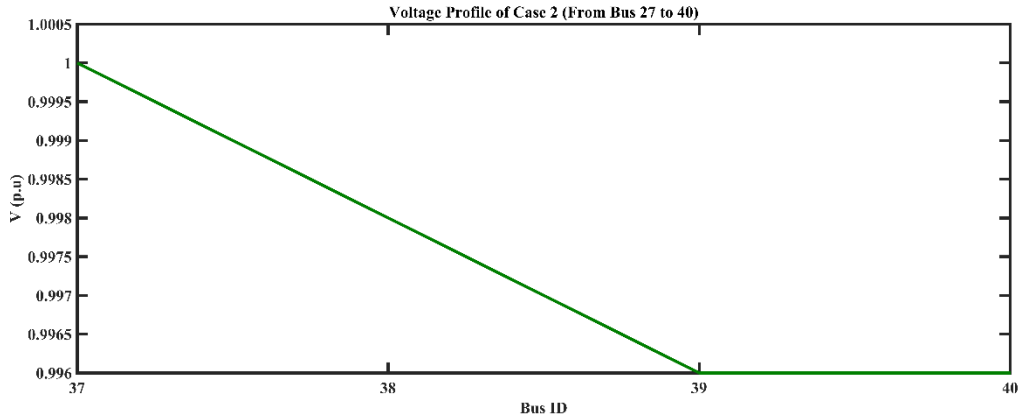

Figure 4.46, Voltage profile of Case 2 (From Bus 37 to 40).

Bus 37 maintains the nominal voltage level of 1 per unit (p.u.). Bus 38 operates at a voltage of 0.998 p.u., while buses 39 and 40 operate at voltages of 0.996 p.u., which is slightly below the nominal voltage level. These voltage levels indicate relatively stable conditions of the ECG 33kV distribution system. Figure 4.47 below shows the voltage profiles of buses 41 to 43 in the ECG 33kV distribution system.

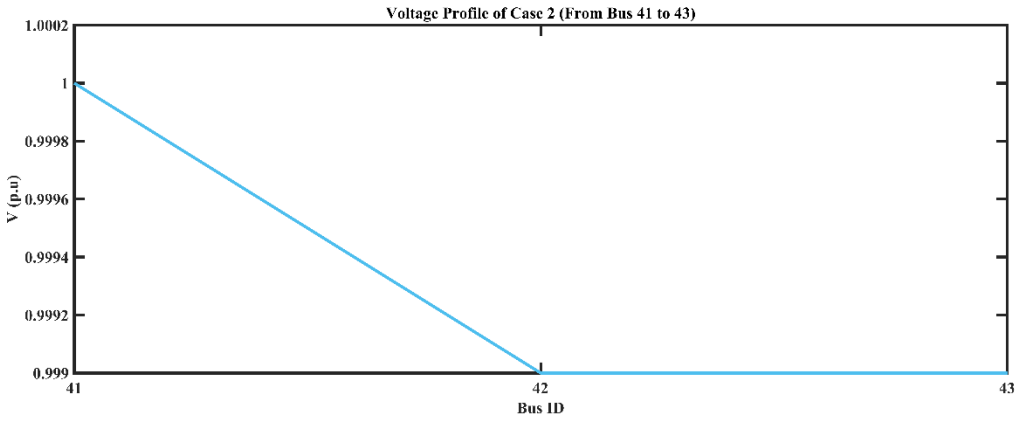

Figure 4.47, Voltage profile of Case 2 (From Bus 41 to 43).

Bus 41 maintains a voltage of 1 per unit (p.u.), while buses 42 and 43 operate at voltages that are very close to the nominal level, with values of 0.999 p.u. These voltage levels indicate a stable and reliable power supply at these buses in the ECG 33kV distribution system. The voltage profiles of buses 44 to 50 in the ECG 33kV distribution system are presented in Figure 4.48 below.

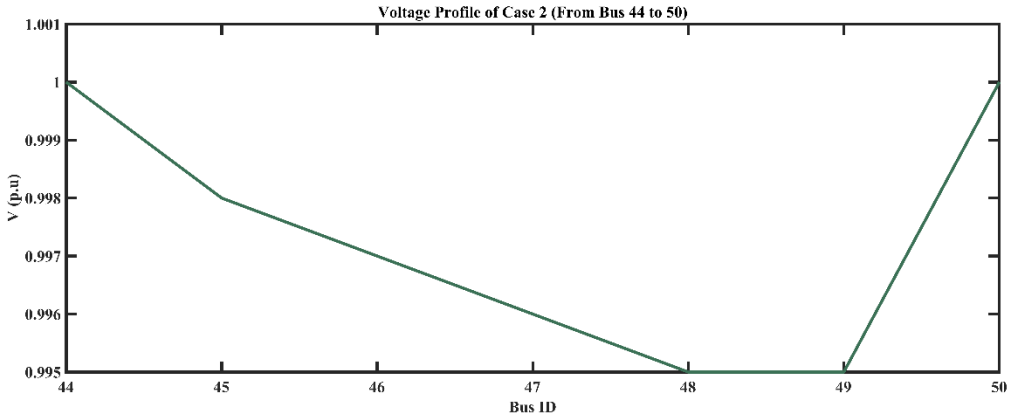

Figure 4.48, Voltage profile of Case 2 (From Bus 44 to 50).

In Case 2, the voltage levels of buses 44 to 50 in the ECG 33kV distribution system were evaluated. Buses 44 and 50 maintains a voltage of 1 per unit (p.u.) and buses 45 to 49 with voltage values ranging from 0.995 p.u. to 0.998 p.u. These buses exhibit minor deviations from the nominal voltage but remain within an acceptable range. Bus 50 also operates at the nominal

voltage level of 1 p.u. In conclusion, Case 2 suggests stable voltage conditions with minimal deviations from the nominal voltage level in the ECG 33kV distribution system.

The outcomes of Case 2 are summarized in Table 4.3, which can be found below. After doing the power flow analysis, here is an extensive overview of the active and reactive power losses that happened in this section as well as the voltage profile that transpired on buses.

Table 4. 3, The Summary Results of Case 2

Performance Measurement	**Case 2**
Minimum Bus Voltage (p.u.)	0.992
Maximum Bus Voltage (p.u.)	1
Total Active Power Loss (MW)	5.99832
Total Reactive Power Loss (Mvar)	2.2205
DSTATCOM Power Injection (kvar) and Location	150 at bus 26 150 at bus 30
Number of DSTATCOM	2
Active Power Loss Percentage	41.28%
Reactive Power Loss Percentage	3.31%

4.4. Discussion of Case 0, Case 1, and Case 2

This section compares the three cases and evaluates the cost-effectiveness of the ECG 33 kV distribution system by examining the total energy cost and annual cost before and after the integration of DSTATCOM. Case 0 represents the reference case, while Case 1 and Case 2 correspond to interventions in the ECG 33 kV distribution system in Ashanti region. The integration of DSTATCOM in the ECG 33 kV distribution system in the Ashanti Region has led to a decrease in power losses and voltage drops, resultant in a reduction of energy cost per year.

4.4.1. Active Power Loss of Case 0, Case 1, and Case 2

Before the integration of DSTATCOM, the Case 0 total active power loss of the ECG 33 kV distribution system in Ashanti Region was 14.530 MW. After the integration of DSTATCOM,

this loss decreased meaningly to 5.975 MW for Case 1 and 5.998 MW for Case 2, representing a reduction of 8.555 MW and 8.532 MW respectively. The data presented in Figure 4.49 provides an lines of the active power losses of Case 0, Case 1, and Case 2. It is evident that the integration of DSTATCOM has led to a significant reduction in active power loss, which improved the efficiency and reduced energy costs.

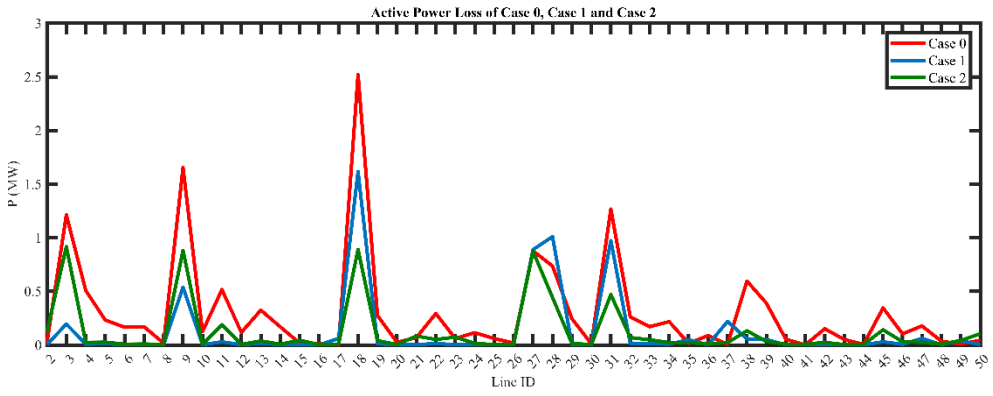

Figure 4.49, Active power loss of Case 0, Case 1, and Case 2.

From figure 4.49 above, it can be observed that there are variations in the active power losses for different lines across the cases. In some cases, the active power decreases, indicating a reduction in power losses, while in other cases, the active power increases, representing an increase in power losses.

Comparing the active power losses of Case 0, Case 1 and Case 2, it can be observed that Case 1 generally leads to reduced power losses in several lines. For example, Lines 2, 4, 5, 6, 7, 10, 12, 14, 16, 19, 20, 21, 24, 25, 26, 28, 30, 32, 33, 34, 35, 36, 38, 40, 41, 42, 43, 44, 46, 47, 48, 50 show decreased active power losses compared to Case 0. This suggests that Case 1 has been successful in improving the efficiency of power distribution by reducing power losses along these lines.

The active power losses in Case 1 are generally lower than those in Case 2 for most lines. While there are a few lines where Case 2 has lower active power losses, the overall trend indicates that Case 1 performs better in minimizing power losses compared to Case 2.

Reducing power losses is crucial for improving the overall efficiency of the power system and minimizing unnecessary energy wastage. By implementing measures that contribute to reduced power losses, such as DSTATCOM integration, Case 1 demonstrates its effectiveness in enhancing the performance of the power distribution network. However, it is important to note that the assessment of the best intervention also depends on system cost-effectiveness. This information can be used to develop strategies to enhance the efficiency and cost-effectiveness of power systems.

4.4.2. Reactive Power Loss of Case 0, Case 1, and Case 2

This section of the study involved a detailed analysis and comparison of various cases of the reactive power losses in the ECG 33 kV distribution system located in the Ashanti Region. The findings are presented in Figure 4.50, which provides an overview of the reactive power losses for three different cases. The analysis of these cases helps to determine the level of reactive power losses in the system.

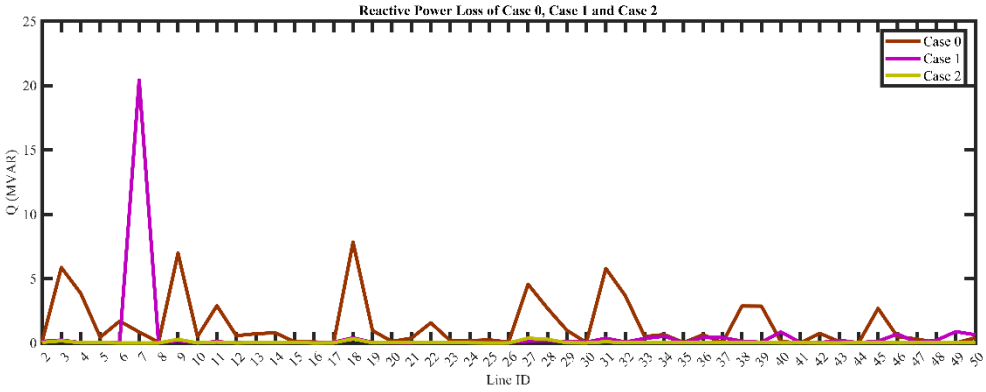

Figure 4.50, Reactive power loss of Case 0, Case 1, and Case 2.

Based on the analysis of reactive power data for Case 0, Case 1, and Case 2, Figure 4.50 clearly indicates that Case 2 emerges as the most effective intervention. It showcases notable

reductions in reactive power losses compared to Case 0 and Case 1, with several lines experiencing significantly lower losses. This reduction signifies enhanced utilization of reactive power and decreased inefficiencies within the system. Case 2 demonstrates improved system stability through efficient management of reactive power, resulting in lower losses.

4.4.3. Voltage Profile of Case 0, Case 1, and Case 2

The integration of DSTATCOM into the ECG 33 kV distribution system was done to enhance the voltage profile and to minimize power losses in the Ashanti Region. Prior to the integration, the voltage profile on some buses of the system were not compliant with the IEC 60038-2009 voltage standard level (Ackermann & Knyazkin, 2002; Standard & Horizontale, 2009). Figure 4.51 depicts the voltage profile of Case 0, Case 1, and Case 2.

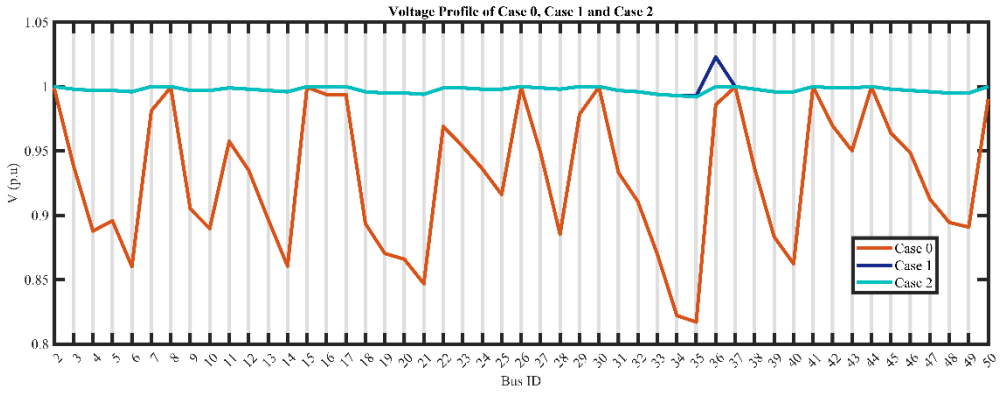

Figure 4.51, Voltage profile of Case 0, Case 1, and Case 2.

It is clear in Figure 4.51 that, there are variances in the voltage profiles at various buses after looking at the findings of the voltage data for Case 0, Case 1, and Case 2. In Case 0, several buses experience noticeable voltage deviations from the nominal level, such as buses 3, 4, 5, 6, 8, 9, 10, 11, 12, 13, 14, 18, 19, 20, 21, 22, 23, 24, 25, 27, 28, 31, 32, 33, 34, 35, 36, 38, 39, 40, 42, 43, 45, 46, 47, 48, and 49. These deviations indicate potential issues in maintaining stable voltage conditions and may impact the overall system performance.

Case 1 demonstrates a closer alignment of voltage levels to the nominal voltage across many buses compared to Case 2. This suggests that the intervention implemented in Case 1 has effectively regulated the voltage profiles and minimized deviations from the desired levels.

In summary, Case 1 exhibits the most favorable voltage profile among the three cases, with improved voltage regulation and fewer deviations from the nominal voltage level. The closer alignment of voltage levels to the nominal values indicates enhanced stability and efficient voltage management within the ECG 33kV distribution system. Generally, the addition of the DSTATCOM played a critical role in stabilizing the voltage profiles of the ECG 33 kV distribution system, bringing the voltage levels within the recommended standard levels.

4.4.4. Energy Cost of Case 0, Case 1, and Case 2

This section of the study aimed to evaluate the cost-effectiveness of integrating DSTATCOM into the ECG 33 kV distribution system. The assessment was carried out by analysing the total energy cost per year before and after the DSTATCOM integration. Figure 4.52, which is presented below, displays a graphical representation of the energy cost of Case 0, Case 1, and Case 2.

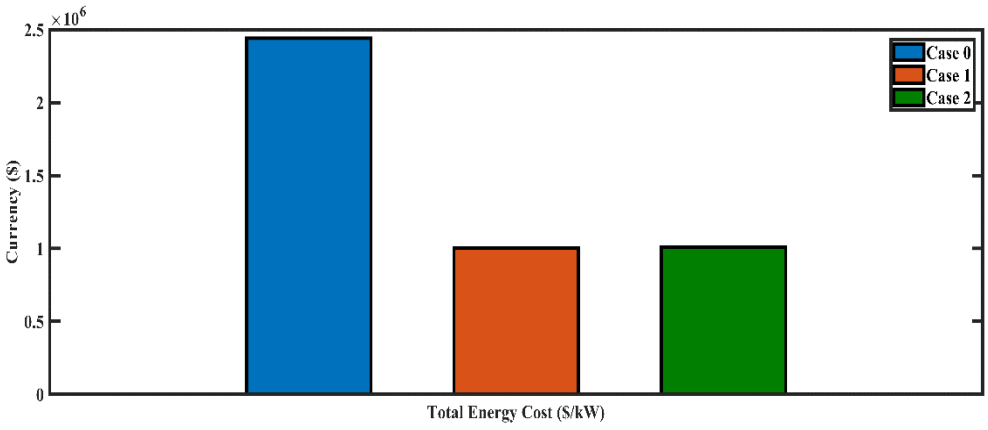

Figure 4.52, Total energy cost per annum of Case 0, Case 1, and Case 2.

The power loss in the Case 0 was measured at 14.530 MW, which equates to a yearly energy cost of $2,441,040. However, after the integration of the DSTATCOM on the 33 kV

distribution system, the power loss reduced to 5.975 MW in case 1 and 5.998 MW in Case 2. After DSTATCOM was integrated, base case (Case 0) energy cost per year was reduced to $1,003,833.6 in case 1 and $1,007,717.76 in Case 2. The difference in energy cost between Case 2 and Case 1 was $3,884.16. These results show that Case 1 is more effective in saving energy when the 1200 kvar size of fixed DSTATCOM is installed on the optimal location of Bus 36 in the distribution system than other cases (Case 0 and Case 2). The general data of ECG 33 kV distribution system in the cases are summarized in Table 4.4 above. It is evident that the integration of the DSTATCOM led to a significant reduction in power loss and a consequent cost saving for the ECG.

By comparing the energy costs of the three cases, we can observe the economic benefits of the fixed DSTATCOM integration. The results of this analysis can be used to make informed decisions about the potential deployment of fixed DSTATCOM in similar distribution systems. Furthermore, it may be possible to identify additional opportunities for cost savings through the optimization of system operations.

4.4.5. Total Cost of Case 0, Case 1, and Case 2

This part of the research was to assess the financial viability of incorporating DSTATCOM into the ECG 33 kV distribution system. The analysis involved examining the overall yearly cost before and after DSTATCOM integration. The Figure 4.53 below, depicts the annual total cost of Case 0, Case 1, and Case 2.

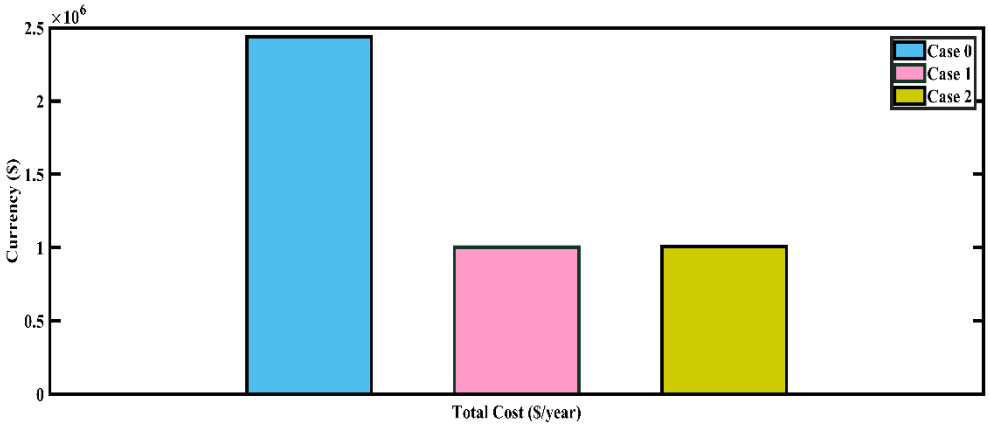

Figure 4.53, Total cost per annum of Case 0, Case 1, and Case 2.

The annual total cost of the ECG distribution system for the Ashanti region was $2,441,040. However, with the integration of DSTATCOM into the ECG 33 kV distribution system, the total cost per year was significantly reduced to $1,004,433.6 in Case 1 and $1,007,867.76 in Case 2. Case 1 is more effective in saving energy compared to Cases 0 and 2. The installation of fixed DSTATCOM helped to reduce the energy loss and save costs, which is a significant benefit for the ECG. Therefore, it is important for companies and organizations to consider the deployment of fixed DSTATCOM in their distribution systems to enhance their economic efficiency and effectiveness.

A summary of the findings from Case 0, Case 1, and Case 2 can be seen in Table 4.4. The data presented in Table 4.4 can be used to assess the feasibility and potential benefits of integrating DSTATCOM in similar distribution systems and can inform decision-making for future projects.

Table 4. 4, The Summary Results of Case 0, Case 1, and Case 2

Performance Measurement	Case 0	Case 1	Case 2
Minimum Bus Voltage (p.u)	0.817	0.993	0.992
Maximum Bus Voltage (p.u)	1	1.023	1
Total Active Power Loss (MW)	14.53	5.9752	5.99832
Total Reactive Power Loss (MVAR)	67.005	28.4925	2.2205
DSTATCOM Power Injection (kvar) and Location	-	1200 at bus 36	150 at bus 26 150 at bus 30
Number of DSTATCOM	-	1	2
Active Power Reduction Percentage	-	58.88%	58.72%
Reactive Power Reduction Percentage	-	57.48%	96.69%
Total Energy Cost ($/kW)	2,441,040.00	1,003,833.60	1,007,717.76
Total Cost ($/year)	2,441,040.00	1,004,433.60	1,007,867.76
Net Saving ($/year)	-	1,436,606.40	1,433,172.24
Percentage of Annual Cost Saving	-	58.85%	58.71%
Payback Period	-	7 months	7 months

The data presented in the Table 4.4 above is related to the performance measurement of the ECG distribution system before and after the integration of DSTATCOM. The performance parameters include the minimum and maximum bus voltages, total active power loss, and total reactive power loss. The Table 4.4 also shows the location and power injection of DSTATCOM, the number of DSTATCOM used, the percentage of active and reactive power reduction, and the total energy cost and net savings.

Before the integration of DSTATCOM (Case 0), the minimum and maximum bus voltages were 0.817 p.u. and 1 p.u., respectively. However, after the integration of DSTATCOM, the minimum and maximum bus voltages improved significantly to 0.993 p.u. and 1.023 p.u., respectively in Case 1, and 0.992 p.u., and 1 p.u. in Case 2. This improvement in voltage profile indicates that DSTATCOM plays a significant role in maintaining the voltage magnitude at the desired value, which is essential for a reliable power supply.

The total active power loss and total reactive power loss also reduced significantly after the integration of DSTATCOM. In Case 1, the total active power loss and total reactive power loss

reduced by 58.88% and 57.48%, respectively, compared to the Case 0. In Case 2, the total active power loss reduced by 58.72%, while the total reactive power loss reduced by only 96.69%.

The Table 4.4 also shows that the DSTATCOM was installed at different buses in different cases. In Case 1, the fixed DSTATCOM was installed at bus 36, and 1200 kvar reactive power was injected. In contrast, in Case 2, two DSTATCOMs were installed at buses 26 and 30, and 150 kvar power was injected at each bus. The results show that the location and power injection of DSTATCOM have a significant impact on the system performance.

Moreover, the integration of DSTATCOM resulted in a significant reduction in the energy cost and net savings. In Case 1, the total energy cost and net savings were $1,004,433.6 and $1,436,606.40 per year, respectively, while in Case 2, the total energy cost and net savings were $1,007,867.76 and $1,433,172.24 per year, respectively. The net savings percentage was 58.85% in Case 1 and 58.71% in Case 2, indicating that both cases provided significant cost savings. The payback period for both cases was seven months. As shown in Table 4.4, the outcomes proved that Case 1 had a more substantial influence than Case 0 and Case 2.

In conclusion, the integration of DSTATCOM in the power system significantly improves the voltage profile, reduces the total active and reactive power losses, and provides cost savings. The performance improvement is highly dependent on the location and power injection of DSTATCOM. Therefore, the results obtained in this research provide evidence of the efficiency and effectiveness of integrating DSTATCOM into the distribution system in Ashanti Region. The results obtained from this study offer valuable insights for decision-making regarding the possible implementation of DSTATCOM in similar distribution systems. These findings can aid in optimizing system operations and attaining cost reductions.

CHAPTER FIVE

CONCLUSION AND RECOMMENDATION

This section presents potential avenues for future research based on the outcomes obtained from the analysis conducted before and after the integration of DSTATCOM, with the aim of enhancing the voltage profile, minimizing power loss and energy cost. The identified possibilities for future work aim to build upon the existing findings and further explore ways to optimize the performance of the electrical system.

5.1. Summary of the research

The thesis discusses the electricity distribution system in Ghana and the challenges it faces in terms of power losses and voltage profile. It highlights the role of Electricity Company of Ghana (ECG) in the country. The distribution system is classified as a radial distribution system and is responsible for supplying electricity to different distribution stations in the Ashanti region.

The thesis emphasizes the importance of addressing power losses and voltage profile issues in the distribution system. It mentions the negative impact of the country's dependence on thermal power generation, both in terms of cost and environmental concerns. It also discusses the high distribution system losses in Ghana and the regions with the highest energy demand.

To improve the distribution system's performance, the thesis suggests the use of compensating devices like DSTATCOM. It mentions the need to properly size and place these devices to enhance the system's stability, reduce losses, and improve the voltage profile. Backward/Forward Sweep was used to analyse the voltage profile, power losses and energy cost while Particle Swarm Optimization (PSO) was used for determining the optimal placement and sizes of DSTATCOMs.

5.2. Conclusion

The distribution system consistently faced various power quality issues, including bus voltage instability, significant voltage drops, and excessive losses. These challenges demanded technical interventions to address and mitigate the problems effectively. This research focused on identifying the ideal placement and capacity of DSTATCOM as a solution to tackle these issues within the Ashanti Region's 33 kV distribution system. To analyse the system's load flow, the Backward/Forward Sweep power flow technique was employed, while the PSO algorithm was utilized to determine the optimal location and size of the DSTATCOM.

This study analysed simulation results from three situations. The first situation analysed the existing system data without the integration of DSTATCOM. In the second and third situations incorporate the fixed and switched DSTATCOM into the network to reduce power losses (active and reactive) and increase voltage profile.

It can be observed in Case 0 that, the reactive power loss, active power loss and minimum voltage magnitude before DSTATCOM integration were 67.005 MVAR, 14.530 MW and 0.817 p.u. respectively. The Case 0 (base case) results show that ECG 33 kV distribution system in Ashanti Region waste energy of 2,441,040.00 $/kW which cost Ghana a huge amount of money that can be used for other purpose in the country.

In the Case 1 and Case 2, the optimal location and size of DSTATCOM was incorporated on the 33 kV distribution system in Ashanti Region using PSO algorithm to improve the voltage profile and minimize the power losses (active and reactive). From Table 4.4, both active and reactive power losses are substantially reduced in Case 1 and Case 2 compared to the Case 0 (base case). Case 1 demonstrates a remarkable improvement in bus voltages and reduction in active power losses, indicating the effectiveness of DSTATCOM integration in mitigating power losses. Case 1 show the substantial solution to decrease the energy loss in existing

system. As shows in Table 4.4, the reactive power loss, active power loss and minimize voltage value after fixed DSTATCOM were 28.493 MVAR, 5.975 MW and 0.993 p.u. respectively. The cost was minimized to 1,004,433.6 $/year after the integration of fixed DSTATCOM. The annual cost saving after the integration of DSTATCOM was 1,436,606.4 $/year with seven (07) months payback period.

The results show that integrating an optimal DSTATCOM in ECG 33 kV distribution system in Ashanti Region would have significant impact to reduce the power loss and improve the voltage profile of the existing distribution system. Again, after the DSTATCOM installed in the existing system, it reduced the active and reactive power loss by 58.88% and 57.48% respectively and enhanced the voltage profile to the international standard voltage deviation range (Standard & Horizontale, 2009).

By achieving these outcomes, the research successfully accomplished its objective. The utilization of the Particle Swarm Optimization algorithm proved to be an effective approach for determining the optimal location and size of the DSTATCOM in the 33 kV distribution system of the Ashanti Region. This technique was instrumental in minimizing both active and reactive power losses while enhancing the voltage profile.

5.3. Recommendation

This research will enable the Electricity Company of Ghana (ECG) to decrease the active and reactive loss in the distribution system. As the results show, the reduced losses help to fulfil the societal demand and minimize the wasted energy which cost the country a huge amount of money. As electricity is necessity for global development for every country, it supposes to be cost-effective and reliable to operate within the permitted limit to stabilize the system. The research was conducted on ECG 33 kV distribution system in Ashanti Region of Ghana to minimize the power loss and improvement voltage profile.

This research approach can be applied to any other primary distribution network to improve its performance by enhancing the voltage profile and minimizing the power losses (active and reactive). However, harmonics and phase imbalance were not considered in this research. To apply the concept used in this research efficiently in other fifteen (15) regions in Ghana, the following recommendations are made,

1. The Electricity Company of Ghana (ECG) need to develop techniques to monitor, record the network system and provide sufficient information for future prediction and academic purposes.
2. The academic institutions must establish a rapport with Electricity Company of Ghana (ECG) in order to develop effective technique for distribution system performance.
3. The proposed method must be considered in other regions in Ghana's primary distribution system.
4. The primary distribution network in Ashanti Region must be reconfigure as ring circuit to stabilize the system.

The future research would consider the harmonics, phase imbalance, frequency stability and voltage stability. It can also consider different metaheuristic techniques to improve the primary distribution system.

REFERENCES

Abdulrazzaq, A. A. (2015). Improving the power system performance using FACTS devices. *IOSR Journal of Electrical and Electronics Engineering Ver. IV*, *10*(2), 2278–1676. https://doi.org/10.9790/1676-10244149

Abebe, B. (2021). September 2021 Adama, Ethiopia. In *Adama Science and Technology University September* (Issue September). Adama Science and Technology University September.

Abou El-Ela, A. A., El-Sehiemy, R. A., Kinawy, A. M., & Mouwafi, M. T. (2016). Optimal capacitor placement in distribution systems for power loss reduction and voltage profile improvement. *IET Generation, Transmission and Distribution*, *10*(5), 1209–1221. https://doi.org/10.1049/iet-gtd.2015.0799

Ackermann, T., & Knyazkin, V. (2002). Interaction between distributed generation and the distribution network: Operation aspects. *Proceedings of the IEEE Power Engineering Society Transmission and Distribution Conference*, *2*(ASIA PACIFIC), 1357–1362. https://doi.org/10.1109/tdc.2002.1177677

ADJOA, G. S. E. (2014). Impact of the National Electrification Scheme on Poverty Reduction in Rural Ghana-a Case Study of the Amansie West …. *Department of Geography and Rural Development …*.

Alam, S., Ismail, N., Norainin, W., & Abdullah, W. (2010). System Using D-STATCOM. *Power Engineering*, *June*, 418–424.

Ali, S. A., & Devi, A. L. (2015). *Multiple DG Placement For Voltage Profile Improvement And Loss Reduction Using IA And PSO Methods*. *3*(10), 14–23.

Amankwah, F., Scott, I. J., Baptista, P. C., & Silva, C. A. (2020). Energy for Sustainable Development Assessing the costs of contributing to climate change targets in sub-Saharan Africa : The case of the Ghanaian electricity system. *Energy for Sustainable Development*, *57*, 32–47. https://doi.org/10.1016/j.esd.2020.05.001

Amara, T., Asefi, S., Adewuyi, O. B., Ahmadi, M., Yona, A., & Senjyu, T. (2019). Technical and economic performance evaluation for efficient capacitors sizing and placement in a real distribution network. *2019 IEEE Student Conference on Research and Development, SCOReD 2019*, 100–105. https://doi.org/10.1109/SCORED.2019.8896285

Amin, A., Kamel, S., Selim, A., & Nasrat, L. (2019). Optimal Placement of Distribution Static Compensators in Radial Distribution Systems Using Hybrid Analytical-Coyote optimization Technique. *2019 21st International Middle East Power Systems Conference, MEPCON 2019 - Proceedings*, 982–987. https://doi.org/10.1109/MEPCON47431.2019.9007924

Arya, A. K., Kumar, A., & Chanana, S. (2019). Analysis of Distribution System with D-STATCOM by Gravitational Search Algorithm (GSA). *Journal of The Institution of Engineers (India): Series B*, *100*(3), 207–215. https://doi.org/10.1007/s40031-019-00383-2

Bakhshideh Zad, B., Hasanvand, H., Lobry, J., & Vallée, F. (2015). Optimal reactive power control of DGs for voltage regulation of MV distribution systems using sensitivity analysis method and PSO algorithm. *International Journal of Electrical Power and Energy Systems*, *68*, 52–60. https://doi.org/10.1016/j.ijepes.2014.12.046

Balakumar, S., Getahun, A., Kefale, S., & Ramash Kumar, K. (2021). *Improvement of the Voltage Profile and Loss Reduction in Distribution Network Using Moth Flame Algorithm: Wolaita Sodo, Ethiopia*. https://doi.org/10.1155/2021/9987304

Balamurugan, P., Yuvaraj, T., & Muthukannan, P. (2018). Optimal Allocation of DSTATCOM in Distribution Network Using Whale Optimization Algorithm. *Engineering, Technology & Applied Science Research*, *8*(5), 3445–3449. https://doi.org/10.48084/etasr.2302

Bosisio, A., Berizzi, A., Amaldi, E., Bovo, C., & Sun, X. A. (2020). Optimal feeder routing in urban distribution networks planning with layout constraints and losses. *Journal of Modern Power Systems and Clean Energy*, *8*(5), 1005–1014. https://doi.org/10.35833/MPCE.2019.000601

Campbell, R. J. (2012). Weather-Related Power Outages and Electric System Resiliency Specialist in Energy Policy Weather-Related Power Outages and Electric System Resiliency. *CRS Report for Congress*.

Chauhan, A., & Rajvanshi, S. (2013). Non-Technical Losses in power system: A review. *Proceedings of 2013 International Conference on Power, Energy and Control, ICPEC 2013*, 558–561. https://doi.org/10.1109/ICPEC.2013.6527720

Chen, T. H., Chiang, L. S., & Yang, N. C. (2012). Examination of major factors affecting voltage variation on distribution feeders. *Energy and Buildings*, *55*, 494–499. https://doi.org/10.1016/j.enbuild.2012.08.021

Chou, M. H., Su, C. L., Lee, Y. C., Chin, H. M., Parise, G., & Chavdarian, P. (2017). Voltage-drop calculations and power cable designs for harbor electrical distribution systems with high voltage shore connection. *IEEE Transactions on Industry Applications*, *53*(3), 1807–1814. https://doi.org/10.1109/TIA.2016.2646658

Chowdhury, S., Chowdhury, S., & Crossley, P. (2009). *Microgrids and Active Distribution Networks, IET RENEWABLE ENERGY SERIES 6*.

Devabalaji, K. R., Yuvaraj, T., & Ravi, K. (2018). An efficient method for solving the optimal sitting and sizing problem of capacitor banks based on cuckoo search algorithm. *Ain Shams Engineering Journal*, *9*(4), 589–597. https://doi.org/10.1016/J.ASEJ.2016.04.005

Egwaile, J., Ogbeide, K., & Osahenvemwen, A. (2018). Technical Loss Estimation and Reduction in a Typical Nigerian Distribution System: A Case Study. *Journal of Electrical Engineering, Electronics, Control and Computer Science-JEEECCS*, *4*(13), 1–8.

El-Fergany, A. A., & Abdelaziz, A. Y. (2014). Capacitor allocations in radial distribution networks using cuckoo search algorithm. *IET Generation, Transmission and Distribution*, *8*(2), 223–232. https://doi.org/10.1049/iet-gtd.2013.0290

Energy Commission. (2016). *2016 Energy Supply and Demand Outlook for Ghana*. *April*, 1–57.

Energy Commission - Ghana. (2019). *Energy Profile of Districts in Ghana*. *December*, 1–93.

Energy Commission Ghana. (2022). *2022 NATIONAL ENERGY STATISTICS* (2022 Natio, Issue April).

Georgilakis, P. S., & Vernados, P. G. (2011). Flexible ac transmission system controllers: An evaluation. *Materials Science Forum*, *670*(8), 399–406. https://doi.org/10.4028/www.scientific.net/MSF.670.399

Guwaeder, A., & Ramakumar, R. (2019). Optimal Integration of PV Generation in Distribution Systems. *2018 IEEE Conference on Technologies for Sustainability, SusTech 2018*, 1–5. https://doi.org/10.1109/SusTech.2018.8671349

Hota, A. P., & Mishra, S. (2021). A forward-backward sweep based numerical approach for active power loss allocation of radial distribution network with distributed generations. *International Journal of Numerical Modelling: Electronic Networks, Devices and Fields*, *34*(1), 1–29. https://doi.org/10.1002/jnm.2788

Hota, A. P., Mishra, S., Mishra, D. P., & Salkuti, S. R. (2021). Allocating active power loss with network reconfiguration in electrical power distribution systems. *International Journal of Power Electronics and Drive Systems*, *12*(1), 130–138. https://doi.org/10.11591/ijpeds.v12.i1.pp130-138

Ismail, B., Abdul Wahab, N. I., Othman, M. L., Radzi, M. A. M., Naidu Vijyakumar, K., & Mat Naain, M. N. (2020). A Comprehensive Review on Optimal Location and Sizing of Reactive Power Compensation Using Hybrid-Based Approaches for Power Loss Reduction, Voltage Stability Improvement, Voltage Profile Enhancement and Loadability Enhancement. *IEEE Access*, *8*, 222733–222765. https://doi.org/10.1109/ACCESS.2020.3043297

Ismail, B., Izzri, N., Wahab, A., Lutfi Othman, M., Radzi, A. M., Vijyakumar, N., Najwan, M., & Naain, M. (n.d.). *A Comprehensive Review on Optimal Location and Sizing of Reactive Power Compensation Using Hybrid-Based Approaches for Power Loss Reduction, Voltage Stability Improvement, Voltage Profile Enhancement and Loadability Enhancement*. https://doi.org/10.1109/ACCESS.2020.3043297

Kadandani, N. B. (2018). *An Overview of FACTS Controllers for Power Quality Improvement An Overview of FACTS Controllers for Power Quality Improvement*. *September 2015*, 9–17.

Kumar, B., Saw, B. K., & Bohre, A. K. (2020). Optimal Distribution Network Reconfiguration to Improve the System Performances using PSO with Multiple-Objectives. *International Conference on Computational Intelligence for Smart Power System and Sustainable Energy, CISPSSE 2020*. https://doi.org/10.1109/CISPSSE49931.2020.9212262

Kumarasundari, P., & Balaraman, S. (2008). Voltage Profile and Loss Reduction Enhancement By Optimal Placement of Dg and Dstatcom in Distribution System. *International Research Journal of Engineering and Technology*.

Kumi, E. N. (2017a). *The Electricity Situation in Ghana: Challenges and Opportunities*. www.cgdev.orgwww.cgdev.org

Kumi, E. N. (2017b). *The Electricity Situation in Ghana: Challenges and Opportunities*.

Lata, P., & Vadhera, S. (2020). Reliability Improvement of Radial Distribution System by Optimal Placement and Sizing of Energy Storage System using TLBO. *Journal of Energy Storage*, *30*(August 2019), 101492. https://doi.org/10.1016/j.est.2020.101492

Maciej Serda, Becker, F. G., Cleary, M., Team, R. M., Holtermann, H., The, D., Agenda, N., Science, P., Sk, S. K., Hinnebusch, R., Hinnebusch A, R., Rabinovich, I., Olmert, Y., Uld, D. Q. G. L. Q., Ri, W. K. H. U., Lq, V., Frxqwu, W. K. H., Zklfk, E., Edvhg, L. V, … (2013) .ح ,فاطمی. Synteza i aktywność biologiczna nowych analogów tiosemikarbazonowych chelatorów żelaza. *Uniwersytet Śląski*, *7*(1), 343–354. https://doi.org/10.2/JQUERY.MIN.JS

Mahmood, M., Shivam, O., Kumar, P., & Krishnan, G. (2014). International Journal of Advanced Research in Electrical, Electronics and Instrumentation Engineering Real Time Study on

Technical Losses in Distribution System. *International Journal of Advanced Research in Electrical, Electronics and Instrumentation Engineering*, *3*(1), 131–137.

MoP. (2005). National Electricity Policy. *Policy*, *3*(October), 1–16.

Murari, K., & Padhy, N. P. (2020). *Graph-theoretic-based approach for solving load flow problem of AC-DC radial distribution network with distributed generations*. https://doi.org/10.1049/iet-gtd.2019.1416

Nemouchi, H., Tiguercha, A., & Ladjici, A. A. (2020). An adaptive decentralized under voltage load shedding in distribution networks. *International Transactions on Electrical Energy Systems*, *30*(11), 1–22. https://doi.org/10.1002/2050-7038.12592

Okwu, M. O., & Tartibu, L. K. (2021). Particle Swarm Optimisation. *Studies in Computational Intelligence*, *927*, 5–13. https://doi.org/10.1007/978-3-030-61111-8_2

Oloulade, A., Imano, A. M., Viannou, A., & Tamadaho, H. (2018). Optimization of the number , size and placement of D-STATCOM in radial distribution network using Ant Colony Algorithm. *American Journal of Engineering Research and Reviews*, *November*, 1–13. https://doi.org/10.28933/AJOERR

Oyedepo, S. O. (2012). *Energy and sustainable development in Nigeria: the way forward*. https://doi.org/10.1186/2192-0567-2-15

Patel, U. (2012). *The Impact of Harmonics on the Power Cable Stress Grading System*.

Pathak, O., & Prakash, P. (2018). Load flow solution for radial distribution network. *2018 2nd IEEE International Conference on Power Electronics, Intelligent Control and Energy Systems, ICPEICES 2018*, 176–181. https://doi.org/10.1109/ICPEICES.2018.8897305

PNNL seeks Visionary Leadership in Grid and Advanced Controls. (2013). *April*.

Prasad, K. R. S. S., Neeraja, T., & Pavani, Y. (2020). Optimal placement of DSTATCOM for power loss reduction and voltage profile improvement in radial distribution systems. *International Journal of Advanced Science and Technology*, *29*(4), 840–847.

Raj, V., & Kumar, B. K. (2020). A New Affine Arithmetic-based power flow analysis for Weakly Meshed Distribution Systems under Uncertainty. *Proceedings - 2020 IEEE International Conference on Environment and Electrical Engineering and 2020 IEEE Industrial and Commercial Power Systems Europe, EEEIC / I and CPS Europe 2020*. https://doi.org/10.1109/EEEIC/ICPSEurope49358.2020.9160489

Rajpoot, S. C., Rajpoot, P. S., Gupta, K., & Yadav, R. R. (2017). Design Modeling and Simulation of Fuzzy Controlled Svc for Long Over Head Transmission Line. *IOSR Journal of Electrical and Electronics Engineering*, *12*(01), 01–15. https://doi.org/10.9790/1676-1201040115

Reddy, V. V., Yesuratnam, G., & Kalavathi, M. S. (2012). Impact of voltage and power factor change on primary distribution feeder power loss in radial and loop type of feeders. *Proceedings - ICETEEEM 2012, International Conference on Emerging Trends in Electrical Engineering and Energy Management*, 70–76. https://doi.org/10.1109/ICETEEEM.2012.6494446

Rukmani, D. K., Thangaraj, Y., Subramaniam, U., Ramachandran, S., Elavarasan, R. M., Das, N., Baringo, L., Imran, M., & Rasheed, A. (2020). *A New Approach to Optimal Location and Sizing of DSTATCOM in Radial Distribution Networks Using Bio-Inspired Cuckoo Search Algorithm*. https://doi.org/10.3390/en13184615

Salau, A. O., Gebru, Y. W., & Bitew, D. (2020). Optimal network reconfiguration for power loss minimization and voltage profile enhancement in distribution systems. *Heliyon*, *6*(6), e04233. https://doi.org/10.1016/j.heliyon.2020.e04233

Salkuti, S. R. (2021a). Optimal Allocation of DG and D-STATCOM in a Distribution System using Evolutionary based Bat Algorithm. *International Journal of Advanced Computer Science and Applications*, *12*(4), 360–365. https://doi.org/10.14569/IJACSA.2021.0120445

Salkuti, S. R. (2021b). Optimal Allocation of DG and D-STATCOM in a Distribution System using Evolutionary based Bat Algorithm. *International Journal of Advanced Computer Science and Applications*, *12*(4), 360–365. https://doi.org/10.14569/IJACSA.2021.0120445

Samimi, A. (2019). Probabilistic day-ahead simultaneous active/reactive power management in active distribution systems. *Journal of Modern Power Systems and Clean Energy*, *7*(6), 1596–1607. https://doi.org/10.1007/s40565-019-0535-4

Sarkar, J., & Bhattacharyya, S. (2012). Application of graphene and graphene-based materials in clean energy-related devices Minghui. *Archives of Thermodynamics*, *33*(4), 23–40. https://doi.org/10.1002/er

Serwaa Mensah, G., Kemausuor, F., & Brew-Hammond, A. (2014). Energy access indicators and trends in Ghana. *Renewable and Sustainable Energy Reviews*, *30*, 317–323. https://doi.org/10.1016/J.RSER.2013.10.032

Shobana, S., Tamil Selvi, K., Abirami, P., Pushpavalli, M., & Sivagami, P. (2019). Implementation of voltage stability system in distribution network by using D-STATCOM. *International Journal of Recent Technology and Engineering*, *8*(2 Special Issue 11), 3374–3379. https://doi.org/10.35940/ijrte.B1567.0982S1119

Standard, H., & Horizontale, N. (2009a). *INTERNATIONAL STANDARD INTERNATIONALE IEC standard voltages*.

Standard, H., & Horizontale, N. (2009b). *INTERNATIONAL STANDARD INTERNATIONALE IEC standard voltages*. https://webstore.iec.ch/publication/72877

Stanelyte, D., & Radziukynas, V. (2019). *Review of Voltage and Reactive Power Control Algorithms in Electrical Distribution Networks*. https://doi.org/10.3390/en13010058

Thangaraj, Y., & Kuppan, R. (2017). Multi-objective simultaneous placement of DG and DSTATCOM using novel lightning search algorithm. *Journal of Applied Research and Technology*, *15*(5), 477–491. https://doi.org/10.1016/j.jart.2017.05.008

UmalRukmani, D. K., Thangaraj, Y., Subramaniam, U., Ramachandran, S., Elavarasan, R. M., Das, N., Baringo, L., & Rasheed, M. I. A. (2020). A new approach to optimal location and sizing of DSTATCOM in radial distribution networks using bio-inspired cuckoo search algorithm. *Energies*, *13*(18). https://doi.org/10.3390/en13184615

Venkatesh, B., Ranjan, R., & Gooi, H. B. (2004). Optimal Reconfiguration of Radial Distribution Systems to Maximize Loadability. *IEEE Transactions on Power Systems*, *19*(1), 260–266. https://doi.org/10.1109/TPWRS.2003.818739

VRA. (n.d.). *Volta River Authority | Profile of VRA*. Retrieved October 20, 2022, from https://vra.com/about_us/profile.php

Williams, J. H., & Ghanadan, R. (2006). Electricity reform in developing and transition countries: A reappraisal. *Energy*, *31*(6–7), 815–844. https://doi.org/10.1016/J.ENERGY.2005.02.008

Yang, C. F., Lai, G. G., Lee, C. H., Su, C. T., & Chang, G. W. (2012). Optimal setting of reactive compensation devices with an improved voltage stability index for voltage stability enhancement. *International Journal of Electrical Power and Energy Systems*, *37*(1), 50–57. https://doi.org/10.1016/j.ijepes.2011.12.003

York, D., Relf, G., & Waters, C. (2019). *Integrated Energy Efficiency and Demand Response Programs*. *September*.

Yuvaraj, T., Devabalaji, K. R., & Ravi, K. (2015). Optimal Placement and Sizing of DSTATCOM Using Harmony Search Algorithm. *Energy Procedia*, *79*, 759–765. https://doi.org/10.1016/J.EGYPRO.2015.11.563

Zhang, L., Liu, Y., Zhang, P., Tang, W., Lv, J., Zhang, L., & Li, D. (2017). Parallel computing of power flow for complex distribution network with DGs. *Journal of Intelligent and Fuzzy Systems*, *33*(5), 2987–2997. https://doi.org/10.3233/JIFS-169350

Ziari, I., Ledwich, G., Member, S., Ghosh, A., & Platt, G. (2013). *Considering Load Growth , Line Loss , and Reliability*. *28*(2), 587–597.

APPENDIX

Appendix I: The Transformer data of twenty-one (21) primary distribution stations.

S/N	Station name	Voltage ratio (kV)	Equipment	Rating
1	Agogo A	33/11	T104	20MVA
	Agogo B	33/11	T102	20MVA
2	Neoplan A	33/11	T79	20MVA
	Neoplan B	33/11	T77	20MVA
3	Edwinase A	33/11	T781	20MVA
	Edwinase B	33/11	T107	20MVA
4	Suame A	33/11	T67	20MVA
	Suame B	33/11	T68	20MVA
5	Barekese A			
	Barekese B	33/11	T62	10MVA
6	KTI A	33/11	T72	20MVA
	KTI B	33/11	T70	20MVA
7	Asekyem A	33/11	T109	20MVA
	Asekyem B	33/11	T113	20MVA
8	Kaase A	33/11	T50	10MVA
	Kaase B	33/11	T52	20MVA
9	Offinso A	33/11	T64	10MVA
	Offinso A	33/11	T65	10MVA
10	Airport A	33/11	T60	20MVA
	Airport B	33/11	T58	20MVA
11	Bekwai A	33/11	T45	10MVA
	Bekwai B	33/11	T48	10MVA
12	Fawoade A	33/11	T40	20MVA
	Fawoade B	33/11	T36	20MVA
13	Boadi A	33/11	T42	20MVA

	Boadi B	33/11	T43	20MVA
14	Akyease A	33/11	T32	20MVA
	Akyease B	33/11	T34	20MVA
15	Mampong A	33/11	T30	20MVA
	Mampong A	33/11	T29	20MVA
16	Agona A			
	Agona B	33/11	T120	10MVA
17	Nsuta A	33/11	T21	5MVA
	Nsuta B			
18	Kumawu	33/11	T23	5MVA
19	Effiduase A	33/11	T122	20MVA
	Effiduase B	33/11	T126	20MVA
20	Akyawkrom A	33/11	T12	20MVA
	Akyawkrom B	33/11	T13	20MVA
21	Switching station (Kuntenase)			

Appendix II: The parameters of secondary transmission lines of 33 kV distribution network.

Line Name	Cable type	Cable size (mm^2)	Distance coverage (km)	Destination
D1	AAC	265	10.5	Neoplan A to Agogo A
D2	AAC	265	10.5	Neoplan B to Agogo B
D3	AAC	265	15	Edwinase B to Agogo B
D4	AAC	409	14.2	Neoplan A to Barekese A
D5	AAC	150	3.6	Edwinase B to Neoplan A
D6	AAC	265	4	Ridge station A to Neoplan A
D7	AAC	265	13	Neoplan B to Barekese B
D8	AAC	265	2.5	Suame A to Barekese A
D9	AAC	400	5	Ridge station B1 to Neoplan B
D10	AAC	265	4	Ridge station A to Edwinase A
D11	AAC	265	4	Ridge station B1 to Edwinase B
D12	AAC	265	2.5	Suame B to Barekese B
D13	AAC	265	5	Airport A to Suame A
D14	AAC	265	5	Airport B to Suame B
D15	AAC	265	16.6	Barekese A to Offinso A
D16	AAC	265	16.6	Barekese B to Offinso B
D17	AAC	265	15	Ridge station A1 to Airport A
D18	AAC	265	5	Ridge station A1 to Kaase A
D19	CU	500	5	Ridge station B to KTI B
D20	AAC	265	15	Ridge station B to Airport B
D21	AAC	265	5	Ridge station B to Kaase B
D22	CU	500	3.6	KTI B to Airport B
D23	AAC	265	7	Kaase A to Asekyem A
D24	AAC	265	7	Kaase B to Asekyem B
D25	AAC	265	20	Kaase A to Switching station A
D26	AAC	265	20	Kaase B to Switching station B

D27	AAC	265	17	Switching station B to Bekwai B
D28	AAC	265	17	Switching station B to Akyawkrom B
D29	AAC	265	17	Switching station A to Bekwai A
D30	AAC	265	17	Switching station A to Akyawkrom A
D31	AAC	265	8	Boadi A to Kaase A
D32	AAC	265	8	Boadi B to Kaase B
D33	AAC	400	9	Airport B to Fawoade B
D34	AAC	400	9	Airport A to Fawoade A
D35	AAC	400	7	Akyease A to Fawoade A
D36	AAC	400	7	Akyease B to Fawoade B
D37	AAC	265	21.5	Fawoade A to Agona A
D38	AAC	265	21.5	Fawoade B to Agona B
D39	AAC	400	10	Awomaso station A to Akyease A
D40	AAC	400	10	Awomaso station B1 to Akyease B
D41	AAC	400	5.4	Awomaso station A to Boadi A
D42	AAC	400	5.4	Awomaso station B1 to Boadi B
D43	AAC	262	32.4	Agona A to Mampong A
D44	AAC	265	27	Agona A to Nsuta
D45	AAC	265	31	Agona A to Kumawu
D46	AAC	265	32.4	Agona B to Mampong B
D47	AAC	265	1	Kumawu to Effiduase A
D48	AAC	400	13.1	Awomaso station A1 to Akyawkrom A
D49	AAC	400	13.1	Awomaso station B to Akyawkrom B

Appendix III: Estimated load on ECG 33 kV distribution network.

Load ID	Rated Load	Current (A)
Agogo A Load	18 MVA	1035
Agogo B Load	21.57 MVA	1247
Agona B Load	3 MVA	167
Airport A Load	13 MVA	729.9
Airport B Load	8 MVA	452.2
Akyawkrom A Load	10 MVA	550.5
Akyawkrom B Load	7 MVA	376.2
Akyease A Load	14 MVA	773.1
Akyease B Load	7 MVA	377.1
Asekyem B Load	8 MVA	435.8
Asekyem A Load	11 MVA	609
Awomaso A1 Load	10 MVA	527.3
Awomaso B Load	5.39 MVA	283.8
Barekese B Load	5 MVA	289.9
Bekwai A Load	8 MVA	469.7
Bekwai B Load	5 MVA	279.4
Boadi A Load	14 MVA	747.5
Boadi B Load	10 MVA	531
Edwinase A Load	18 MVA	968.6
Edwinase B Load	21.57 MVA	1164
Effiduase A Load	8 MVA	456.7
Effiduase B Load	4.69 MVA	254.9
Fawoade A Load	13 MVA	725.7
Fawoade B Load	7 MVA	381.3
Kaase A Load	8 MVA	440.2
Kaase B Load	8 MVA	432
KTI B Load	4 MVA	211.2

KTI B Load2	3 MVA	158.4
Kumawu Load	4.22 MVA	247.9
Mampong A Load	4.062 MVA	244.4
Mampong B Load	3 MVA	169.8
Neoplan A Load	18.26 MVA	1007
Neoplan B Load	22 MVA	1212
Nsuta A Load	3 MVA	181
Offinso A Load	8 MVA	469.8
Offinso B Load	5 MVA	294.5
Ridge A1 Load	9.73 MVA	513.7
Ridge B1 Load	7.31 MVA	385.4
Suame A Load	13 MVA	742
Suame B Load	9 MVA	520.3

Appendix IV: Bus and Line data of ECG 33 kV distribution network in Ashanti region.

BUS DATA			LINE DATA				
Bus ID	**P (MW)**	**Q (Mvar)**	**Bus ID**	**From Bus**	**To Bus**	**R**	**X**
1	374.414	137.639	1	1	2	0.04	0.12
2	61.611	23.883	2	2	3	6.21	20.58
3	42.778	13.192	3	3	4	13.03	43.30
4	16.843	4.764	4	3	5	29.12	61.10
5	7.584	2.554	5	5	6	20.60	68.45
6	7.419	2.059	6	2	7	4.97	16.47
7	17.252	5.498	7	1	8	0.04	0.12
8	61.487	24.63	8	8	9	18.62	61.85
9	24.9	4.459	9	9	10	6.21	20.62
10	12.251	2.838	10	8	11	6.21	20.62
11	25.101	11.474	11	11	12	8.69	28.86
12	10.042	4.106	12	11	13	40.98	86.19
13	7.588	2.565	13	13	14	21.10	70.10
14	7.42	2.059	14	1	15	0.04	0.12
15	61.035	23.491	15	15	16	2.91	20.03
16	6.748	1.814	16	16	17	0.01	0.02
17	2.84	0.965	17	15	18	18.62	61.85
18	25.784	5.574	18	18	19	6.21	20.62
19	17.832	4.081	19	19	20	2.00	9.80
20	9.42	1.928	20	20	21	20.60	68.45
21	4.668	0.883	21	15	22	6.21	20.62
22	19.418	8.148	22	22	23	8.69	28.86
23	7.363	2.909	23	22	24	40.98	86.19
24	4.796	1.296	24	24	25	21.10	70.10
25	4.737	1.157	25	1	26	0.04	0.12
26	63.91	25.452	26	26	27	4.01	19.57

27	41.921	14.567	27	27	28	13.03	43.30
28	20.148	6.043	28	26	29	4.97	16.47
29	20.868	5.937	29	1	30	0.04	0.12
30	47.979	15.877	30	30	31	8.01	39.21
31	33.224	6.896	31	31	32	5.60	27.45
32	19.472	2.966	32	32	33	26.69	88.67
33	6.721	1.944	33	33	34	33.51	111.33
34	6.492	1.313	34	34	35	6.70	22.27
35	3.678	0.735	35	30	36	4.32	21.17
36	13.608	3.464	36	1	37	0.04	0.12
37	31.954	10.725	37	37	38	10.49	51.36
38	21.469	6.101	38	38	39	21.60	71.75
39	11.54	2.558	39	39	40	23.59	78.36
40	3.92	1.102	40	1	41	0.04	0.12
41	11.357	3.843	41	41	42	10.49	51.36
42	11.206	3.158	42	42	43	21.60	71.75
43	4.457	1.198	43	1	44	0.04	0.12
44	34.995	9.456	44	44	45	8.01	39.21
45	19.584	4.14	45	45	46	5.60	27.45
46	12.652	2.508	46	46	47	44.07	92.67
47	5.759	0.708	47	47	48	33.51	111.33
48	2.821	0.613	48	48	49	6.70	22.27
49	2.811	0.608	49	44	50	4.32	21.17
50	9.745	2.333					

Appendix V: Existing system data against simulation results.

Bus ID	Existing system voltage	Simulated Voltage	Error
AGOGO A	29.5	29.3	0.2
AGOGO B	29.4	29.2	0.2
AGONA A	29.6	28.7	0.9
AGONA B	30	30.1	-0.1
AIRPORT A	32.2	29.9	2.3
AIRPORT B	32.1	29.5	2.6
AKYAWKROM A	32.8	31.9	0.9
AKYAWKROM B	32.4	30.9	1.5
AKYEASE A	32.1	30.8	1.3
AKYEASE B	32.7	31.8	0.9
ASEKYEM A	31.7	30.9	0.8
ASEKYEM B	31.3	30.5	0.8
AWOMASO STATION A	33	33	0
AWOMASO STATION A1	33	33	0
AWOMASO STATION B	33	33	0
AWOMASO STATION B1	33	33	0
BAREKESE A	30.6	29.6	1
BAREKESE B	31.2	28.6	2.6
BEKWAI A	29.2	28.4	0.8
BEKWAI B	31	30.2	0.8
BOADI A	32.6	32.5	0.1
BOADI B	32.8	32.7	0.1
EDWINASE A	32.6	32.4	0.2
EDWINASE B	32.5	32.3	0.2
EFFIDUASE A	31.9	29.1	2.8
EFFIDUASE B	31.9	31.4	0.5
FAWOADE A	31.3	30	1.3

FAWOADE B	32.2	31.3	0.9
GridCo	33	33	0
KAASE A	32.4	31.6	0.8
KAASE B	32.8	32	0.8
KTI A	32.8	32.8	0
KTI B	32.8	32.8	0
KUMAWU	29.8	28.5	1.3
MAMPONG A	27.9	27	0.9
MAMPONG B	29.3	29.4	-0.1
NEOPLAN A	32	31	1
NEOPLAN B	32.2	31.3	0.9
NSUTA A	28	27.1	0.9
NSUTA B	29.4	29.5	-0.1
OFFINSO A	28.6	28	0.6
OFFINSO B	29.7	28.4	1.3
RIDGE STATION A	33	33	0
RIDGE STATION A1	33	33	0
RIDGE STATION B	33	33	0
RIDGE STATION B1	33	33	0
SUAME A	31	28.7	2.3
SUAME B	32	29.4	2.6
SWITCHING STATION A	30.4	29.6	0.8
SWITCHING STATION B	31.7	30.9	0.8

Appendix VI: Active and Reactive Power Loss of Case 0, Case 1, and Case 2.

Active Power Loss (MW)					Reactive Power Loss (Mvar)				
From Bus	To Bus	Case 0	Case 1	Case 2	From Bus	To Bus	Case 0	Case 1	Case 2
1	2	0.01629	0.002	0.122	1	2	0.05385	0.118	0.041
2	3	1.2127	0.195	0.916	2	3	5.8607	0.216	0.165
3	4	0.5064	0.007	0.023	3	4	3.8464	0.023	0.007
3	5	0.232	0.012	0.026	3	5	0.4401	0.026	0.012
5	6	0.1648	0.002	0.007	5	6	1.6953	0.007	0.002
2	7	0.1692	0.003	0.009	2	7	0.8446	20.424	0.003
1	8	0.01637	0.001	0.005	1	8	0.05411	0.005	0.002
8	9	1.6532	0.538	0.881	8	9	6.972	0.161	0.278
9	10	0.1239	0.002	0.006	9	10	0.4953	0.006	0.002
8	11	0.5156	0.029	0.188	8	11	2.8932	0.098	0.069
11	12	0.1169	0.002	0.005	11	12	0.5626	0.005	0.002
11	13	0.3246	0.017	0.037	11	13	0.7156	0.037	0.017
13	14	0.1687	0.002	0.007	13	14	0.7868	0.057	0.009
1	15	0.01596	0.001	0.043	1	15	0.08275	0.026	0.021
15	16	0.01436	0.001	0.003	15	16	0.07795	0.043	0.001
16	17	0.0000057	0.06	0.008	16	17	-0.0000013	0.057	0.005
15	18	2.5214	1.617	0.89	15	18	7.8315	0.39	0.317
18	19	0.2742	0.012	0.04	18	19	0.9649	0.04	0.012
19	20	0.02468	0.001	0.004	19	20	0.1129	0.008	0.022
20	21	0.06871	0.001	0.083	20	21	0.3674	0.004	0.023
15	22	0.293	0.015	0.051	15	22	1.5635	0.051	0.015
22	23	0.05983	0.001	0.073	22	23	0.1784	0.047	0.051
22	24	0.1143	0.007	0.015	22	24	0.1696	0.015	0.007
24	25	0.05961	0.001	0.003	24	25	0.2386	0.036	0.001
1	26	0.01766	0.002	0.005	1	26	0.05838	0.045	0.002
26	27	0.877	0.889	0.873	26	27	4.5601	0.142	0.369

27	28	0.7357	1.01	0.443	27	28	2.6879	0.153	0.283
26	29	0.244	0.004	0.013	26	29	0.9763	0.113	0.008
1	30	0.00953	0.001	0.004	1	30	0.03144	0.064	0.003
30	31	1.2671	0.973	0.469	30	31	5.7864	0.359	0.093
31	32	0.2621	0.014	0.069	31	32	3.6775	0.069	0.016
32	33	0.1705	0.014	0.048	32	33	0.4969	0.348	0.016
33	34	0.2171	0.007	0.022	33	34	0.6483	0.522	0.019
34	35	0.01412	0.049	0.021	34	35	0.03211	0.021	0.043
30	36	0.08756	0.001	0.009	30	36	0.6362	0.417	0.06
1	37	0.00424	0.219	0.021	1	37	0.01391	0.421	0.016
37	38	0.5957	0.057	0.132	37	38	2.8663	0.132	0.027
38	39	0.3894	0.05	0.032	38	39	2.8588	0.052	0.022
39	40	0.0524	0.001	0.007	39	40	0.1151	0.852	0.006
1	41	0.000536	0.008	0.006	1	41	0.00165	0.041	0.008
41	42	0.151	0.005	0.024	41	42	0.7456	0.024	0.005
42	43	0.05077	0.001	0.003	42	43	0.1033	0.203	0.004
1	44	0.0049	0.001	0.005	1	44	0.01611	0.023	0.012
44	45	0.3451	0.029	0.141	44	45	2.6794	0.141	0.029
45	46	0.1036	0.006	0.03	45	46	0.4802	0.69	0.006
46	47	0.1775	0.061	0.023	46	47	0.3008	0.043	0.014
47	48	0.0347	0.002	0.007	47	48	0.02542	0.207	0.032
48	49	0.00698	0.039	0.042	48	49	0.00565	0.877	0.018
44	50	0.04416	0.003	0.104	44	50	0.3936	0.634	0.026

Appendix VII: Voltage Profile of Case 0, Case 1, and Case 2.

Voltage Profile (p.u.)				
Bus Name	Bus ID	Case 0	Case 1	Case 2
GridCo	1	1	1	1
RIDGE STATION A	2	0.99948	1	1
NEOPLAN A	3	0.93867	0.998	0.998
AGOGO A	4	0.88776	0.997	0.997
BAREKESE A	5	0.89573	0.997	0.997
OFFINSO A	6	0.86012	0.996	0.996
EDWINASE A	7	0.98118	1	1
RIDGE STATION A1	8	0.99945	1	1
AIRPORT A	9	0.90509	0.997	0.997
SUAME A	10	0.88964	0.997	0.997
KAASE A	11	0.95742	0.999	0.999
ASEKYEM A	12	0.93506	0.998	0.998
SWITCHING STATION A	13	0.89694	0.997	0.997
BEKWAI A	14	0.86048	0.996	0.996
RIDGE STATION B1	15	0.99948	1	1
KTI B	16	0.99382	1	1
KTI A	17	0.99382	1	1
AIRPORT B	18	0.89352	0.996	0.996
SUAME B	19	0.87027	0.995	0.995
BAREKESE B	20	0.86585	0.995	0.995
OFFINSO B	21	0.84682	0.994	0.994
KAASE B	22	0.96909	0.999	0.999
ASEKYEM B	23	0.95339	0.999	0.999
SWITCHING STATION B	24	0.93624	0.998	0.998
BEKWAI B	25	0.91609	0.998	0.998
RIDGE STATION B	26	0.99945	1	1

NEOPLAN B	27	0.94855	0.999	0.999
AGOGO B	28	0.88515	0.998	0.998
EDWINASE B	29	0.97845	1	1
AWOMASO STATION A	30	0.99964	1	1
AKYEASE A	31	0.93324	0.997	0.997
FAWOADE A	32	0.91064	0.996	0.996
AGONA A	33	0.86973	0.994	0.994
NSUTA A	34	0.82206	0.993	0.993
MAMPONG A	35	0.817	0.993	0.992
BOADI A	36	0.98594	1.023	1
AWOMASO STATION A1	37	0.99976	1	1
AKYAWKROM A	38	0.93618	0.998	0.998
EFFIDUASE A	39	0.8833	0.996	0.996
KUMAWU	40	0.86224	0.996	0.996
AWOMASO STATION B1	41	0.99991	1	1
AKYAWKROM B	42	0.96964	0.999	0.999
EFFIDUASE B	43	0.95021	0.999	0.999
AWOMASO STATION B	44	0.99976	1	1
AKYEASE B	45	0.96382	0.998	0.998
FAWOADE B	46	0.94848	0.997	0.997
AGONA B	47	0.91267	0.996	0.996
NSUTA B	48	0.89442	0.995	0.995
MAMPONG B	49	0.89079	0.995	0.995
BOADI B	50	0.99039	1	1